BIO-BASED FIBRES FOR USE IN CEMENT COMPOSITE MATERIALS

Ashley Calleja

Dissertation submitted to the Faculty for the Built Environment, University of Malta in part fulfilment of the requirements for the Master of Engineering (Structural Engineering)

July 2023

L-Università ta' Malta

FACULTY/INSTITUTE/CENTRE/SCHOOL for the Built Environment

DECLARATIONS BY POSTGRADUATE STUDENTS

(a) Authenticity of Dissertation

I hereby declare that I am the legitimate author of this Dissertation and that it is my original work.

No portion of this work has been submitted in support of an application for another degree or qualification of this or any other university or institution of higher education.

I hold the University of Malta harmless against any third party claims with regard to copyright violation, breach of confidentiality, defamation and any other third party right infringement.

(b) Research Code of Practice and Ethics Review Procedures

I declare that I have abided by the University's Research Ethics Review Procedures. Research Ethics & Data Protection form code BEN-2022-00066.

As a Master's student, as per Regulation 77 of the General Regulations for University Postgraduate Awards 2021, I accept that should my dissertation be awarded a Grade A, it will be made publicly available on the University of Malta Institutional Repository.

ACKNOWLEDGEMENTS

I would like to express my deepest appreciation to all those who have contributed to the completion of this dissertation. Firstly, I am very grateful to my supervisor Prof. Ruben Paul Borg Ph.D.(Sheffield), Spec.Struct.Eng.(Milan), B.E&A.(Hons.), MICE, C.Eng., Eur.Ing. for his guidance, support, and invaluable insight throughout this research journey.

I would also like to thank Prof. Joseph Buhagiar B.Ed.(Hons), M.Phil., Ph.D.(Nott.) for his contribution and guidance in the initial phase of the research, on the extraction method for Agave fibres.

Special appreciation goes to Mr. John Sammut from Central Cement Ltd for sponsoring all the aggregates and cement required for this research. Additionally, I am also grateful to Philip A. Tabone Ltd. for provide the superplasticizer needed for the production of SCC.

I am also grateful to the laboratory technicians, Mr. Nicholas Azzopardi and Mr. Alex Falzon, for their constant assistance throughout my laboratory work.

Lastly, I would like to express my profound gratitude to my parents, sister, boyfriend and closest friends for their patience and encouragement throughout the years. Their presence and belief in my abilities have been a constant source of motivation.

ABSTRACT

The invasive Agave plant has been rapidly spreading in the Maltese islands, displacing native species and potentially harming local structures and biodiversity. Extensive removal efforts have been undertaken, but the disposal of these alien species through incineration poses a significant environmental challenge. To mitigate this issue, it is crucial to utilize this by-product in an innovative and sustainable way that contribute to a more circular and sustainable economy.

This study investigates the potential use of Agave Sisalana fibres in self-compacting concrete (SCC) and their impact on its fresh properties, early age characteristics and hardened properties of concrete. The influence of different fibre lengths, specifically 15mm, 25mm and 35mm, with various fibre volume percentages of 0.25%, 0.50% and 1%, were considered. To evaluate the performance of the concrete specimens, experimental tests were conducted to assess the compressive, flexural, tensile and shrinkage behaviour.

The findings obtained from the testing of the fresh properties indicated that the introduction of fibres in the concrete mix reduced its self-compacting characteristics. This reduction was primarily observed in the passing ability of the mix, with instance of clogging resulting in loss of performance. However, despite this expected decrease in performance, the SCC still maintained certain flow characteristics.

For the early age characteristics, both concrete and mortar were subjected to controlled environmental conditions. The concrete specimens were placed in an environmental chamber, while the mortar panels were exposed to directed wind from high-velocity fans. The results indicated that the addition of Agave fibres contributed to a decrease in plastic shrinkage cracks widths and delayed crack development. Additionally, the restrained concrete ring test also demonstrated higher strains exerted on the steel ring with an increase in fibre percentage.

Regarding the mechanical properties, the addition of fibres resulted in a decrease in density, ultrasonic pulse velocity and compressive strength of the concrete. However, it also led to an increase in the flexural peak load and tensile splitting strength.

Keywords: *self-compacting concrete, fibre reinforced concrete, agave sisalana fibres*

Table of Contents

List of Figures

List of Tables

List of Abbreviations

CSH	Calcium Silicate Hydrate
GHGs	Greenhouse gases
ERA	Environment and Resource Authority
SCC	Self-Compacting Concrete
NaOH	Sodium Hydroxide
H_2O_2	Hydrogen Peroxide
UPV	Ultrasonic Pulse Velocity
CMOD	Crack Mouth Opening Displacement
LVDT	Linear Variable Differential Transformer

CHAPTER 1

Introduction

1.1 Background

Concrete is one of the most widely utilized construction material due to its versatility and is employed in various applications in the construction sector, such as buildings, bridges, roads and dams. It is a mixture of materials made of fine and coarse aggregate, water, sand, cement and occasionally admixtures. Admixtures are used to alter the qualities of concrete by affecting its properties including workability and setting time to ensure good quality concrete. The bond of these constituents are due to a chemical reaction between water and cement, called hydration. C-S-H determines the majority of the concrete's properties, including its high compressive strength, fire resistance, durability and low permeability. However, despite its beneficial characteristics, concrete also has its drawbacks such as poor tensile strength, brittleness and weak crack resistance. Thus, fibre reinforcements are introduced in cement-based materials to improve its toughness and ductility and to control cracks.

Fibres can be classified into man-made and natural fibres. Man-made fibres generally consist of synthetic fibres such as glass, carbon and polypropylene. Synthetic fibres are employed in diverse applications worldwide to enhance the strength and durability of concrete structures. These fibres have consistently demonstrated substantial improvements in the performance of concrete. These include increase in tensile strength, ductility and impact resistance and the control of shrinkage cracking. However, the manufacture of synthetic fibres contributes significantly to environmental pollution, particularly greenhouse gas (GHG) emissions. This is because these fibres are non-renewable, require great energy consumption for manufacture and are not biodegradable, which may take thousands of years to decompose (Rashmi Nayak, Bochen, & Gołaszewska, 2022). Utilizing waste products from industrial operations and using renewable resources in construction is a practical approach to increase the sustainability of building materials. Thus, this generates considerable demand for natural fibres that may be employed in cement composites.

Natural fibres have been extensively used since the Egyptian Era, were they used straw and horsehair in the construction of mud bricks. Additionally, early Japanese and Chinese buildings frequently employed straw as reinforcement for the structural elements. By the late 1800s, the United States had chosen straw as a primary component of load bearing walls (Mohajerani, et al., 2019).

There are various natural fibres that can be used in concrete reinforcements, which include animal-based, plant-based and mineral-derived fibres. This dissertation will focus primarily on plant-based fibres using Agave Sisalana. The Agave plant has become an invasive species in the Maltese islands. This plant has taken over substantial areas, replacing native and endemic plants and posing as a potential threat to local structures and the overall biodiversity of the islands. Consequently, effort was made to eliminate the Agave species from areas including Buskett, Ġnejna, Għajn Tuffieħa and Comino. Once removed, the plant material was transported to the PARK & Initiatives Directorate composting facility in Ta' Qali to be incinerated (Life Saving Buskett, 2018). During this process, a significant amount of leaf waste is generated. According to the Environment and Resource Authority (ERA), around 200 tons of alien species were removed including the Agave plant (Malta Today, 2020).

Therefore, the properties of cementitious materials can be significantly enhanced by promoting the use of low-impact concrete and adopting more sustainable construction established on nature-based solutions (Onuaguluchi & Banthia, 2016).

1.2 Aims and Objectives

The main aim of this research is to study the potential use of natural plant fibres in self-compacting concrete (SCC) for low impact and a more environmentally friendly construction. The objectives of this dissertation are:

- To assess extraction methods for obtaining Agave fibres.
- To assess the fresh properties and rheology of SCC mixes incorporating agave fibres and determine if the fibres affect the self-compacting characteristics of the concrete.
- To assess cracking behaviour of SCC with Agave fibres during the early stages.
- To determine the mechanical performance of plant-based fibres cement composite mixes in the hardened state.
- To compare the results of different fibre lengths and volume percentages of Agave fibres and identify the most efficient one.

1.3 Dissertation Overview

Chapter 1 Introduction – This chapter provides an overview of the research topic, outlines the main aims and objectives and gives a structural overview of the dissertation.

Chapter 2 Literature Review – This chapter deals with an introduction on Agave Sisalana fibres, the chemical composition and biological structure of the fibre, fibre preparation techniques, limitations and challenges of fibres in concrete, applications of plant-fibres in construction and a study on several different tests to identify its properties in cement composite materials.

Chapter 3 Methodology – The methodology gives a description of the extraction and preparation process of Agave fibres, the materials used in the study, the mix design and the testing methods adopted in this dissertation.

Chapter 4 Results and Discussion – This chapter is a summary of the outcomes obtained from several tests performed and discuss the achieved results.

Chapter 5 Conclusion – This chapter gives a summary of the research outcomes and determines whether the goals of the study have been achieved. It also provides further suggestions for future research in this field.

CHAPTER 2

Literature Review

2.1 Introduction to Agave Fibres

Natural plant fibres are extracted from various parts of the plant, and the characteristics of these fibres can be influenced by multiple factors including, the specific plant species, extraction location, plant age and soil conditions (E. Njoku, K. Alaneme, A. Omotoyinbo, & O. Daramola, 2019).

Agave fibres are classified under leaf fibres, which are obtained from the tissues or stalks of the plants. These plants have parallel veins and only one seed leaf. The typical characteristics of these fibres include high strength, which are usually used for the manufacture of ropes and carpets (Onuaguluchi & Banthia, 2016).

There are more than 250 species of agave plants. Amongst them, the Agave Americana, Agave Angustifolia, Blue Agave (A. Tequilana), Agave Sisalana and Agave Attenuata are the most cultivated species in countries like Brazil, Tanzania and Kenya (Mwaikambo, 2006). As seen in Figure 2-1, the plant's trunk is covered in a rosette of around 150-250 dark green leaves. Each leaf measures about 2m in length, 10cm in width and 6mm in thickness. It is estimated that every leaf has around 1000 fibre bundles, of which only 4% are utilised as fibres (Pickering, 2008, p. 18).

These fibres have various eco-friendly benefits, including low density and high strength, which makes them a cost-effective alternative. Thus, this makes them suitable for reinforcement in concrete and other manufacturing products (Jawaid & Thariq, 2018).

Fig 2-1: Agave Sisalana trunk and leaves (Man P., 2022)

2.2 Chemical Composition and Biological Structure of Agave Fibres

2.2.1 Chemical Composition

The structure of the fibres comprises of various elements, such as lignin, cellulose, hemicellulose, pectins and waxes. The quantities of these different components are significantly determined by several parameters which include, age, plant location, fibre type, extraction, processing method and growth state (Alshaya, Alhomidan, Alromizan, & Labib, 2018). Table 2-1 exhibit the various chemical structures of typical plant fibres including the Agave Sisalana fibres (Mwaikambo, 2006).

Lignin

Lignin gives rigidity to the plants and provides protection against microbial attack of plants. Thus, it is extremely resistant to many chemical agents and biological degradation due to its chemical composition (Ntenga, et al., 2022). Lignin is a thermoplastic polymer that becomes flexible at a temperature of approximately 90°C and melts at 170°C. It can dissolve in hot alkaline solutions but does not decompose when exposed to acids (Kaur, Kaith, & Kalia, 2011, p. 12).

Cellulose

Cellulose is the primary constituent of natural fibres. According to research done by Komuraiah et al., it was observed that the cellulose provides reinforcement properties such as high stiffness, strength and stability. Hence, the physical and chemical properties of a fibre, such as strength and Young's Modulus, are determined by their molecular structure (Komuraiah et al., 2014 as cited in Labib, 2022).

Hemicellulose

A hemicellulose consists of a group of substance made up of different sugars that remains attached to the cellulose after the lignin has been eliminated. Due to their hydrophilic nature, they are responsible for the increase in moisture absorption (Ntenga, et al., 2022). Hemicellulose varies from cellulose in three significant ways, which include (Kaur, Kaith, & Kalia, 2011, p. 12):

1. The variety of sugar units present
2. The level of branching in its structure (cellulose is more linear).
3. The length of the polymer chains (cellulose has longer chains when compared to hemicellulose).

Pectins and Waxes

Pectin is mostly composed of polygalacturon acid, which is soluble in water and helps the plants maintain flexibility. The final component of fibres is made up of waxes, which consists of various alcohols which do not dissolve in water or certain acids (Kaur, Kaith, & Kalia, 2011, p. 12).

Table 2-1: Chemical Composition of typical natural fibres (Mwaikambo, 2006)

Fibre	***Cellulose***	***Hemicellulose***	***Lignin***	***Pectin***
Sisal	**43-78**	**10-13**	**4-12**	**0.8-2**
Banana	60-65	6-19	5-10	3-5
Bamboo	26-43	15-26	21-31	-
Cotton	82-96	2-6	0.5-1	5-7
Flax	60-81	14-19	2-3	0.9
Hemp	70-92	18-22	3-5	0.9
Jute	51-84	12-20	5-13	0.2
Kenaf	44-57	21	15-19	2
Pineapple	80-81	16-19	4.6-12	2-3
Wood	45-50	23-30	27	2-2.5

2.2.2 Biological Structure

A single plant fibre cell from Agave Sisalana leaves generally ranges from 1-2m in length and around 0.2-0.4mm in diameter. They are made of multiple cell walls that surrounds the central lumen. Figure 2-2 gives an example of the fibre's cell structure (Kaur, Kaith, & Kalia, 2011, p. 6).

The cell walls consist of two sections: the primary wall and the secondary wall. The primary wall is the outer layer of the fibre and contains a network of closely packed microfibrils (Kaur, Kaith, & Kalia, 2011, p. 8). On the other hand, the secondary wall is composed of three different layers which include, the outer layer (S_1), the middle layer (S_2) and the inner layer

(S_3) (Mwaikambo, 2006). The outer layer (S_1) is located close to the primary wall and is very resistant to water and acid. This layer's structural arrangement stabilises the fibre against any lateral forces. Conversely, the middle layer (S_2) represents the thickest section of the fibre (Mwaikambo, 2006).

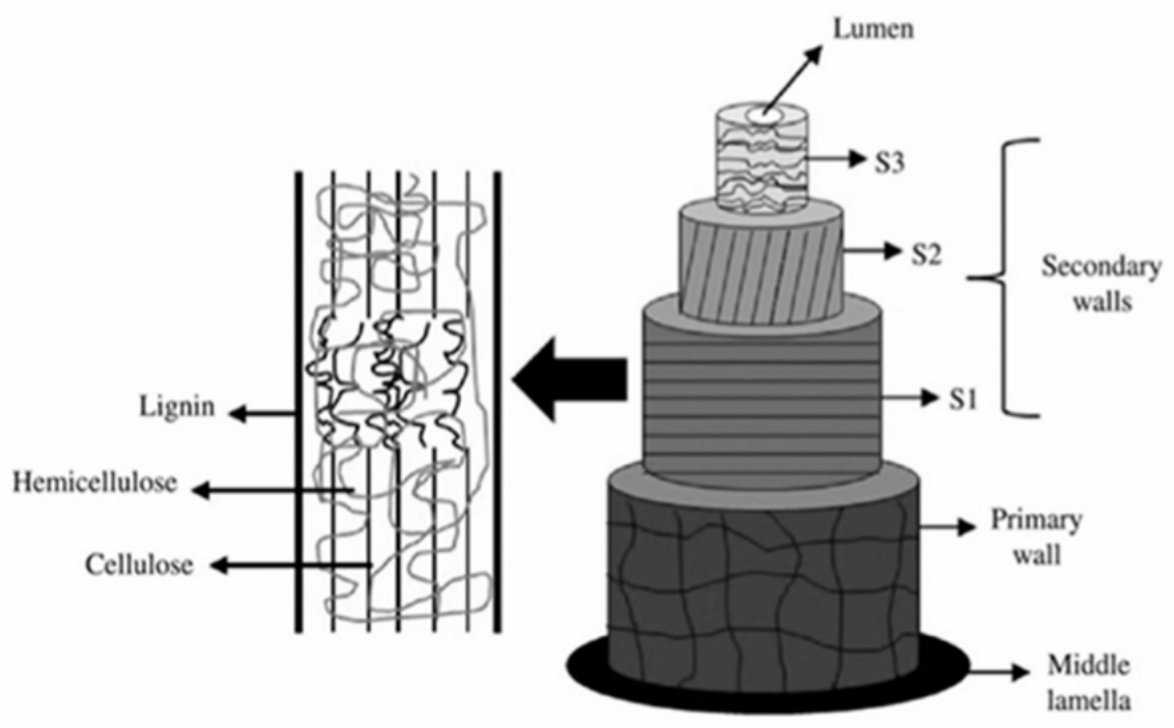

Fig 2-2: Biological structure of fibre cell walls (Maya et al., 2017)

The strength and durability of natural fibres are influenced by their chemical composition, which includes constituents such as cellulose, hemicellulose and lignin. These components are responsible for the bonding behaviour and degradation of the fibres. The primary structural element in the fibre cell is the cellulose/hemicellulose network. This is created through hydrogen bonding between the molecules, which act as a binding matrix between the microfibrils (Onuaguluchi & Banthia, 2016). Table 2-2 provides a comparison of the mechanical properties of different fibres, including Agave Sisalana, and how these may differ (Pickering, 2008, p. 40).

Table 2-2: Mechanical properties of typical natural fibres (Labib, 2022)

Fibre	***Tensile Strength (MPa)***	***Young's Modulus (GPa)***	***Elongation at break (%)***	***Density (kg/m^3)***
Sisal	**511-635**	**9.4-22**	**2-2.5**	**1450**
Flax	345-1035	27.6	2.7 – 3.2	1380
Jute	393-773	26.5	1.5-1.8	1300
Hemp	690	70	1.6	1350
Kenaf	930	53	1.6	1200
Bamboo	140-230	11-17	-	600-1100
Pineapple	400-627	1.44	14.5	1500
Coir	175	4-6	30	1200

2.3 Fibre Extraction Processing Techniques of Fibres

The extraction process has an impact on both the production and fibre quality. This can affect the structure, chemical composition and the overall characteristics of the fibres. The three most common types of retting processes are: biological, mechanical and chemical fibre separation (Kaur, Kaith, & Kalia, 2011, p. 9).

2.3.1 Biological Retting

Biological retting includes both natural and artificial methods. Natural retting involves techniques such as cold water or dew retting, while for artificial retting, warm water is used (K Singh, Bansal, Gope, & Gupta, 2017).

- *Cold Water Retting:* During this method, plants are immersed into large water tanks, rivers or ponds. Pectin substances are dissolved, which allows the fibres to be separated from its cores. This process typically ranges from 7 to 14 days, depending on the quality of water and its temperature. As shown in Figure 2-3, In India and Bangladesh, fibres have been traditionally pond retted for several years, where the plant is submerged in the water and left to decompose naturally. The bark and bast are then removed and separated from the core (Pickering, 2008, p. 38). In a research paper conducted by Sathiamurthi et al., a similar method of fibre extraction was used. When the Agave fibres were collected, the thorns and spines on the tip were removed. To eliminate moisture content, the leaves were cut into vertical parts and left to dry in the natural sun for two days. The leaves were then immersed in the water for around 14 days to promote microbial action, which help the tissues of the leaf's matrix to soften. After removing the leaves from the water, they were cleaned and dried for another two days (Sathiamurthi, Karthi Vinith, Sathiskumar, Arunkumar , & Anaamalaai, 2021).

- *Dew Retting:* This is a commonly used techniques, especially in areas with suitable moisture and temperature conditions (Kaur, Kaith, & Kalia, 2011, p. 10). Over-retting must be avoided as it can lead to cellulose degradation. Similarly, under-retting must also be prevented as fibres can be difficult to separate from the plant and processed any further (K Singh, Bansal, Gope, & Gupta, 2017).

- *Warm Water Retting:* In the case of artificial retting, warm water retting is used. Warm water tanks are utilised to soak plants and produce a homogenous, high-quality and clean fibre in around 3 to 5 days. After the fibres are separated from the plant, the remaining stalks and stems are extracted by using a scotching procedure (Kaur, Kaith, & Kalia, 2011, p. 10).

Fig 2-3: Plant Fibres Retting by microbial action (Research Outreach, 2021)

2.3.2 Mechanical Retting

A decorticator is a mechanical device specifically used for mechanical retting. This is used to remove fibres from the stem. After the pulp is removed, the plant stems are squeezed between two drum rollers to obtain the fibres. Water is then used to wash away any remaining parts of the leaf, and the fibres are rinsed and dried in a hot environment (Mwaikambo, 2006). This method is considered to be more efficient when compared to a manual procedure, as it was revealed that the use of the use of decorticators increases fibre production by around 20-25 times (Ntenga, et al., 2022).

2.3.3 Chemical Retting

Chemical retting is another method used to separate fibres from plants. The process involves a heated water tank in which the fibre crop is immersed into the water containing sulphuric acid or sodium hydroxide, to dissolve the pectin component. This method generally provides high quality fibres but is very costly (Kaur, Kaith, & Kalia, 2011, p. 11).

2.3.4 Physical Retting

There are several physical retting techniques such as ultrasound retting, enzyme retting and steam explosion methods (Ramamoorthy, Skrifvars, & Persson, 2015).

2.3.4.1 Ultrasound Retting

Ultrasound retting involves the crushing and cleaning of harvested stems. These crushed stems are then placed in a hot water tank containing alkali and surfactants before being subjected to the ultrasound. Due to the high intense ultrasound, the fibres and the hurds are separated (Kaur, Kaith, & Kalia, 2011, p. 10).

2.3.4.2 Steam Explosion

Another viable solution to the classic field-retting approach is the steam explosion method. Steam and additives penetrate the fibre interspaces when subjected to pressure and an increase in temperature. The fibre composite is effectively broken up by the abrupt relaxation of the steam, which causes a significant disintegration into fine fibres (Kaur, Kaith, & Kalia, 2011, p. 10).

2.3.4.3 Enzyme Retting

Enzymes are used to degrade the pectin and separate the fibres from the wood parts. The enzyme activity may increase with a rise in temperature, however when a certain temperature is reached the enzymes starts to degrade. This technique produces fibres of high quality (Ramamoorthy, Skrifvars, & Persson, 2015).

2.4 Limitations and challenges of natural fibres in cement composites and the effect of chemical treatments

Natural fibres are generally easily accessible, low-cost and sustainable. They provide several benefits which can be used to improve the structural, thermal and energy performance of a material (Luhar, et al., 2020). However, there are also some drawbacks when using natural fibres in concrete. The subsequent sections will address topics such as the water absorption properties, durability, compatibility and adhesion between the cement and fibre matrix, along with various treatment methods (Labib, 2022).

2.4.1 Limitations and Challenges of Plant-based Fibres

2.4.1.1 High Water Absorption

A fundamental drawback of plant-based fibres is their high-water absorption. Natural fibres are generally obtained from plants which have hydroxyl groups (-OH). Fibres that are high in cellulose content have more free hydroxyl groups present, which makes it much more likely that the fibre will absorb more water. Thus, moisture absorption capacity depends on the chemical structure and crystallinity of the fibre (Begum, Tanni, & Shahid, 2021). When plant fibres are used as reinforcement in cementitious materials, several issues may arise, including (Savastano Junior, Fiorelli, & Dos Santos, 2017, p. 366):

- When moisture is absorbed by the fibres, swelling may occur. Similarly, when moisture is lost as a result of dry environments and high temperatures, plant fibres will shrink. This can cause crack formations, affecting the performance and durability of concrete.
- During the mixing process, plant fibres tend to absorb a significant amount of water. This can result in a reduction of the water available for cement hydration, leading to lower mechanical performance.
- The presence of moisture can weaken the mechanical strength of plant fibres, as the hydrogen bonds between the fibres and matrix can be broken.

2.4.1.2 Compatibility

Compatibility between fibres and the matrix is another major issue. It refers to the ability of two materials to bond and improve the mechanical properties of the composite. The cement matrix serves as a binder to transfer the stiffness of the fibres within the material. Therefore, if there is poor adhesion between the fibres and the matrix, the material may not exhibit the desired properties (Célino, Fréour, Jacquemin, & Casari, 2014).

The length of the fibres influences the bond with the cement matrix. A simple technique to improve the compatibility is to use longer fibres as they generally provide better properties than shorter fibres due to their greater surface area for bonding. Other techniques which have been suggested to improve the compatibility of the fibres include (Labib, 2022):

- *Chemical Reagents:* Chemical reagents are generally used to treat plant-based fibres. In multiple studies, it was investigated that several chemical reagents were tested to improve the compatibility of composites. This will be further discussed in section 2.4.2.

- *Pulping Technique (Chemical or Mechanical):* The pulping technique is also another approach to improve adhesive of fibres and cement matrix. Pulping refers to the process of fibre separation. This can be achieved either by chemical or mechanical procedures. In research carried by Basch and Lewin, they found that the mechanical properties of the material were affected by chemical pulping.

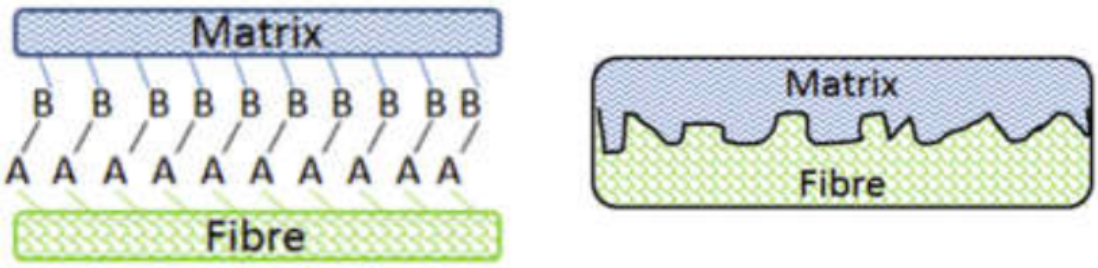

a) b)

Fig 2-4: Bonding of fibre-matrix mechanism with the methods of a) chemical pulping, and b) mechanical pulping (Lee et al. 2021)

2.4.1.3 Durability

Durability is crucial to the design of cement-based materials because it has an impact on the long-term resistance of composites when exposed to harmful chemicals. Since plant fibres have a high moisture absorption, they are very susceptible to degradation. This is because when an alkaline pore solution is present, the lignin and hemicellulose linking the fibre cells, starts to dissolve (Onuaguluchi & Banthia, 2016).

2.4.2 Chemical Treatments of Plant-based Fibres

Chemical treatments are employed to improve the adhesion between the cement matrix and natural fibres, as well as to modify its surface characteristics. The most used treatments on plant fibres are alkaline, silane, benzoylation and peroxide treatments (Gholampour & Ozbakkaloglu, 2020).

2.4.2.1 Alkaline Treatment

The Alkaline treatment is an effective chemical method used to improve the bond between the fibre and the matrix. In this process, the fibres are submerged in a solution of NaOH, which causes the lignin and hemicellulose components of the fibre to break down. Following this treatment, the cellulose molecules become exposed, thereby strengthening their bond (Geremew, De Winne, De Backer, & Demissie, 2021).

In research conducted by Mehrez et al., fibres were subjected to treatment using different concentrations of NaOH, specifically 4.2%, 5% and 9%. The fibres were immersed in the solution for a duration of 12 hours. After treatment, the fibres were cleaned and left to dry in the sun for 2 days (Mehrez, Hachem, Gheith, & Jemni, 2022). From a study done by Mishra et al., it was indicated that lower concentrations of alkali gave a better performance. The sisal fibres which were treated with 5% alkali solution showed a higher performance in tensile strength when compared to fibres treated with 10% alkali (Mishra, S, et al., 2003).

2.4.2.2 Peroxide Treatment

This involves treatment of fibres using Hydrogen Peroxide (H_2O_2). The peroxide is induced on the surface of the fibre and introduced in hydroxyl groups, where these can affect the bonding of the fibre. Thus, the peroxide treatment can improve the compatibility of the fibres, decrease its moisture absorption and increase the thermal stability of the fibres. This can ultimately lead to better mechanical properties of the composite (Gholampour & Ozbakkaloglu, 2020).

From a study done by Rayung et al., a similar approach to the Sodium Hydroxide is used. The fibres were subjected to a concentration of 5% Hydrogen Peroxide for around 90 minutes. Subsequently, the fibres were then washed and dried at a temperature of 60°C for a duration of 24 hours (Rayung, et al., 2014).

2.5 Application of Plant-based fibres in Construction

The use of plant-based fibres is steadily increasing all around the world, especially in the construction industry. Fibre-reinforced materials have several advantages when compared to properties of regular materials. Such advantages include (Mohajerani, et al., 2019):

- Enhanced properties such as strength and durability.
- Has the ability to withstand physical and chemical attacks under various environments.
- The density and specific weight of the product are reduced, which results in a lighter, more economical and energy-efficient product.
- Reduces the chance of shrinking, cracking, spalling and swelling.

There are various applications in the construction sector where plant fibres can be used which will be discussed below. These will include normal concrete, asphalt pavements, soil conservation, blocks and bricks.

2.5.1 Plant Fibres in Normal Concrete

Concrete is often used for a variety of purposes including slabs, pavements, columns, beams and shotcrete. Fibres can be formed and utilised as reinforcing bars to replace traditional steel bars and meshes. These can be beneficial as they are more lightweight and require less energy to produce (Mohajerani, et al., 2019). A study by Jiao et al., demonstrated that the addition of natural fibres in a cement paste has increased it flexural strength by 15% and 20% respectively (Jiao, et al., 2016).

2.5.2 Plant Fibres in Asphalt Concrete Pavement and Binders

In road infrastructure construction, the design of asphalt concrete is crucial, since it is a major element used for roads and pavements. When fibres are added in asphalt mixes, its resistance to cracks is improved and helps in the stabilisation of asphalt binders (Mohajerani, et al., 2019). Thus, the performance, service life and cost efficient of the roads are affected with the addition of fibres. In order to prevent binder drainage, Arshad et al. examined two different types of cellulose fibres by using synthetic and kenaf fibres. It was concluded that the kenaf fibres performed better in maintaining the binders' mix, making it a less expensive and more sustainable replacement for synthetic fibre (Arshad, Mansor, Shafie, & Hashim, 2016).

2.5.3 Plant Fibres in Soil Conservation

The soil's characteristics are influenced by the environmental conditions and climate of the area. Soils can be classified into four types being: clay, sand, silt and gravel. Generally, soils are very weak in tension and shear strength, thus soil reinforcement using fibres is implemented to improve its tensile strength, shear strength and density. The improvement of these properties will result in stabilised slopes, increased bearing load capacities and a reduction in settlement (Mohajerani, et al., 2019).

Research conducted by Gosavi et al. has shown that when plant fibres were added to the mix, the results in strength increased significantly when used to reinforce soil. When compared with a reference sample, a mixture of nylon fibres and jute fibres increased the strength by 50%, while coconut fibres increased it by 96% (Gosavi, et al., 2004 as cited in Mohajerani, et al., 2019).

2.5.4 Plant Fibres in Earth Materials, Blocks and Bricks

Since a very long time ago, earth has been used as a building material, and it is still widely utilised today, especially in developing countries. Using natural fibres for earth materials and blocks could be beneficial, as it is environmentally friendly and can also save energy and costs, since it may reduce or eliminate the need for burning procedures used to dispose of waste in landfills (Mohajerani, et al., 2019).

A study done by Binici et al., it has been found that there were several benefits of using fibre reinforced mud bricks. It was observed that they were much lighter than the traditional mud bricks and their compressive strength was greater (Binici, Aksogan, & Shah, 2005). Binici et al. also discovered that straw fibres improve the thermal insulation properties which results in a reduction of energy costs in buildings (Binici, Aksogan, Bodur, Akca, & Kapur, 2007). Similarly, Khedari et al. noted that coir fibre reinforced soil-cement blocks were less thermally conductive and lighter in weight when compared to an unreinforced block samples (Khedari, Watsanasathaporn, & Hirunlabh, 2005).

2.6 Experimental Reviews on the properties of fibres in concrete and mortars

Various studies have explored the effects of incorporating Agave fibres into concrete mixes to examine their characteristics in their fresh and hardened state. The investigations have considered different factors such as the preparation methods, varying fibre proportions and length of fibres. Several properties have been investigated including the workability, compressive strength, tensile strength, flexural strength, plastic shrinkage and drying shrinkage tests (Alshaya, Alhomidan, Alromizan, & Labib, 2018).

2.6.1 Fresh Properties of Agave Fibres

2.6.1.1 Consistency

In a study by Savastano et al., a decrease in workability of the cement paste has been observed when it is reinforced with coir combined with sisal fibres. The fibre aspect ratio and the volume percentage in the mix design are factors which affect workability. To increase the workability, chemical pre-treatments can be used before adding them to the mix (Savastano, Agopyan, Nolasco, & Pimentel, 1999).

In another study conducted by Sugathan on self-compacting concrete with sisal fibres, three different tests were considered, which include the Slump flow, V-Funnel and L-Box tests. The fibres used had a length of 12mm and different fibre dosage of 0.5%, 1%, 1.5% and 2% were added to the mixes. The findings showed a decrease in the slump flow diameter as the fibre volume increased. Moreover, higher fibre dosages led to an increase in the time required for the slump flow to reach 500mm. The V-Funnel tests also indicated that as the fibre percentage increased, the V-Funnel time also increased, suggesting a decrease in flowability. Lastly, in the L-Box test, a blockage was observed for mixes containing 2% fibres (Sugathan, 2017).

2.6.1.2 Plastic Shrinkage

Plastic shrinkage cracks are developed when there is a sudden loss of water from the surface of the fresh cement mix. In a study on crack control by Toledo Filho and Sanjuan, a sisal fibre length of 25mm was used with a ratio of water-cement of 0.5. It has been found that the sisal fibres were very effective in preventing mortar cracking. It was also observed that there was a slight delay to reinforcement corrosion (Toledo Filho, Ghavami, Sanjuán, & England, 2005).

2.6.2 Hardened Properties of Agave Fibres

2.6.2.1 Drying Shrinkage

Drying shrinkage problems is often an issue in hardened concrete. According to research done by Toledo Filho, with the addition of 25mm sisal fibres, the drying shrinkage was increased by around 27%, with a presence of up to 3% volume of fibres. The research revealed that sisal fibres exhibited higher drying shrinkage compared to coconut fibres (Toledo Filho, Ghavami, Sanjuán, & England, 2005).

2.6.2.2 Compressive Strength

Rashmi et al. examined the effect of natural sisal fibres in comparison with synthetic fibres. Sisal fibres with a length of 15mm and proportions of 1% and 2% to cement weight were used. From the results obtained, sisal fibres increased the compressive strength with 10% after 28 days, as compared to synthetic fibres (Rashmi Nayak, Bochen, & Gołaszewska, 2022).

In a similar study by Fadhil and Yaseen, the effect of sisal fibres on the mechanical properties of concrete was investigated. Sisal fibres were cut into pieces of 40mm and added in proportions of 0.6%, 1.2% and 1.8% by volume of the mix. The findings indicated that the inclusion of 1.2% fibres led to a 3.3% increase in compressive strength (Fadhil & Yaseen, 2015).

Furthermore, Sugathan conducted a study on SCC with sisal fibres. The sisal fibres were cut into lengths of 12mm and different fibre percentages of 0.5%, 1%, 1.5% and 2% were investigated. From the tests results obtained, an increase in compressive strength was recorded for fibres up to 1.5%. This was observed for both 7 and 28 days (Sugathan, 2017).

2.6.2.3 Splitting Tensile Strength

Sathiamurthi et al. investigated the Agave Americana fibres reinforced with epoxy hybrid composites. They added different fibre lengths of 10mm, 20mm, 30mm and 40mm which were mixed in different proportions of 10%, 15%, 20% and 25%. It was found that the tensile strength increased gradually as the fibre length increased. The highest tensile strength and tensile modulus were found in 30mm fibre lengths and at 20% proportion (Sathiamurthi, Karthi Vinith, Sathiskumar, Arunkumar , & Anaamalaai, 2021).

Sugathan also conducted a research on the impact of sisal fibre on the tensile splitting strength of SCC. The results indicated an increase in tensile strength for fibre percentages of 0.5%, 1% and 1.5%. This suggest that the addition of fibres contributed to the overall tensile strength of concrete. However, a decrease in strength was observed at a fibre percentage of 2%. Nevertheless, even at this high fibre dosage, the strength of the SCC with sisal fibre remained higher than that of plain concrete (Sugathan, 2017).

2.6.2.4 Flexural Tensile Strength

Sathiamurthi et al. investigated the flexural strength of various concrete mixes. The results demonstrated that when all four samples were examined at the same fibre length, the 20% specimen had the highest flexural strength. In contrast, the 10% specimen showed the lowest flexural strength with 10mm and 20mm fibre lengths (Sathiamurthi, Karthi Vinith, Sathiskumar, Arunkumar , & Anaamalaai, 2021).

A similar study carried out by Solai Mathi et al., examined the use of sisal fibres in SCC. The findings revealed that the inclusion of 0.25%, 0.75% and 1% sisal fibres resulted in increased load strength when compared to conventional concrete. Additionally, a load vs deflection graph was also plotted to analyse the behaviour of the beams. The results show that as the percentage of fibres increases, the failure load and deflection also vary. Traditional concrete exhibited a maximum load of 6.4 tonnes with a corresponding deflection of 7.52mm. For 0.75% fibre addition, a maximum load of 7.2 tonnes was recorded with a deflection of 5.5mm (Solai Mathi, 2021).

CHAPTER 3

Methodology

3.1 Overview

The main aim of this study is to assess the fresh, hardened and shrinkage properties of self-compacting concrete (SCC) reinforced with natural fibres using Agave Sisalana. This chapter provides an overview of the fibre preparation techniques and the testing methods necessary.

3.2 Considered Variables

From various research papers as described in the literature review, the most significant parameters impacting the fresh, hardened and shrinkage properties of concrete are the following:

- The length of fibres
- The fibre volume percentage

Therefore, it was concluded that three different fibre lengths would be studied as follows: 15mm, 25mm and 35mm. Furthermore, the fibre dosage used in the mix are of 0.25%, 0.5% and 1% of the concrete volume.

Table 3-1: Different mix variable considered

Mix	***Fibre Length***	***Volume Fraction***	***Mix Code***
1	-	-	CM
2	15mm	0.25%	F15-0.25
3	25mm	0.25%	F25-0.25
4	35mm	0.25%	F35-0.25
5	15mm	0.5%	F15-0.50
6	25mm	0.5%	F25-0.50
7	35mm	0.5%	F35-0.50
8	15mm	1%	F15-1

3.3 Preparation of Materials

3.3.1 Cement

In accordance with EN 197-1 Ordinary Portland cement, CEM II /A-LL 42.5 R, was used during this research. This type of cement is most often used locally, and it consists of 80 to 94% clinker content and 6 to 20% limestone powder. CEM II /A-LL 42.5 R is generally employed for high strength concrete and self-compacting concrete.

3.3.2 Coarse & Fine Aggregate

Dolomite Aggregate was used for both coarse and fine aggregate. The particles for coarse aggregate range from 10mm to 4mm, having both an oven dry particle density and a saturated surface-dried density of 2.83g/cm^3. Furthermore, the fine aggregate particles used during this study range from 4mm to 0mm, having an oven dry particle density of 2.75g/cm^3 and a saturated surface-dried density of 2.76g/cm^3. From the data sheets provided, the coarse aggregates had a 0.2% water absorption, while the fine aggregate had a 0.3% water absorption. According to BS 812-109 (1990), the aggregates were oven dried for 24 hours at a temperature of 105°C before mixing.

3.3.3 Chemical Admixture

To obtain a SCC mix, a liquid superplasticizer, MasterGlenium SKY 698 was used. This type of superplasticizer was obtained from P.A Tabone Ltd. and produced by BASF Construction Chemicals. It is designed particularly to offer concrete fluidity and self-compaction capabilities. With the use of this superplasticiser, the water-to-cement ratio can be decreased without compromising the concrete's ability to resist segregation while yet maintaining high workability characteristics. The suggested dose for this superplasticizer is between 1.2 and 1.6 litres per 100 kg of binder, and it has a relative density of 1.059 to 1.099 g/cm^3 at 20°C.

3.3.4 Fibres

The Agave Sisalana leaves were obtained from a plant in Baħar iċ-Ċagħaq as seen in Figure 5a. It is noted that the Agave Sisalana plant, although commonly used as a decorative plant, is also a non-endemic and invasive species.

The following steps were taken to extract the fibres from their leaves:

- The lower part of the leaves and the spikes at the top were cut using a sharp tool, as seen in figure 5b.
- To remove any moisture content, the leaves were cut into vertical strips as shown in figure 5c and left to dry in the sun for about two days.
- Figure 5d below, show the strips submerged in water for 14 days to induce microbial activity and help soften the leaf's matrix.
- The leaves were then beaten with a rubber mallet to cause further de-cohesion of fibres and were put again in the water as shown in figure 5e.
- The fibres were removed from the water after 7 days and were rinsed and left to dry for another two days. Figure 5f shows the Agave fibres after being dried.

a) b) c)

d) e) f)

Fig 3-1: Fibre extraction method of Agave Sisalana Fibres a) Agave Sisalana Plant in Baħar iċ-Ċagħaq, b) Agave Sisalana leaves after cut, c) Leaves cut into vertical strips and left to dry, d) Submerged leaves into the water, e) De-cohesion of fibres, f) Extracted Agave fibres

3.4 Aspect Ratio of Fibres

The aspect ratio of fibres is a crucial parameter in fibre-reinforced concrete as it determines the effectiveness of fibres to enhance the properties of concrete. Generally, fibres with a high aspect ratio, i.e., longer and thinner fibres, provide better reinforcement to improve the properties of concrete. To determine the average diameter of Agave fibres, multiple measurements were taken since they exhibit variations in diameter. This process is depicted in Figure 3-2, which represents a normal distribution curve. The average diameter was found to be 0.167mm. The fibre lengths used in this study are of 15mm, 25mm and 35mm. To determine the aspect ratio, the length of fibre is divided by its diameter. Therefore, the aspect ratios for the fibres used are tabulated in Table 3-2.

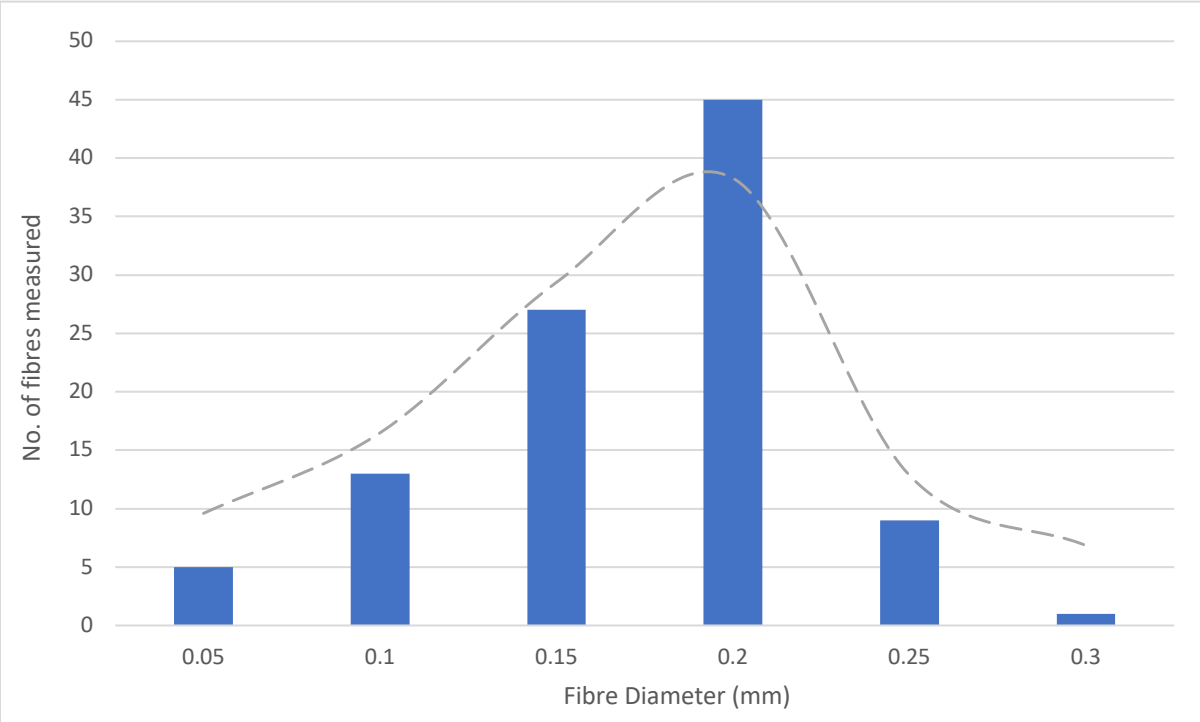

Fig 3-2: Normal Distribution Curve of fibre diameter

Table 3-2: Fibre Aspect Ratio

Fibre Length	***Aspect Ratio***
15mm	89.82
25mm	149.70
35mm	209.58

a)

b)

Fig 3-3: Agave Sisalana fibres under the microscope a) Cross-section of fibres, b) Longitudinal section of fibres

3.5 Mix Design

The preparation of the SCC mix does not follow any standard procedures. Therefore, the mix design methodology adopted by Vella (2018), was used for the SCC mixes. Table 3-3 shown below, represents the control mix without any fibres. Furthermore, Table 3-4 shows the addition of Agave fibres to the other mixes, which led to a reduction in the weight percentage of coarse aggregate. All other constituents, including the fine aggregate, cement, water, and superplasticizer, remained constant in their respective quantities.

Table 3-3: Control Mix ratios

Mix Design per m³

W/C	0.45				
Aggregate / Sand	0.6				
Water Absorption	5.184				
Material		**Units**	**Quantities**	**Material Density g/cm³**	**Volume m³**
Cement		kg/m³	495	3.01	0.164
Water		kg/m³	222.75	1.00	0.223
Fine Aggregate (0-4mm)		kg/m³	1080	2.83	0.382
Coarse Aggregate (4-10mm)		kg/m³	648	2.85	0.227
Admixture		kg/m³	5.94	1.10	0.005
		Total	2451.69		1.00

Table 3-4: Mix proportions for all other mix designs

Mix		***CM***	***F15-0.25***	***F25-0.25***	***F35-0.25***	***F15-0.5***	***F25-0.5***	***F35-0.5***	***F15-1***
Fibre Length	mm	-	15	25	35	15	25	35	15
Volume Fraction	%	0	0.25	0.25	0.25	0.5	0.5	0.5	1
W/C	-	0.45	0.45	0.45	0.45	0.45	0.45	0.45	0.45
Cement	kg/m³	495	495	495	495	495	495	495	495
Water	kg/m³	222.75	222.75	222.75	222.75	222.75	222.75	222.75	222.75
Fine Aggregate	kg/m³	1080	1080	1080	1080	1080	1080	1080	1080
Coarse Aggregate	kg/m³	648	645	645	645	642	642	642	636
Superplasticiser	kg/m³	5.94	5.94	5.94	5.94	5.94	5.94	5.94	5.94
Water Absorption	kg/m³	5.184	5.175	5.175	5.175	5.166	5.166	5.166	5.148

3.6 Mixing Methodology

3.6.1 Concrete Mixing

SCC is a highly fluid mixture that can flow and fill all the voids in a mould without requiring external compaction. The following is a procedure which was adopted by Vella (2018) for mixing self-compacting concrete:

- Firstly, the buttering of the mixer is applied in which some cement and water were mixed for 1 minute.
- The mixer was then loaded with both coarse and fine aggregate, which were mixed for a duration of 3 minutes.
- Around two minutes into the mixing process, approximately 60% of the total water was added to the aggregates, which was then followed by another 1 of mixing.
- The pan mixer was switched off for 2 minutes to allow the aggregates to absorb the water.
- The superplasticizer was added with the remaining water and placed in the mixer.
- Once again, the mixing process was restarted to mix the cement and the aggregates for another 2 minutes.
- After 1 minute of mixing, the agave fibres were introduced in the mix.
- The mixture was then left to mix for an additional 2 minutes.

Fig 3-4: Pan mixer

Fig 3-5: Agave fibres in concrete mix

3.6.2 Casting of Specimen

The moulds were prepared and greased with a de-moulding agent. After the concrete was mixed and the fresh properties tests were performed, the concrete was cast into the moulds according to the specifications of each test. The following moulds were used to cast the specimen:

- Compressive cubes measuring 100 x 100 x 100mm
- Flexural prisms measuring 150 x 150 x 550mm
- Tensile cylinder measuring 150 diameter x 300mm
- Environmental Chamber specimen measuring 560 x 355 x 100mm
- Ring specimen

Following the casting process, all moulds were left to harden. The moulds were then removed after 24 hours and kept in a water tank for further curing until testing.

3.7 Fresh Properties

To assess the capability of a self-compacting mix to adequately fill confined spaces which also maintaining its consistency in its fresh state, the following parameters are used such as flow, viscosity, passing ability and segregation resistance (SCC European Project Group, 2005). The evaluation of these properties was carried out through the Slump flow, V-Funnel and L-Box experiments.

To evaluate the fresh properties of all the mixes, an identical testing procedure used by Vella (2018) and Abdilla (2021) was employed. The testing commenced with the Slump Flow test, followed by the V-funnel and L-box tests, all of which were conducted within two minutes from each other.

These tests were ultimately performed at three different intervals (t_0, t_{15} and t_{30}) corresponding to 0, 15 and 30 minutes following the mixing procedure. This approach was applied to each mix to investigate how the fresh properties of a SCC mixes respond to different agave fibre dosages and time intervals.

3.7.1 Slump Flow

For this test, a slump cone was utilised and positioned in the centre of a glass sheet that measures 900mm by 900mm. The cone was filled with a layer of concrete without the use of mechanical compaction, and any excess concrete that spilled onto the glass sheet was carefully removed. As the cone was raised vertically, the time taken for the concrete to expand to a diameter of 500mm (t_{500}) was noted. Once the concrete flow stabilised, the average diameter of the slump flow was calculated by measuring two diameters perpendicular to each other. The slump flow test was conducted as specified in the BS EN 12350-8 Standard.

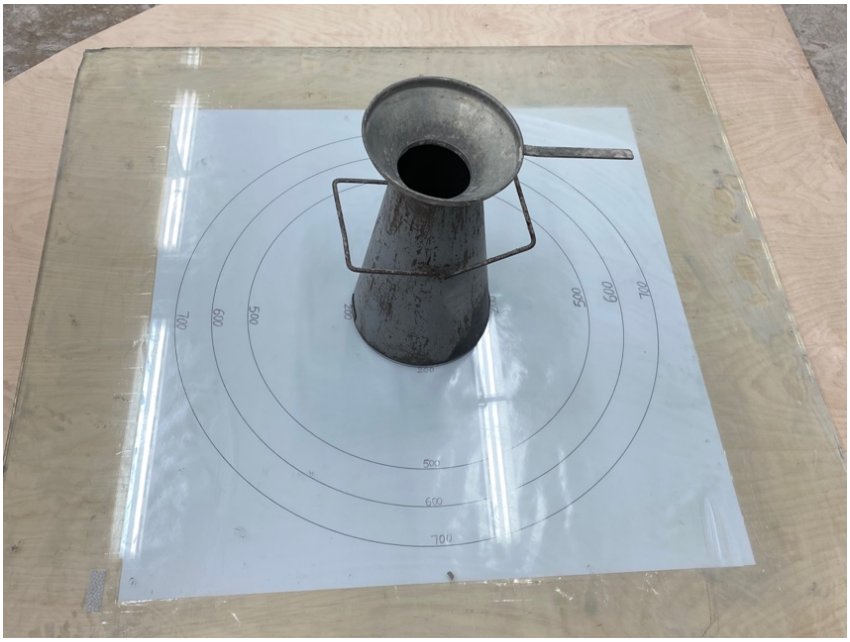

Fig 3-6: Slump Flow Test

3.7.2 V-Funnel

The V-Funnel test was performed on a flat surface, and the SCC was poured into it without any mechanical compaction, ensuring that the hinged gate is closed. After levelling the top surface of the concrete, it was left to settle for 10 ± 2 seconds before opening the gate. The time (t_v) taken for the concrete to flow out from the funnel was recorded. This test was conducted following BS EN 12350-9.

Fig 3-7: V-Funnel Test

3.7.3 L-Box

The L-Box test was performed on a steady surface. The concrete was poured vertically without mechanical compaction, with the sliding gate closed. The concrete was left to settle for approximately 60 ± 10 seconds before opening the gate to allow the concrete to flow. Three values of H_1 and H_2 were obtained, and their averages were calculated to determine the PL ratio for each mix. This test was carried out following the guidelines of BS EN 12350-10.

Fig 3-8: L-Box Test

3.7.4 ICAR Rheometer

The rheological properties of concrete are assessed using an ICAR Rheometer. It is commonly used to test the flow characteristics and workability of self-compacting concrete. A fresh concrete sample is poured into the steel container with a diameter of 205mm and a height of 312mm. The Rheometer measures the torque and rotation as a four-bladed vane is inserted in the container. Two tests, namely the stress growth test and the flow curve test, were conducted for all the concrete mixes. To establish the maximum torque and static yield, an input speed of 0.025 rps was used in the stress growth test. As for the flow curve test, a rotation speed of 0.5 rps was employed. Additionally, the relative Bingham parameters were determined by taking torque measurements at seven different speeds ranging from 0.5 rps to 0.05 rps. The study was conducted using BS EN 12350-13 Standard.

Fig 3-9: ICAR Rheometer Test

3.8 Mechanical Properties

3.8.1 Hardened Concrete Density

The hardened concrete density test is performed to assess the strength of the concrete. The cubes were removed from the curing tank, and any residual water was wiped from their surfaces using a damp cloth. The cubes were then measured, and their mass was recorded using a weighing scale. Subsequently, the specimen was placed on a stirrup and the scale was set to zero. The cube was then immersed in the water tank and their mass was measured again. This procedure was conducted in accordance with EN12390-7.

Fig 3-10: Hardened Concrete Density Test

Fig 3-11: Cube Specimen immersed in water

3.8.2 Ultrasonic Pulse Velocity

This method is conducted to determine the time of an ultrasonic pulse to travel through the concrete sample being tested. Prior to each test, it was ensured that the equipment was calibrated, and petroleum jelly was applied to the flat surfaces of the concrete specimens as a coupling medium. Two transducers were positioned on opposite faces of the specimen to allow for direct transmission and measured the time it took to pass through the specimen. This test was performed on the 28th day after casting, following the guidelines outlined in BS EN 12404-4 (2004). The pulse velocity was calculated using the equation below:

$$V = \frac{L}{T}$$

Where:

V = Pulse Velocity (km/s)

L = Path Length (mm)

T = Time taken by the pulse to transverse (µs)

Fig 3-12: Ultrasonic Pulse Velocity Test

3.8.3 Compressive Strength

Cube specimen measuring 100 x 100 x 100mm were tested on the 7th and 28th day, for each mix variable. The cubes were wiped, measured and weighed after being removed from the curing tank. They were then placed in the machine and a loading rate of 0.6 Mpa/s was applied until failure. The cubes were checked to ensure they failed in a satisfactory manner by removing any loose concrete with a hammer. This testing procedure followed the guidelines as specified in MSA EN 12390-3 (2009).

Fig 3-13: Cube Compression Test

3.8.4 Flexural Strength

Two concrete beams measuring 150 x 150 x 550mm were tested on the 28th day for each mix variable. Before testing, the beams samples were wiped from excess water and measured. A 5mm cut was made at mid-span across the bottom width of the beam, to insert a CMOD transducer. A three-point bending rig was used to evaluate the flexural tensile strength capacity of each specimen. This consists of two rollers supports and a top central roller, which applied a point load to the specimen. Additionally, two LVDTs connected to a data logger, were positioned on each side of the top roller to record the deflection. An initial load rate of 0.08mm per minute was applied, which was then increased to 0.21mm per minute after the first crack appeared within the sample. The test was carried out following EN 14651 (2005) Standard.

Fig 3-14: Flexural test setup

Fig 3-15: CMOD transducer at crack

3.8.5 Tensile Splitting Strength

Cylinder specimens, measuring 150mm in diameter and 300mm in height, were tested for each mix variable 28 days after casting. The cylinders were cleaned, measured, and centred in the testing machine. The specimens were then subjected to a compression load of 0.05 MPa/s until they reached failure. This test was performed following the guidelines outlined with BS EN 12390-6 (2009). The tensile splitting strength can be determined using the equation below:

$$F_{ct} = \frac{2\ x\ F}{\pi\ x\ D\ x\ L}$$

Where:

F_{ct} = Tensile Splitting Strength (MPa)

F = maximum Load (N)

L = length of specimen (mm)

D = diameter (mm)

Fig 3-16: Tensile Splitting Test, Control Mix

3.9 Shrinkage Properties

3.9.1 Environmental Chamber Test

3.9.1.1 Test Setup

To evaluate the plastic shrinkage of SCC and study the impact of Agave Sisalana fibres on this behaviour, various samples were subjected to controlled environmental conditions. These conditions were achieved by using an environmental chamber that followed procedures outlined in ASTM Standard C1579-06. The setup employed in this study is similar to that used in previous research conducted by Baldacchino (2014), Vella (2018) and Abdilla (2021).

The chamber setup is made up of thick chipboard panels, having dimensions of 1460mm in length, 840mm in width and 560mm in height. Transparent Perspex panels with a thickness of 5mm are installed on the top part of the chamber to allow for visual inspection of the sample while maintaining a sealed environment. A steel frame table is used to provide support to the concrete specimen and the container of water, which was placed on an electronic balance. To ensure a continuous airflow, aluminium sheets were used to direct the air generated by the industrial fan. This is done to create a consistent and controlled air flow within the chamber.

For this setup, three halogen heaters were used to maintain a consistent ambient temperature of 36 ± 3 °C within the chamber as specified in accordance to ASTM C 1579-06. Two heaters were positioned inside the chamber, while the third one was located outside, placed behind the industrial fan. The mould used for the specimen was made from 6mm welded metal sheets, with internal dimensions of 560mm length, 355mm width and 100mm depth. Three stress risers are present on the inside of the mould to control the development and locations of cracks within the specimen. To provide further constraint to the concrete specimen, 17mm bolts were fixed to the ends of the mould.

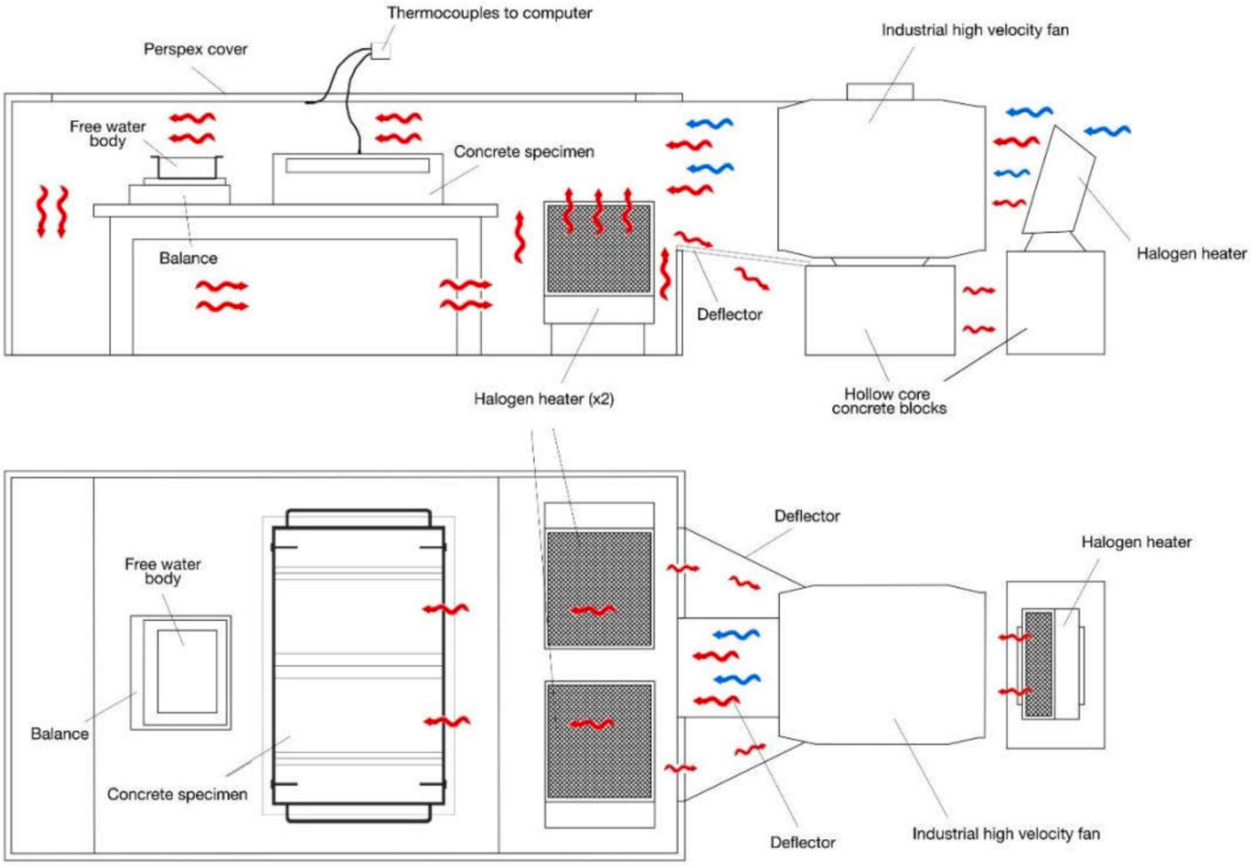

Fig 3-17: Environmental Chamber setup (Baldacchino, 2014)

3.9.1.2 Test Procedure

To create the desired environmental conditions, the heaters and industrial fan were turned on 30 minutes prior to each mix. The conditions include a wind speed greater than 4.7m/s, a relative humidity within the range of 30 ± 10% and a temperature of 36 ± 3^{o}C. These parameters were monitored by the use of two thermocouples which were connected to a data logger. One thermocouple was fixed to the inside of the Perspex cover above the specimen, while the other was inserted in the sample at depth of around 50mm. The placement of the

second thermocouple was carefully chosen, ensuring it was positioned 100mm away from the central riser to prevent any interference to the crack formation. The ambient and concrete temperature readings were recorded every 30 minutes during the initial 3 hours, and subsequently every 1 hour for the following 3 hours. Additionally, the time taken for the concrete specimen to develop its first crack was also noted. The evaporation rate was also measured by reading the weight of the water on the electronic balance at the same time intervals mentioned earlier. These specific conditions were crucial to achieve a rate of evaporation of approximately 1.0kg/m^2 per hour. This was determined by measuring the weight loss of the water container with a surface are of 0.1m^2.

Following a duration of six hours, the specimen was removed from the chamber and kept in in a controlled environment. The specimen was inspected 24 hours after casting, and the crack width was measured along 10 distinct positions. The measurements and photos were taken by a USB microscope and scaled in a CAD program to obtain an average for the crack width.

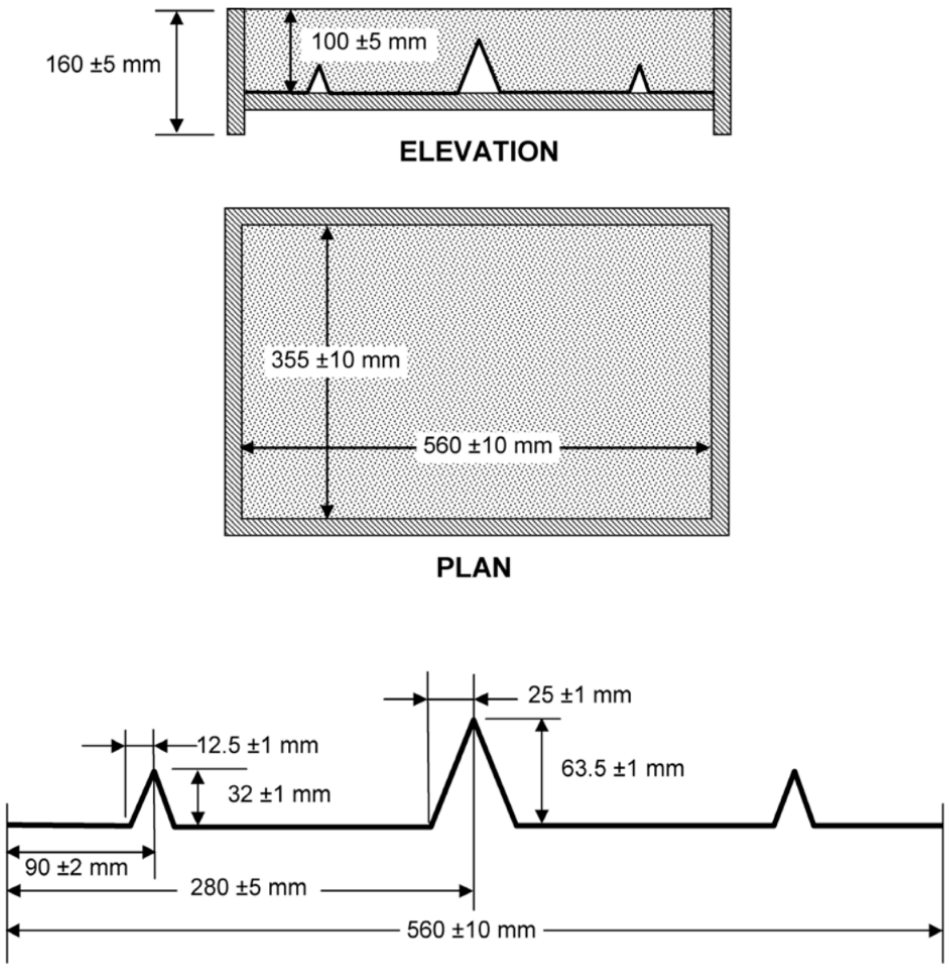

Fig 3-18: Mould and stress risers dimensions (ASTM C 1579-06)

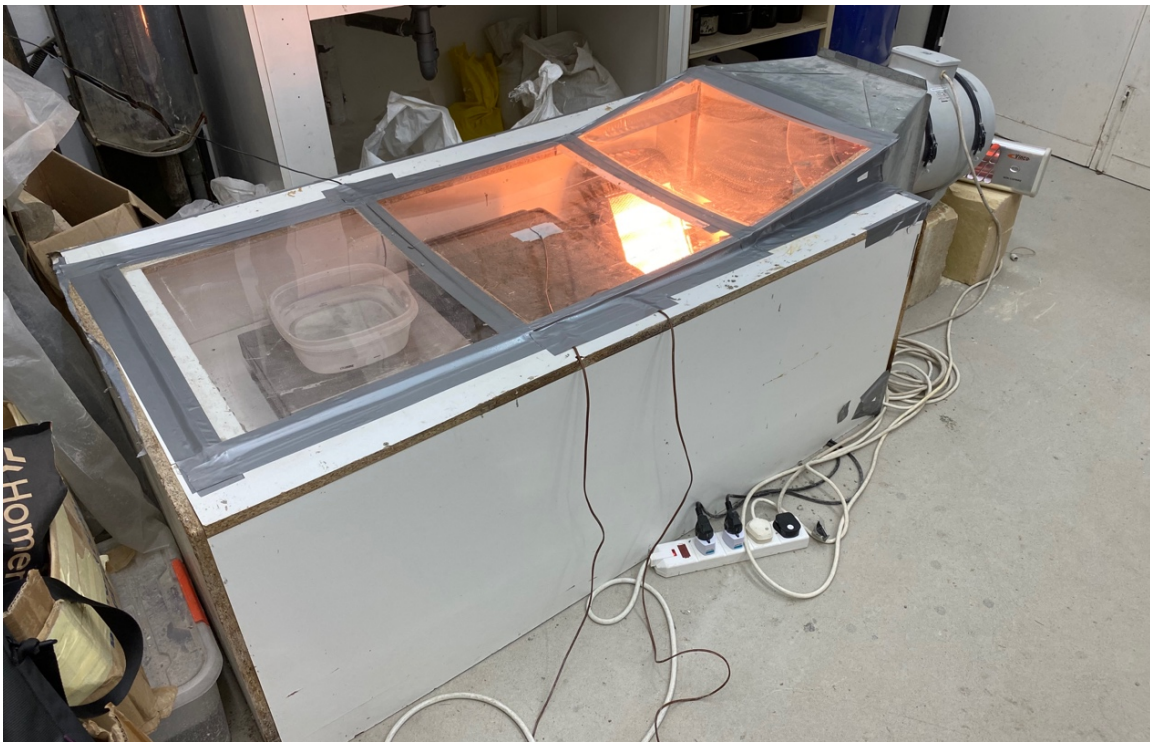

Fig 3-19: Environmental Chamber Test setup

3.9.2 Ring Test

The objective of conducting the Ring test was to identify the specific age at which shrinkage cracks occurred in the concrete specimen resulting from the development of tensile stresses under restrained shrinkage conditions. This setup consisted of an inner steel ring and an outer PVC ring, which were secured in place during casting using four washers, as depicted in Figure 3-20. To measure the strain experienced by the inner ring, two FLA-30-11-5L strain gauges, were fixed at mid-height of the inner steel ring, positioned across from each other.

Before the casting process, the ring was placed in a controlled environment with a temperature of 23 ± 2^{o}C. All surfaces were layered with an epoxy coating to minimise any frictional resistance. Once the concrete was poured, the washers were loosened, and the data logger started recording the strain at intervals of 10 minutes. After 24 hours, the outer PVC ring was removed, and daily visual inspections were conducted to detect any cracks in the specimen. Typically, a sudden decrease in the strain values of the steel ring indicate the occurrence of cracking in the specimen. This test was performed in compliance with ASTM C 1581-04 Standards.

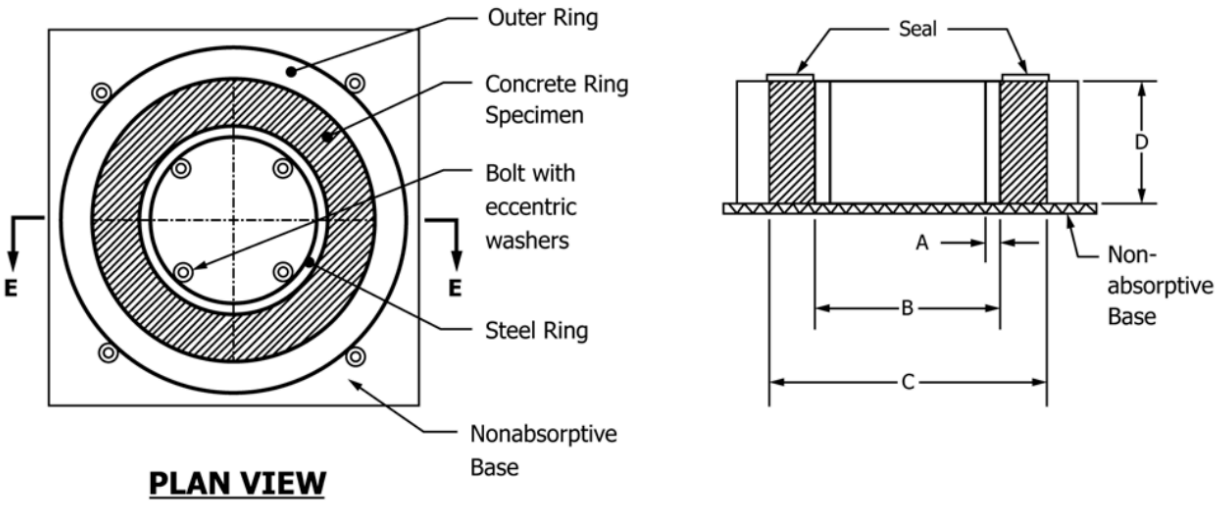

Figure Dimensions	SI Units	Inch-Pound Units
A	13 ± 1 mm	0.50 ± 0.05 in.
B	330 ± 3 mm	13.0 ± 0.12 in.
C	405 ± 3 mm	16.0 ± 0.12 in.
D	150 ± 6 mm	6.0 ± 0.25 in.

Fig 3-20: Ring Test Dimensions (ASTM C 1581-04)

Fig 3-21: Ring Test, Control Mix

3.10 Mortar Shrinkage Properties

3.10.1 Kraai Test

3.10.1.1 Test Setup

This test was performed to evaluate the possibility of fibre mortar mixes to develop cracks in thin slabs. The moulds used for this test has dimension of 610 x 914mm and a depth of 19mm. The mould was made from plywood sheet that were glued and nailed together. To prevent water absorption by the plywood and avoid mortar restraint during shrinkage, the inner surfaces were covered with polythene sheeting. Perimeter restraints were provided using chicken-wire steel mesh, which was placed at regular intervals. The mesh was bent at right angles so that it protruded into the mortar and was secured to the base with pins. This setup followed the recommendations outlined by Kraai (1985).

Fig 3-22: Kraai Panel

Fig 3-23: Steel Mesh around perimeter restraint

3.10.1.2 Test Procedure

The mortar mix used in this test followed the same design as the concrete mix, however the coarse aggregate and its corresponding water absorption were eliminated. After thorough mixing, the mortar was poured in the panel mould and levelled using a trowel to ensure a satisfactory finish. Subsequently, the panels were then placed in a controlled environment with a temperature of 22 ± 2°C and relative humidity of 50 ± 2%. The mortar was subjected to a wind speed of 6m/s generated from an industrial fan for the initial 5 hours, in order to stimulate crack formation. A handheld anemometer was used to measure the wind speed.

The mortar mix was assessed 24 hours after casting to evaluate their condition. For each specimen, the average crack length and width were measured. As indicated in Table 3-5, the crack widths were divided into four different groups, each given a particular weighted value. The weighted value was then multiplied by the crack length to get the 'average weighted value'. The sum of these 'average weighted values', referred to as the 'total weighted average value', provided a comparative measure of the specimen's crack potential. The specific details of the fibre mortar mixes used in these tests are outlined in Table 3-6.

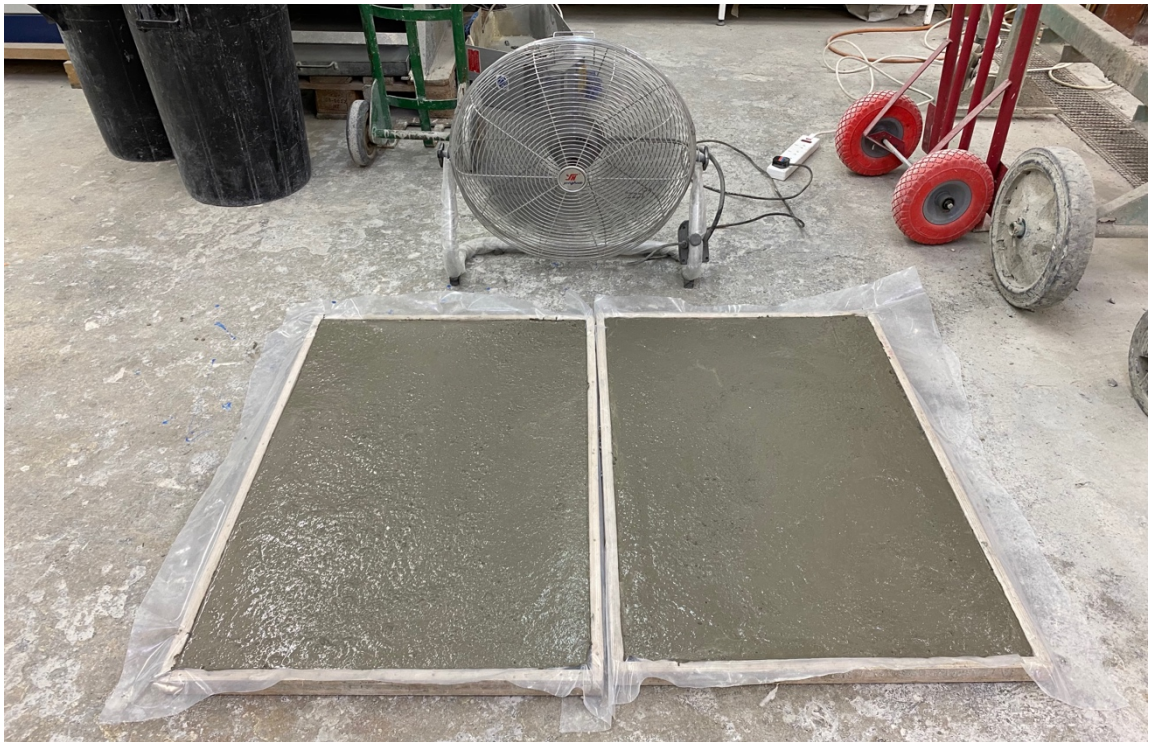

Fig 3-24: Kraai Test

Table 3-5: Crack Weighting

Crack Width	*Weighted Value*
Large (about 3mm)	3
Medium (about 2mm)	2
Small (about 1mm)	1
Hairline (about 0.5mm)	0.5

Table 3-6: Mortar Mix Variables for Kraai Test

Mix	*Fibre Length*	*Volume Fraction*	*Mix Code*
1	-	-	CMM
2	35mm	0.50%	F35-0.50
3	35mm	1%	F35-1

3.11 Treated and Untreated Fibres Properties

Chemical treatments were used in this study to examine the potential improvement of mechanical properties in fibre-cement composites such as the compressive and flexural strength. The tests were conducted on a mortar mix design as indicated in table 3-7 . Two distinct chemical treatments such as, Hydrogen Peroxide and Sodium Hydroxide, were applied to the fibres to compare their effects on the mortar properties.

Table 3-7: Mortar Mix Variables

Mix	***Fibre Length***	***Volume Fraction***	***Mix Code***
1	-	-	CMM
		Untreated Fibres	
2	15mm	0.50%	UF15-0.50
3	25mm	0.50%	UF25-0.50
4	35mm	0.50%	UF35-0.50
5	15mm	1%	UF15-1
6	25mm	1%	UF25-1
7	35mm	1%	UF35-1
		Treated Fibres with Hydrogen Peroxide	
8	15mm	0.50%	HPF15-0.50
9	25mm	0.50%	HPF25-0.50
10	35mm	0.50%	HPF35-0.50
11	15mm	1%	HPF15-1
12	25mm	1%	HPF25-1
13	35mm	1%	HPF35-1
		Treated Fibres with Sodium Hydroxide	
14	15mm	0.50%	SHF15-0.50
15	25mm	0.50%	SHF25-0.50
16	35mm	0.50%	SHF35-0.50
17	15mm	1%	SHF15-1
18	25mm	1%	SHF25-1
19	35mm	1%	SHF35-1

3.11.1 Treatment of Fibres

3.11.1.1 Hydrogen Peroxide

Similar methodologies were adopted in previous research carried out by Rayung et al. and Fonseca et al. for fibre treatments. Initially, the fibres were washed in hot water to eliminate any wax or impurities present. The fibres were then subjected to a 5% solution of Hydrogen Peroxide concentration for a duration of 90 minutes, followed by a thorough rinse with water. Finally, the fibres were dried in the sun for 2 days.

3.11.1.2 Sodium Hydroxide

The treatment of fibres with Sodium Hydroxide was based on a method outlined in a research carried out by Mehrez et al. This approach resembled a similar process which was employed for the Hydrogen Peroxide treatment. The fibres were treated in a 5% alkali solution of Sodium Hydroxide and left to soak for 12 hours. Following the treatment, the fibres were washed and then sun-dried for 2 days.

a) b) c)

Fig 3-25: a) Untreated Fibres, b) Treated Fibres with Hydrogen Peroxide, c) Treated fibres with Sodium Hydroxide

a)

b)

c)

Fig 3-26: Fibres under the microscope a) Untreated Fibres, b) Treated Fibres with Hydrogen Peroxide, c) Treated fibres with Sodium Hydroxide

3.11.2 Slump Flow Test

A 100mm diameter slump cone, conforming to the EFNARC Guidelines for Self-Compacting concrete was used, and placed centrally on a glass sheet that measures 500mm by 500mm. The cone was filled with concrete, and any excess mortar spilled onto the glass was carefully removed. The cone was then lifted vertically, and the average diameter was recorded by measuring two diameters perpendicular to each other.

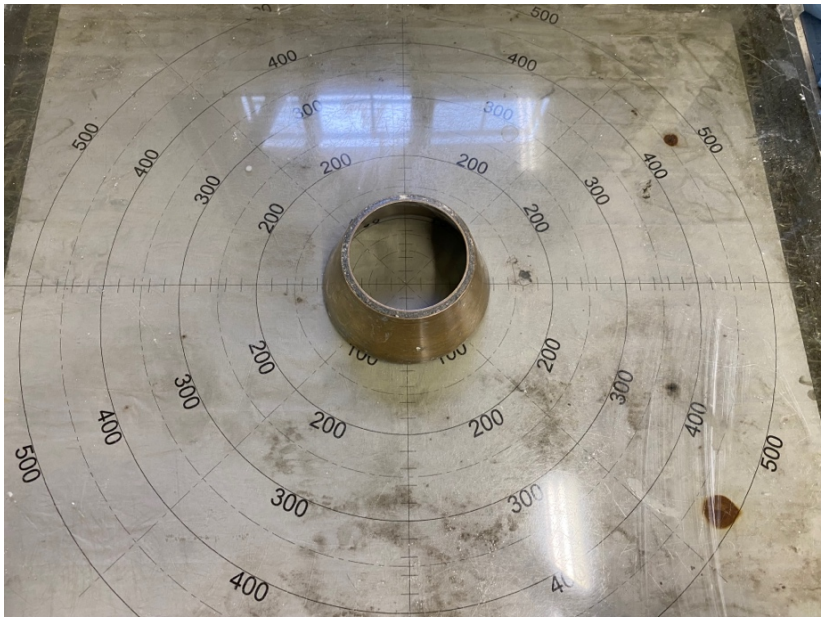

Fig 3-27: Slump Flow Test

3.11.3 Flexural Test

Two prisms measuring 160 x 40 x 40mm were tested on the 7th day for each mortar mix variable. Prior to testing, the prisms were taken out from the curing tank, wiped from any excess water, and measured using a Vernier Calliper. A load rate of 50 N/s was applied. The following equation was used to determine the flexural strength:

$$f_{cf} = \frac{3\ x\ F\ x\ I}{2\ x\ d_1\ x\ {d_2}^2}$$

Where:

f_{cf} = Flexural Strength (MPa)

F = maximum Load (N)

I = distance between rollers (mm)

d_1 and d_2 = dimensions of the cross-section (mm)

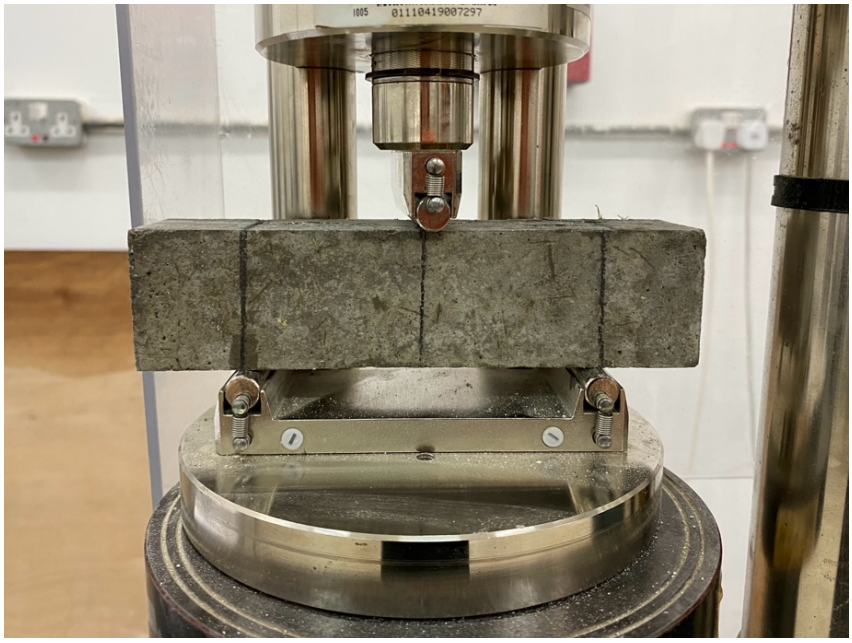

Fig 3-28: Flexural Strength Test

3.11.4 Compression Test

The compressive strength test was conducted on the 7th day following the casting process for each mix variable. The specimen measuring 40 x 40 x 40mm was placed in the compression machine with their rough surfaces facing outwards, and subjected to a loading rate of 2400 N/s. The cubes were carefully examined to ensure that they failed in a satisfactory manner, and any loose mortar on the specimen was removed.

Fig 3-29: Compressive Strength Test

CHAPTER 4

Results and Discussion

4.1 Overview

This chapter presents an analysis of the findings obtained from various tests conducted on the fresh properties, mechanical properties (including compressive, flexural and tensile strength), as well as shrinkage properties, using Agave fibres in both concrete and mortar.

4.2 Fresh Properties

4.2.1 Slump Flow (Flow Ability)

The slump flow test was conducted to assess the flowability of SCC in different concrete mixes. The results indicated a reduction in the diameter of the slump flow as the volume percentage of fibres increased. Figure 4-1 demonstrates the flowability performance decreased over time with an average of 4.96%. Notably, mix F15-1 exhibited poor performance, which can be attributed to the higher dosage of fibres, resulting in a stiffer mix. This can be depicted in Figure 4-2, which shows the impact of increasing fibre length and volume on the concrete mix. According to EFNARC SCC European Project Group's classification (May 2005), it can be observed that only the Control Mix was classified as SF2, while mixes containing fibres were classified as SF1. Furthermore, mix F15-1 and F35-0.5 did not conform to the guidelines provided by EFNARC.

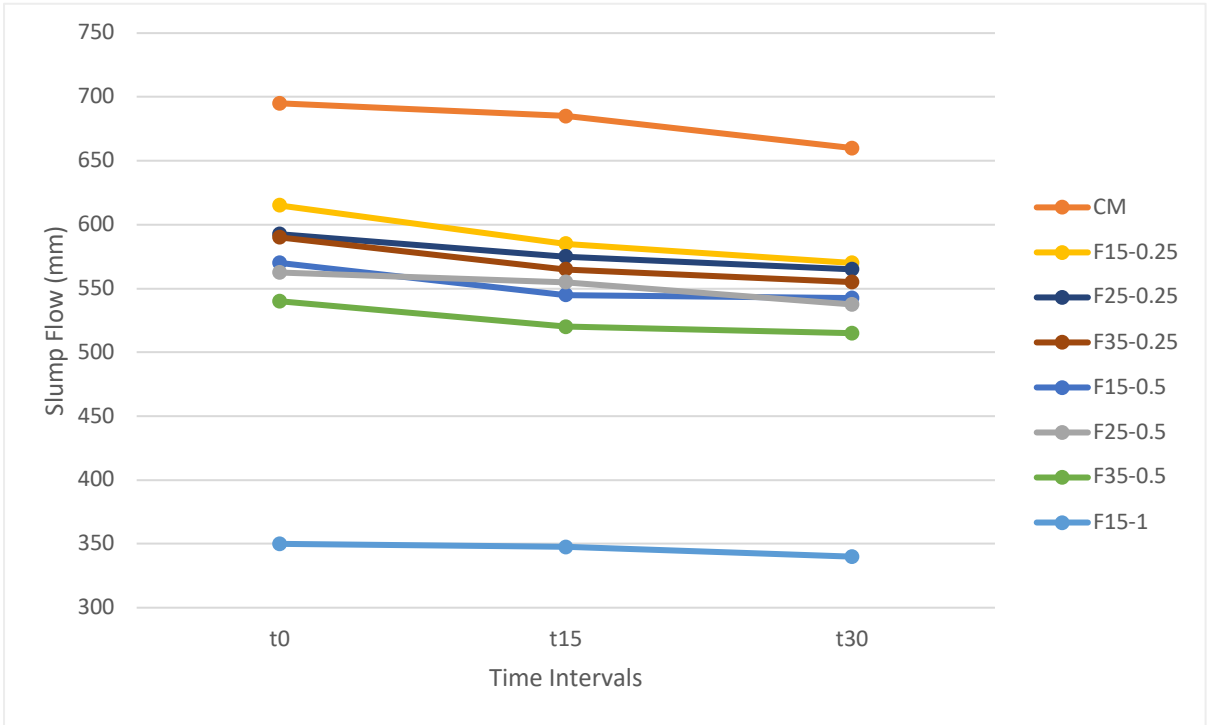

Fig 4-1: Slump flow at different time intervals

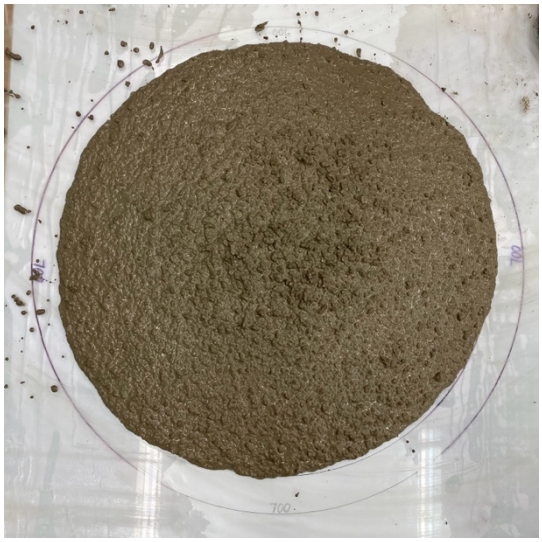

Control Mix

F15-0.25

F25-0.5

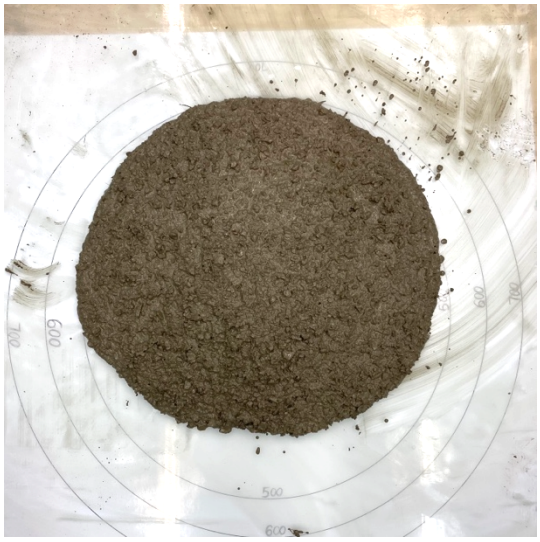

F35-0.25

F35-0.5

F15-1

Fig 4-2: Slump flow test results at t_0

Additionally, the SCC viscosity was assessed through the slump flow test by measuring the time taken for the concrete to achieve a slump flow diameter of 500mm (t_{500}). Figure 4-3 illustrates, that as the fibre dosage increased from the Control Mix to Mix F35-0.5, the time required to reach the desired diameter also increased. However, Mix F15-1 did not reach the 500mm, likely due to the high water absorption of the fibres, resulting in a stiffer mix.

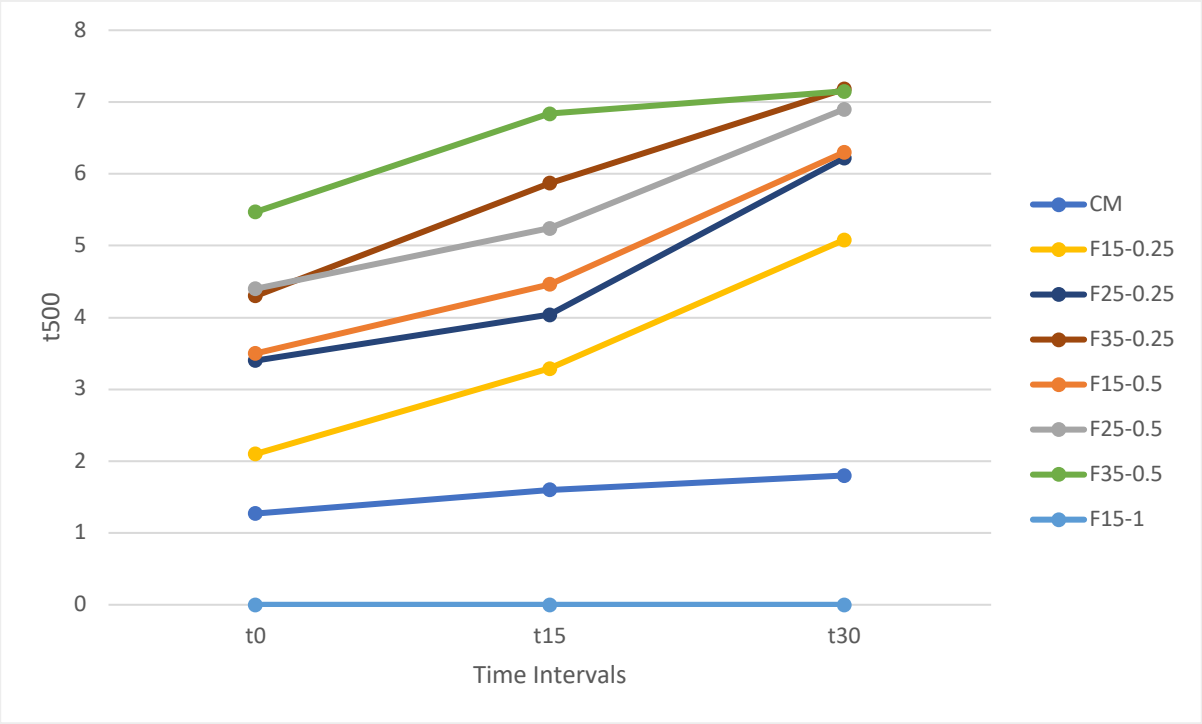

Fig 4-3: Slump flow (t_{500}) at different time intervals

4.2.2 V-Funnel (Viscosity)

The viscosity of the SCC was also assessed using the V-Funnel test. In Figure 4-4, it is shown that an increase in concrete viscosity was observed for all the mixes with an increase in fibre percentage. The flow time of the concrete through the V-Funnel varied from 5 to 43 seconds from the Control Mix to Mix F15-1.

Furthermore, as the results were compared to the EFNARC classification, it can be concluded that the inclusion of Agave fibres resulted in a decrease in the classifications of the SCC mixes. In relation to the time intervals, it was noted that as time progressed, there was a gradual increase in the viscosity of the mixes.

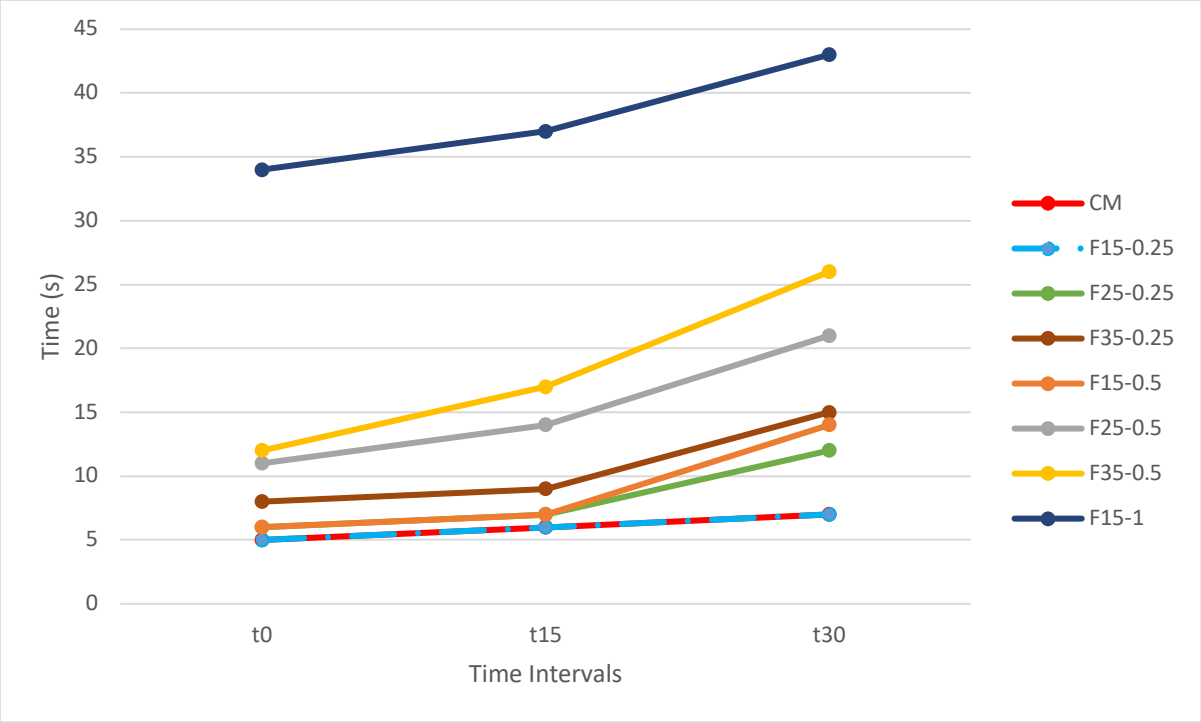

Fig 4-4: V-Funnel at different time intervals

4.2.3 L-Box (Passing Ability)

The purpose of the L-Box test was to evaluate the passing ability of a self-compacting mix. Figure 4-6 illustrates that the inclusion of fibres had a detrimental impact on the passing ability of SCC. It is evident that as the fibre length and dosage are increased, the mixes experience a decrease in their passing ability. Additionally, a gradual decline in passing ability was observed for all mixes over time. This was particularly noticeable in mixes F25-0.5 and F35-0.5 where readings were only obtained up to t_{15} due to clogging. Similarly, mix F15-1 also did not yield any readings due to immediate clogging.

Fig 4-5: Clogging of L-Box at t_0 ,Mix F15-1

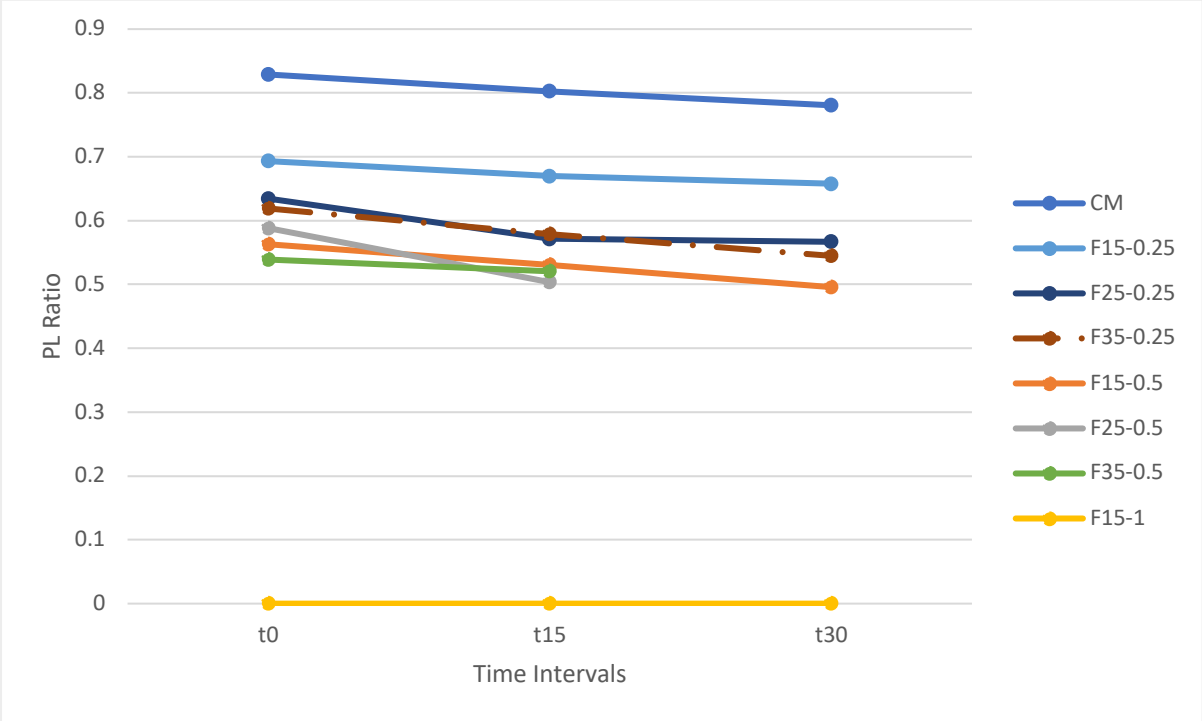

Fig 4-6: L-Box (PL Ratio) at different time intervals

4.2.4 Rheometer (Rheological Properties)

The rheometer test was conducted using an ICAR Rheometer, to evaluate the fresh characteristics of concrete and its thixotropic behaviour. The test specifically examined properties such as static yield stress and plastic viscosity. The results from the stress growth test, as illustrated in Figure 4-7, indicate an increase in static yield stress with an increase in fibre length, while keeping the fibre dosage constant. Similarly, as shown in Figure 4-8, as the fibre dosage was increased from 0.25% to 0.50%, the static yield stress demonstrated the same behaviour with an increase in fibre length. Furthermore, when comparing mixes with the same fibre length but with an increased fibre percentage, the static yield stress also increased. Therefore, this indicates that a greater shear stress is necessary to initiate the flow of concrete from rest when the fibre dosage or length is increased.

With regards to the flow curve test, from the results shown in Figure 4-9, the graph demonstrates that a greater shear stress is obtained with an increase in fibre length and a constant fibre dosage. The plastic viscosity, represented by the gradients of the lines in Figure 4-9, shows variations among the mixes. When compared to the other three mixes, the Control Mix showed a higher viscosity. Similarly, in Figure 4-10, the Control Mix also exhibited a higher viscosity than the other mixes.

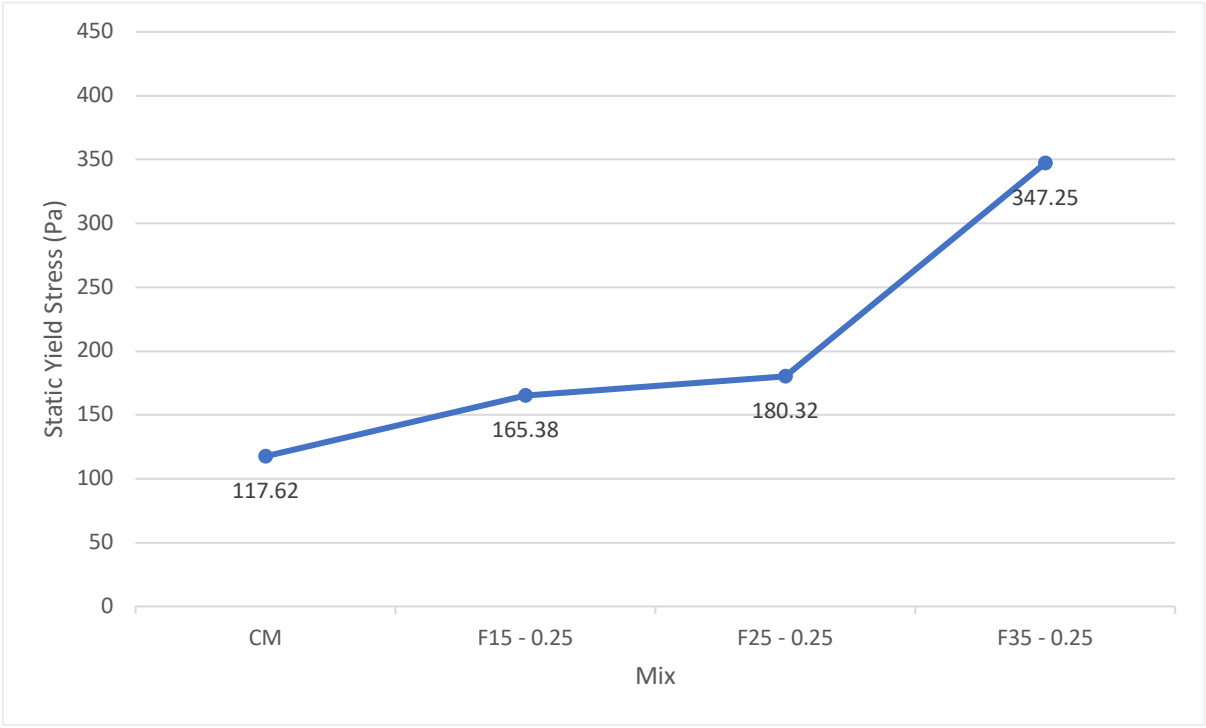

Fig 4-7: Static Yield stress for mixes with 0.25% fibre dosage

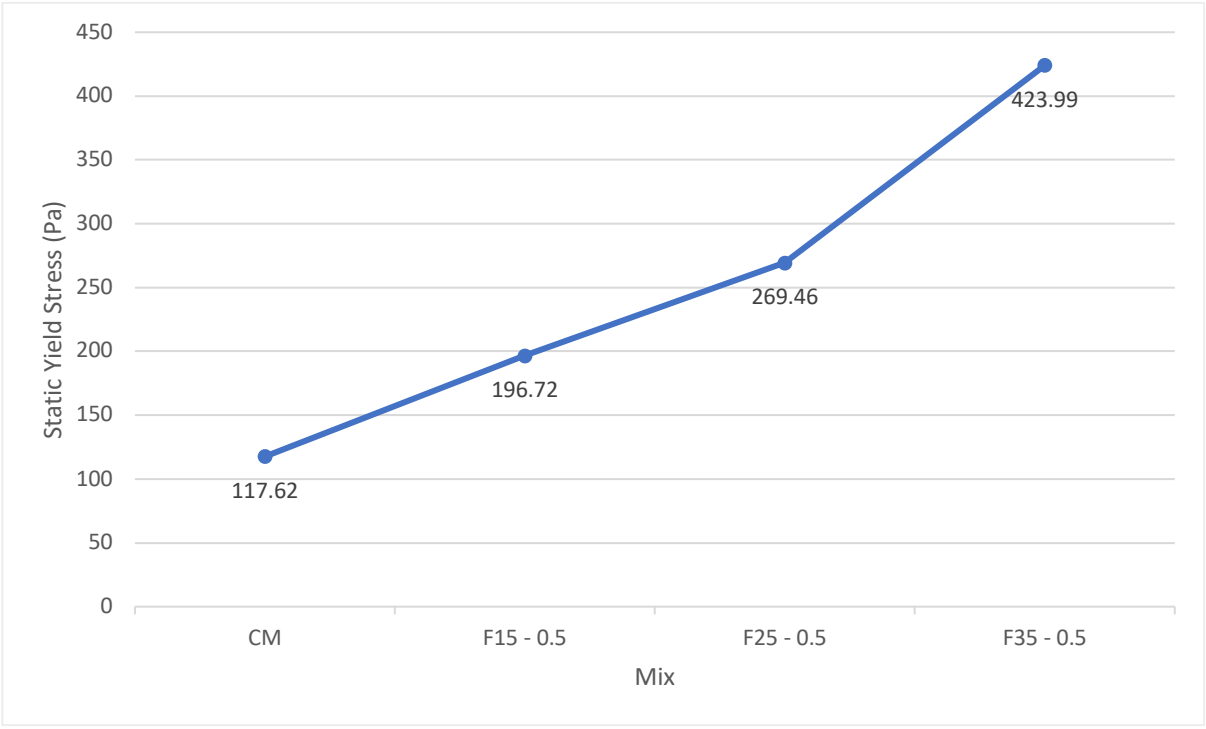

Fig 4-8: Static Yield stress for mixes with 0.50% fibre dosage

Furthermore, when comparing mixes with the same fibre length but with an increased fibre percentage, a greater shear stress is obtained. The results obtained from the Rheometer test can be found in Appendix B.

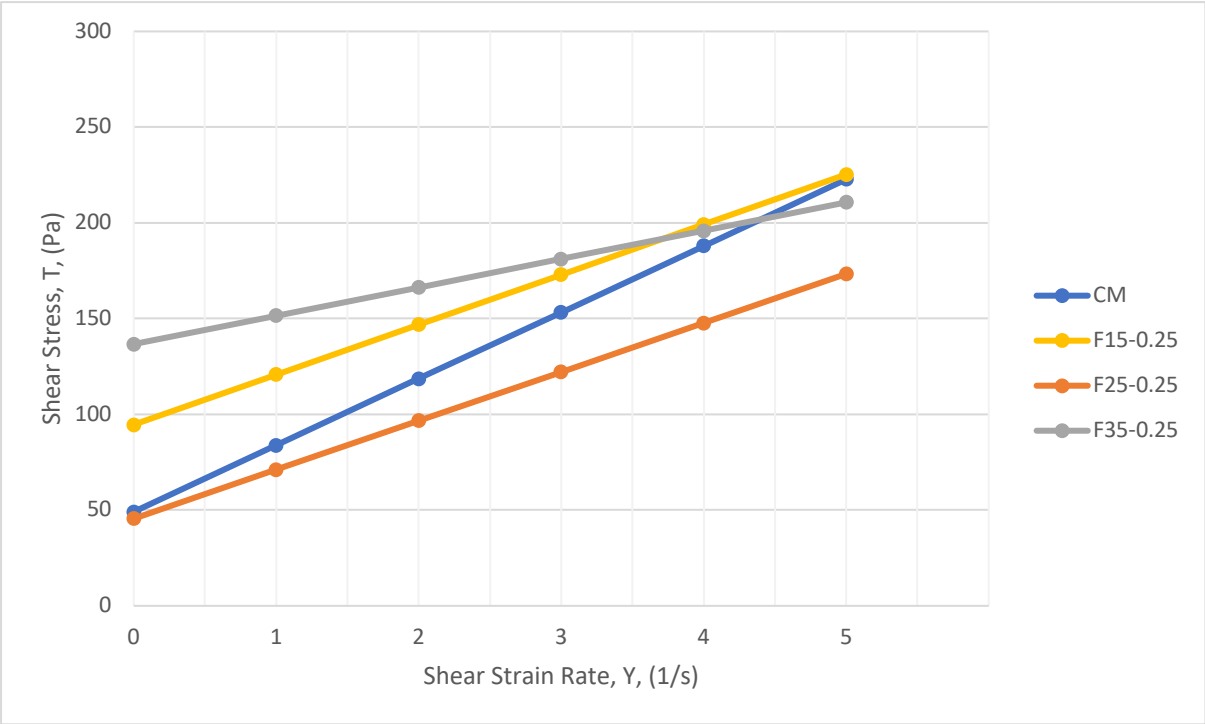

Fig 4-9: Shear stress vs shear strain rate for mixes with 0.25% fibre dosage

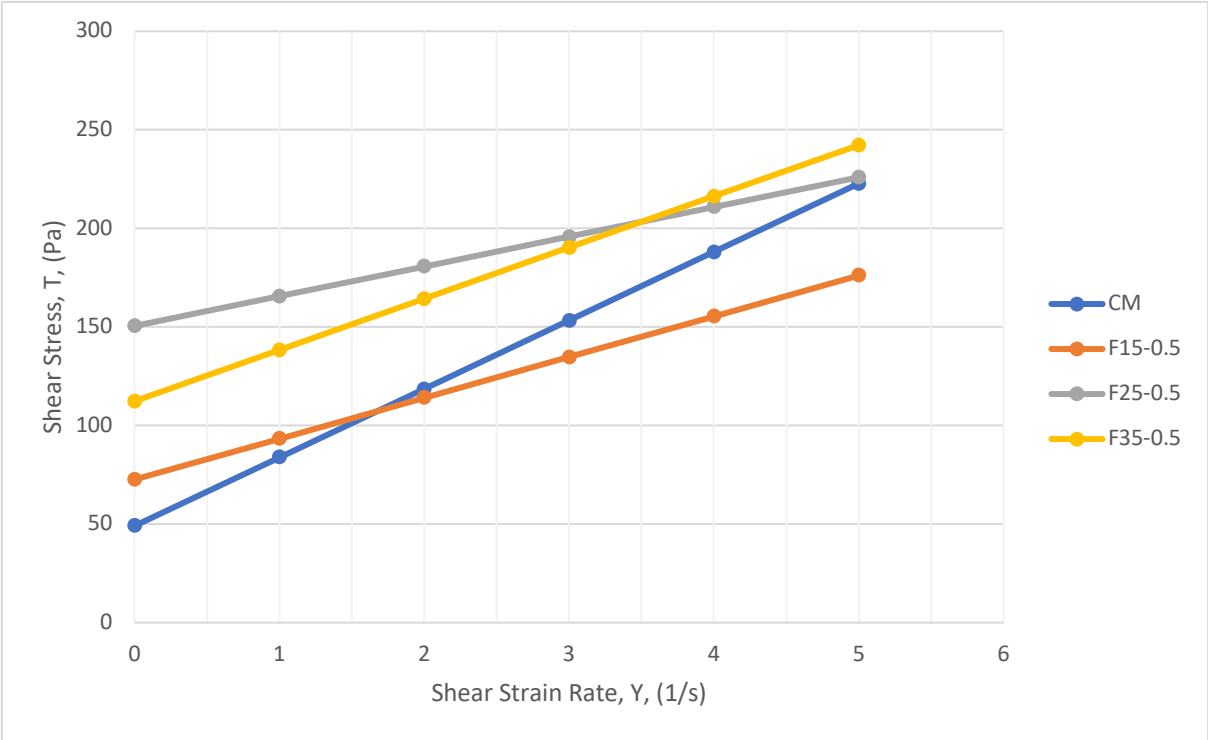

Fig 4-10: Shear stress vs shear strain rate for mixes with 0.50% fibre dosage

Comparison with literature

When comparing the obtained results with previous research findings, it was found that similar trends were observed. Sugathan (2017) conducted a study on SCC using sisal fibres and found that the flowability of concrete decreased as the percentage or the length of sisal fibres increased. Similar decrease in workability was also reported in another study done by Savastano et al. (1999) when fibres were added to normal concrete. Moreover, the findings related to the viscosity and passing ability are similar with the results obtained from studies conducted by Sugathan (2017) and Solai Mathi et al. (2021). From both studies it was concluded that an increase in fibre dosage led to a higher viscosity and a decrease in flowing ability. From further studies conducted by Abdilla (2021) and Vella (2018), they both reported a reduction in the fresh properties results with the addition of fibres.

A similar investigation on the rheological performance of SCC was also conducted by Abdilla (2021). The findings of this research indicated that as the fibre content was increased, the static yield stress also increased. In the flow curve test, Abdilla (2021) obtained a higher viscosity for the control mix when compared to the fibre mixes. Thus, these outcomes align with the results obtained in the present study.

4.3 Mechanical Properties

4.3.1 Hardened Concrete Density

The addition of Agave fibres in SCC resulted in changes to the density of the hardened concrete. As illustrated in Figure 4-11, the density of the concrete decreased as different lengths and fibre proportions are incorporated to the mix. The average reduction in density from the Control mix to mix F15-1 was of 5.70%.

The reduction in density can be attributed to the presence of air voids that are formed due to the entanglement of fibres within the concrete mix. The longer fibres tend to create more entanglements, resulting in a higher volume of air voids leading to a decrease in density. Furthermore, the increase of the volume percentage of fibres may also affect the packing density of concrete, further contributing to the reduction in density.

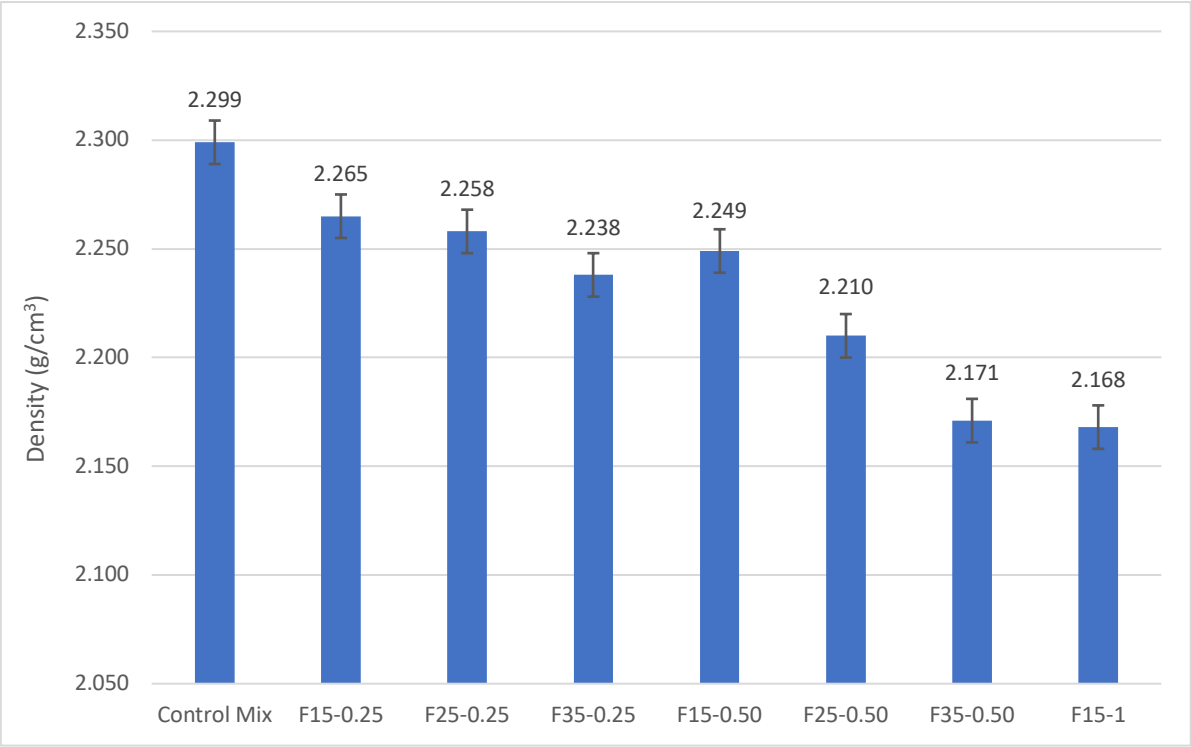

Fig 4-11: Hardened concrete density for different mix proportions

4.3.2 Ultrasonic Pulse Velocity

The Ultrasonic Pulse Velocity (UPV) test was performed to assess the homogeneity of the hardened concrete. Figure 4-12 shows the UPV values obtained for the different mix variables after 28 days. The graph illustrates a decrease of 7.77% in the pulse velocity from the Control Mix to Mix F15-1. This indicates that the addition of Agave fibres in the mix resulted in a decrease in both concrete density and homogeneity.

The results depicted in Figure 4-12 can be compared to the observations presented in Figure 4-11, which also demonstrates a similar trend in density properties when fibres are incorporated. This decrease in pulse velocity can be attributed to similar factors discussed in section 4.3.1. Therefore, the presence of fibres and air voids can interfere with the transmission of the ultrasonic waves, leading to a decrease in UPV. Detailed outcomes of this test can be found in Appendix C.

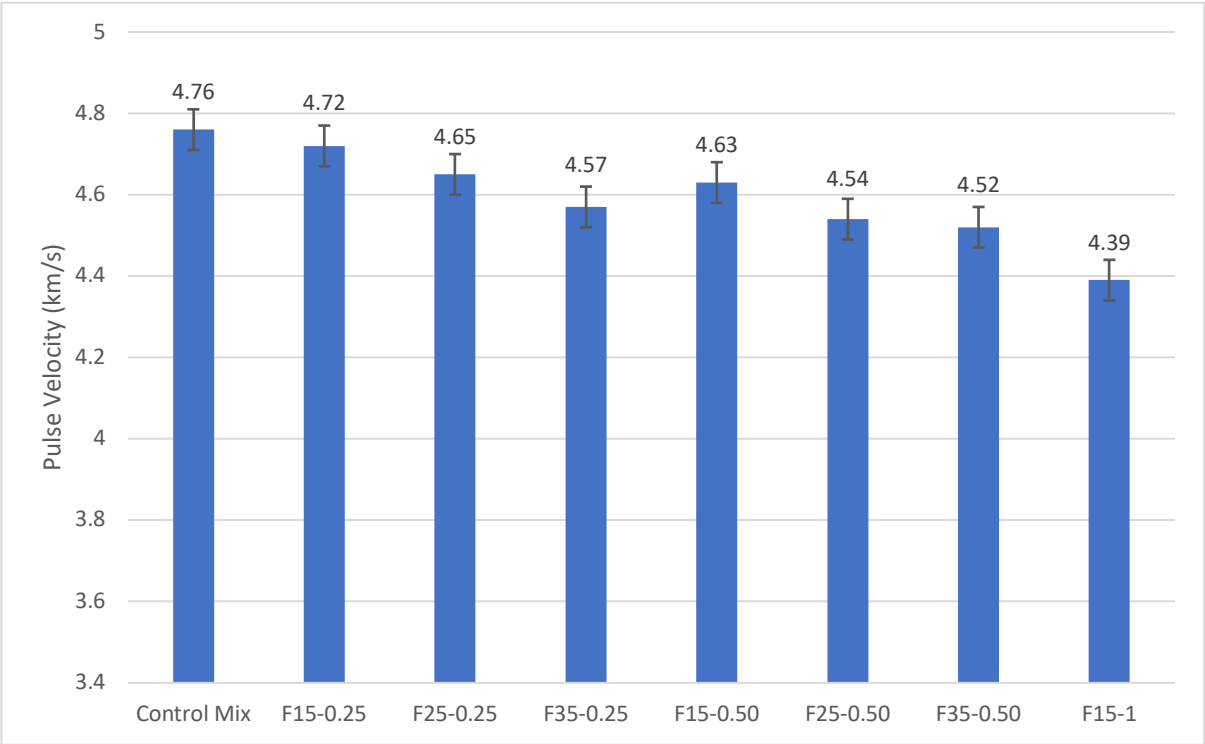

Fig 4-12: UPV for different mix proportions

Comparison with literature

Limited data is available regarding the hardened concrete density on SCC containing Agave Sisalana fibres. From a study conducted by Okeola et al. (2018), it is evident that the inclusion of fibres reduced the concrete's density. Similarly, Abdilla (2021) also obtained a decrease in density when using Steel Waste Tyre Fibres (SWTF).

As for the investigation of the Ultrasonic Pulse Velocity (UPV), Solai Mathi et al. (2021) observed a decrease in pulse velocity when sisal fibres were used in the concrete mix. This decrease in pulse velocity was noted until a volume percentage of 1%. Additionally, other studies on UPV with different fibres were examined. Abdilla (2021) reported a decrease in pulse velocity when SWTF were used in the concrete mix. This observation is consistent with the findings of Gebretsadik (2013), who also observed a decrease in pulse velocity as the steel fibre content increase. This decrease in both the density and pulse velocity can be attributed to the formation of voids which are generated between the concrete and the fibres.

4.3.3 Compressive Strength

The purpose of this test was conducted to examine the influence of Agave Sisalana fibres on the compressive strength of hardened concrete. The results are illustrated in Figure 4-13, indicating the strength values obtained at both 7 and 28 days. The findings demonstrate a notable reduction in strength as the volume percentage of Agave fibres is increased.

As the results are compared, it is evident that the Control Mix exhibited the highest mean compressive strength at 28 days, resulting in 59.68 Mpa. In contrast Mix F15-1, recorded a compressive strength of 45.88 Mpa, indicating a decrease of 23.12%. This noticeable decrease in strength can be attributed to loss of workability in the SCC caused by the addition of Agave fibres, leading to the formation of air voids within the concrete mix. Similar results were obtained for the 7th day. All test results can be found in Appendix C.

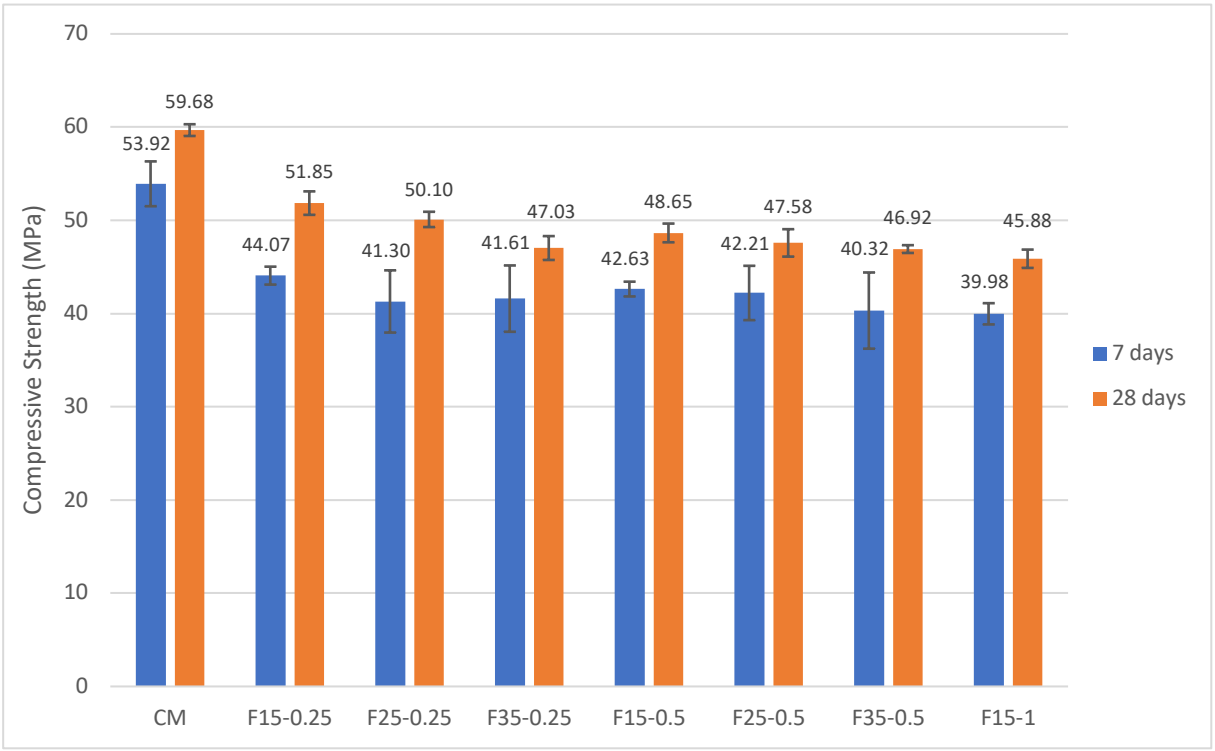

Fig 4-13: Compressive Strength for different mix proportions

Fig 4-14: Cube after failure for 15mm fibres

Fig 4-15: Cube after failure for 35mm fibres

Comparison with literature

Okeola et al. (2018) conducted similar research to investigate the mechanical properties of concrete using sisal fibres. Their findings are consistent with the results obtained in this study, as they observed a decrease in compressive strength with an increase in fibre percentage, both for the 7^{th} and 28^{th} days. This reduction was more evident when the volume fraction of fibres reached 2% and 3%, resulting in a decrease of 25% to 30% in the compressive strength.

However, these findings contradict a study done by Sugathan (2017), which reported an increase in compressive strength of SCC with fibre percentages of up to 1.5%. It is important to note that sisal fibres have a natural tendency to absorb moisture, which can affect the water-cement ratio and the overall hydration process of the concrete mix. Therefore, this increase in compressive strength may be attributed to the consideration of water absorption by the sisal fibres in the concrete mix, mitigating the potential reduction on the compressive strength. These contrasting findings highlight the importance of the water absorption characteristics of the sisal fibres.

4.3.4 Flexural Strength

This test was done to determine the relationship between the applied load at mid-span and the corresponding deflection for each mix variable. The samples were subjected to a three-point bending test after 28 days of casting. The deflection was measured using two LVDT's, while a load cell was used to record the applied load. The results obtained from the load-deflection relationship and the peak loads achieved are presented in Figure 4-16 and Figure 4-18, respectively.

In the case of the tested specimens, a brittle failure mode was observed across all mix variations. Figure 4-16 illustrates that once the peak load was reached, the specimens failed abruptly. Upon failure, further examinations of the cross-sections of the beams were done. It was noted that the fibres at both ends of the cross-section were interconnected, suggesting that the fibres experienced yielding rather than pull out. This is illustrated in Figure 4-17.

Furthermore, the load-deflection curve displayed varying gradients, indicating that the Agave fibres had higher resistance to deflection and increased stiffness when compared to the Control Mix. Notably, the deflection achieved for a specific load showed a direct correlation with the fibre dosage or length used in the mix, except for Mix F15-1.

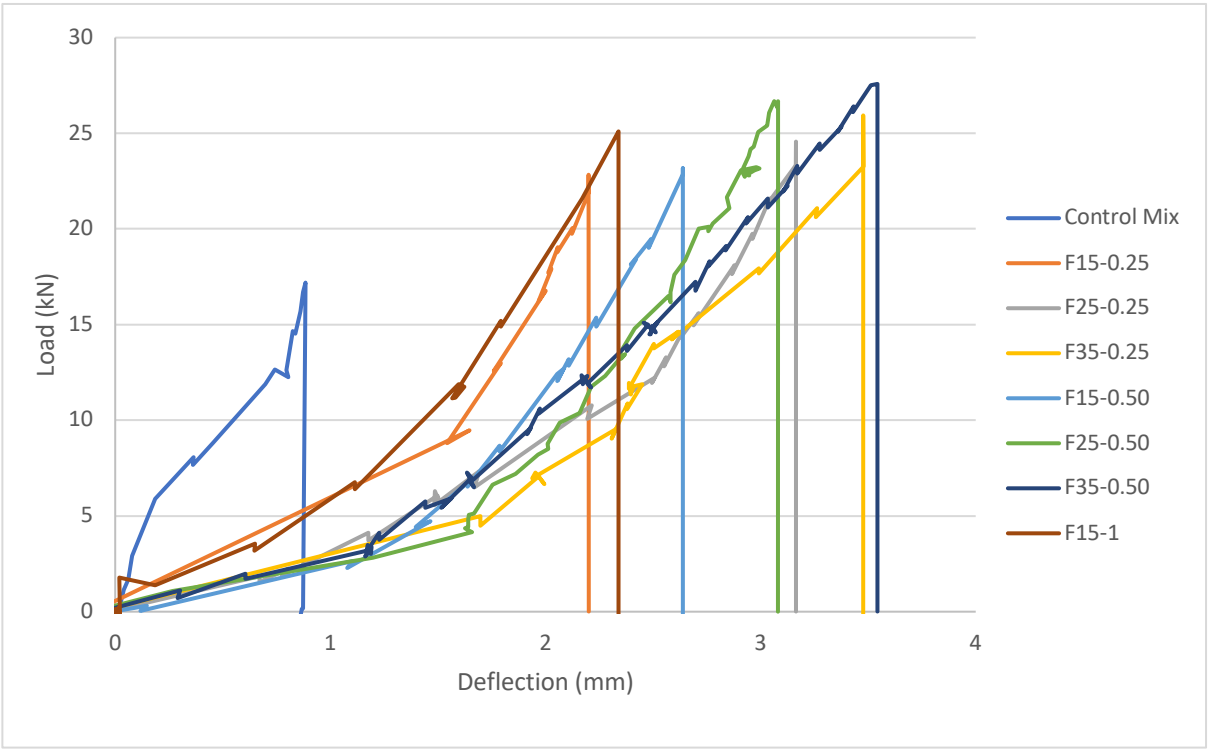

Fig 4-16: Load against mid-span deflection

Fig 4-17: Surface cross-section containing fibres after failure

Figure 4-16 provides an overview of the peak loads achieved for each mix. It was observed that an increase in the peak load was recorded as the fibre volume percentage or length in the concrete was also increased. The highest peak load of 27.58 kN was obtained for Mix F35-0.50, representing an increase of 37.65% when compared to the Control Mix.

However, it is worth noting that Mix F15-1 showed a decrease of 9.03% in the peak load. One possible reason for this reduction could be related to the aspect ratio of fibres used, as Mix F15-1 employed the shortest fibres with a length of 15mm. Furthermore, when comparing Mix F15-1 with other mixes that had the same fibre length but a lower dosage, it is interesting to note that Mix F15-1 still exhibited the highest peak load among those mixes.

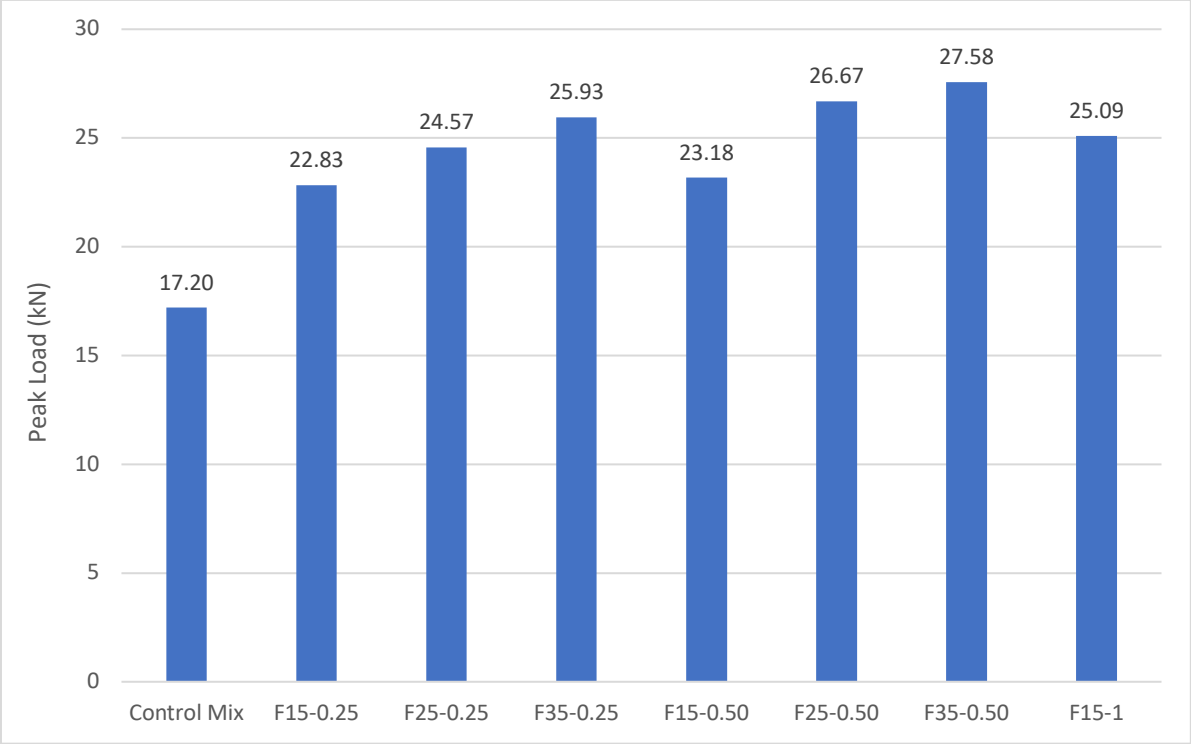

Fig 4-18: Flexural peak loads for different mix proportions

Flexural Toughness

In addition to the previously discussed factors, another important characteristic to consider is the toughness factor. This factor was assessed for each mix according to the JSCE-SF4 standard. The flexural toughness factor was determined using the following formula:

$$\sigma b = \frac{Tb}{\delta tb} \; x \; \frac{l}{bh^2}$$

Where:

σb = Flexural toughness factor (N/mm^2)

Tb = Flexural toughness – area under load-deflection graph (Nmm)

δtb = Deflection of L/150 of span (mm)

l = span between rollers (mm)

b = breadth of sample (mm)

h = height of sample (mm)

Figure 4-19 illustrates the results obtained for each mix, highlighting the influence of Agave fibres on the flexural toughness. The Control Mix displayed the lowest toughness factor of 0.27 N/mm^2. An increase of 85.06% was observed from the Control Mix to Mix F35-0.5, indicating a better toughness with the Agave fibres. All results are tabulated in Appendix C.

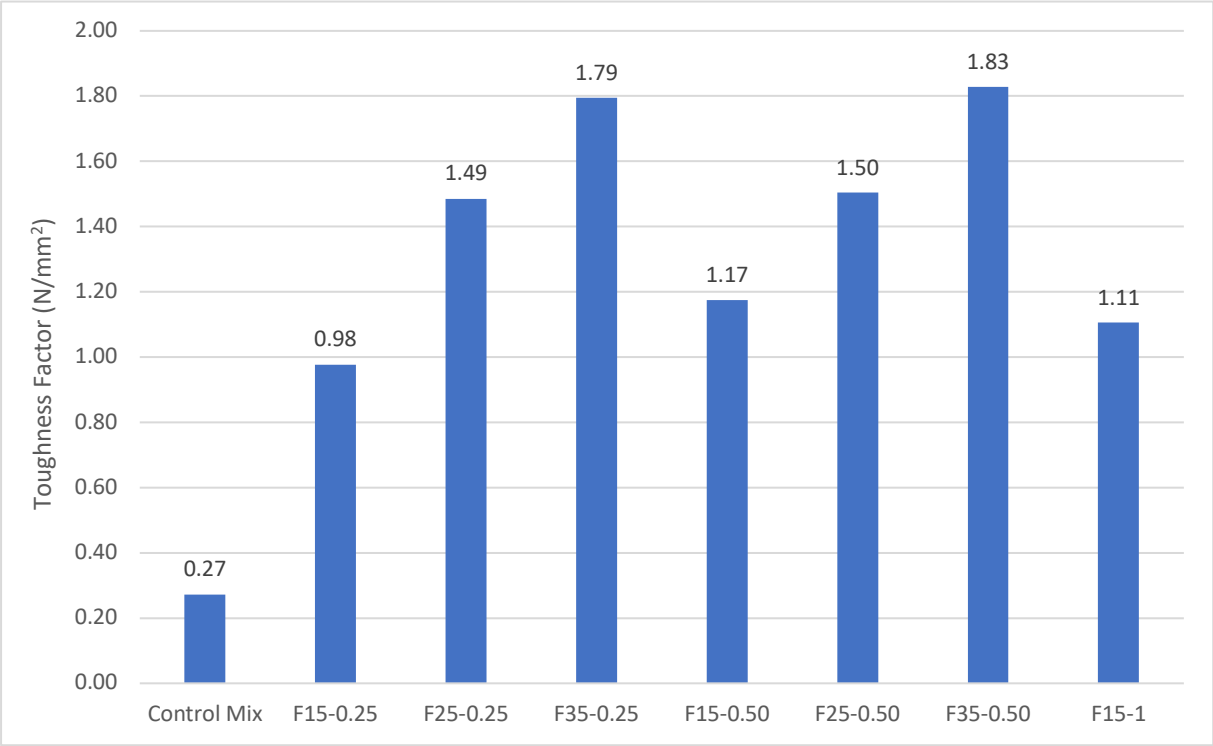

Fig 4-19: Toughness factor for different mix proportions

Comparison with literature

The findings from this study are consistent with the findings of previous research conducted by Fadhil and Yaseen (2015), Solai Mathi et al. (2021) and Vella (2018). Fadhil and Yaseen (2015) investigated the inclusion of sisal fibres in normal concrete. The concrete exhibited an increase in flexural strength as the fibre percentage increases up to 1.2%. From this study, the strength increased by 43.01% from the plain concrete, supporting the results obtained in this study.

Similarly, Solai Mathi et al. (2021) conducted research on SCC incorporating sisal fibres. From the results, it was also observed that an increase in concrete mixes with 0.25%, 0.75% and 1% sisal fibres was obtained when compared to the Control Mix. However, a decrease in flexural strength was noted for 1.25% and 1.5%, which can be attributed to fibre curling or bundling during the mixing process.

Furthermore, Vella (2018) investigated the effects of SWTF in SCC and also reported an increase in the peak load and flexural toughness with the addition of SWTF. However, the samples incorporating fibres experienced a ductile behaviour after failure. Since Agave fibres are typically stiff, they have limited ability to deform, resulting in an abrupt failure. On the other hand, steel fibres are generally more flexible when compared to agave fibres. This means that when a concrete specimen is subjected to loading, the steel fibres can bridge cracks more effectively and increase the overall ductility of the concrete.

4.3.5 Tensile Splitting Strength

This test was conducted to evaluate the tensile splitting strength of the concrete specimen after 28 days of casting. Figure 4-20 presents the recorded data, showing the performance of different mixes with varying length and percentages. Amongst the tested mixes, Mix F35-0.50 demonstrated the highest tensile strength at 4.47 MPa. Therefore, an increase of 20.43% was recorded when compared to the Control Mix. However, as the fibre percentage increased, a slight reduction of 0.38% tensile strength was observed for Mix F15-1. Despite this decrease, it is important to note that the overall tensile strength remained relatively high. This reduction in strength may be attributed to factors such as fibre length, which can influence the overall performance of the concrete.

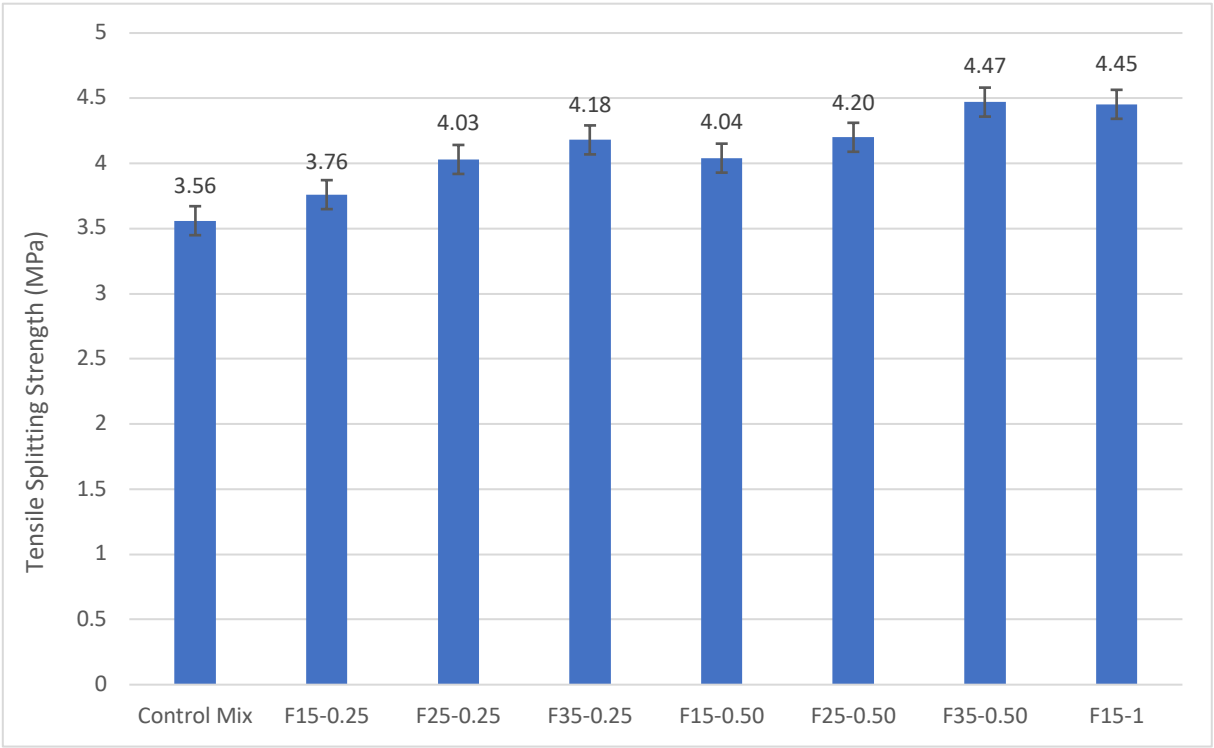

Fig 4-20: Tensile Splitting Strength for different Mix proportions

Moreover, during the testing procedure, the Control Mix experienced a brittle failure, whereas all the other samples containing the Agave fibres displayed a ductile mode of failure. This observation suggests that the addition of fibres had an impact on the behaviour of concrete as they provided a bridging effect, effectively distributing the applied load. This is illustrated further in Figure 4-21 and Figure 4-22. All the results are provided in Appendix C.

Fig 4-21: Tensile Splitting Strength test for Control Mix

Fig 4-22: Tensile Splitting Strength test for Mix F15-1

Comparison with literature

The obtained results for the Tensile Splitting test in this study are consistent with those reported in previous research findings. Fadhil & Yaseen (2015) conducted a study on normal concrete incorporating sisal fibres and observed an increase in tensile splitting strength. The highest strength was achieved at a fibre percentage of 1.2%, while a decrease in strength was observed at 1.8%. Remarkably, the current study recorded a significant increase of 32.71% in tensile splitting strength.

Furthermore, Sugathan (2017) performed a similar investigation on SCC with sisal fibres and also reported an increase in splitting tensile strength. The strength increased for a fibre percentage of 1.5% but decreased at 2% fibre volume. In this study, an increase of 13.54% was noted. Thus, these results from this research are very consistent to these findings. All results of these tests are tabulated in Appendix C.

4.4 Shrinkage Properties

4.4.1 Environmental Chamber

The plastic shrinkage behaviour of concrete can be influenced by various factors such as the relative humidity, wind speed, concrete and ambient temperature and the evaporation rate. These factors were carefully monitored to ensure that the concrete specimens were subjected to the specified environmental conditions as defined in ASTM C 1579-06 (2006).

In Figure 4-23 an average evaporation rate for all mixes is illustrated. This was measured by monitoring the mass of water in the container placed alongside the specimen inside the chamber. This method provides a comparable estimation of water loss to that of the concrete specimen. However, the concrete cracking occurred before reaching the evaporation limit. Thus, Figure 4-24 depicts the increase in concrete temperature during the first six hours. The initial recorded temperatures ranged from 23.18°C to 24.05°C, while the final temperatures ranged between 31.55 °C to 33.74 °C. Furthermore, it was noted that higher temperatures were recorded as the fibre dosage is increased.

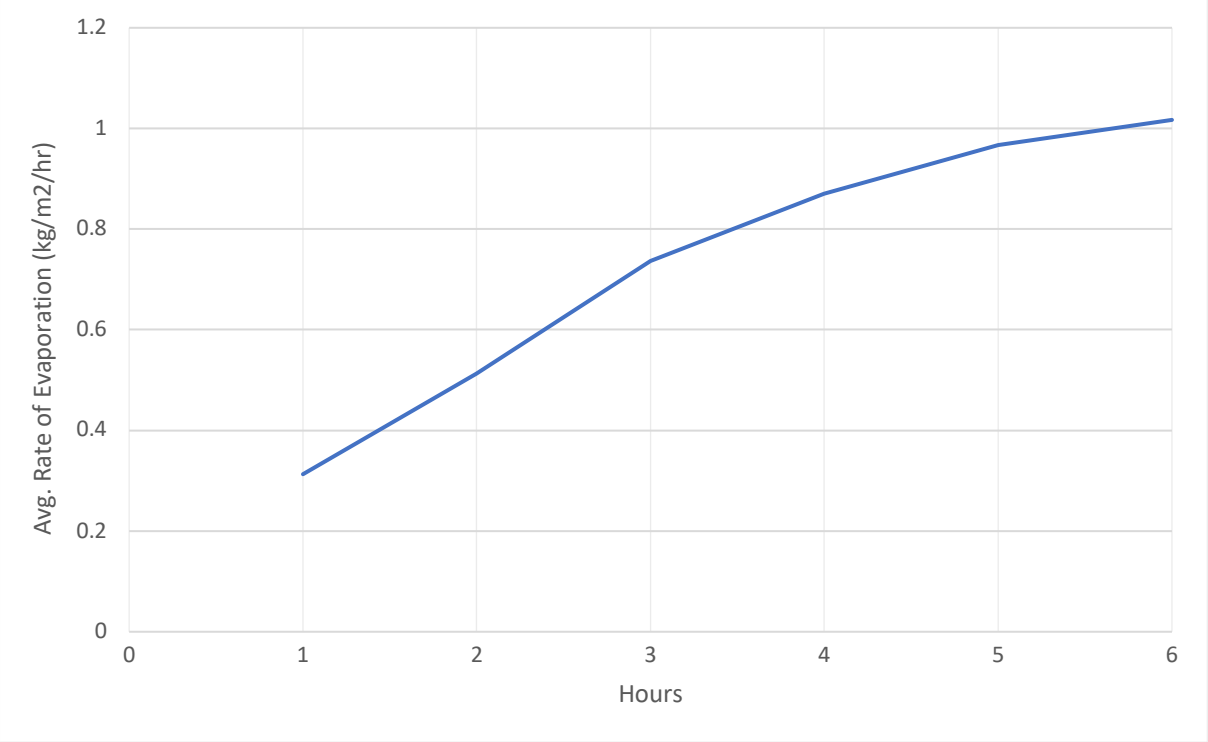

Fig 4-23: Average rate of evaporation

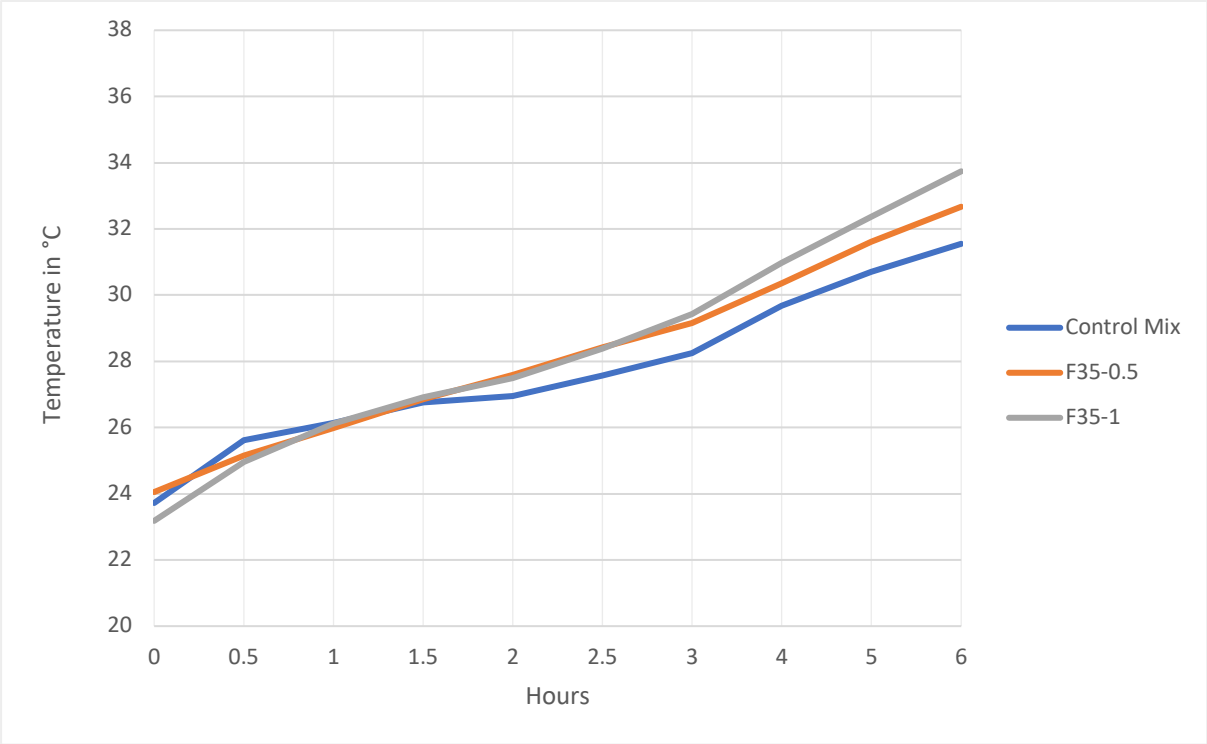

Fig 4-24: Concrete temperature for different mixes

The time at which cracks began to develop in the concrete specimens were recorded at every 15 minutes. As shown in Figure 4-25, the Control Mix exhibited the first crack at 2.25 hours, while mixes F35-0.5 and F35-1 experienced cracking at a later stage. This suggests that the incorporation of Agave fibres resulted in a delay in crack development, with mixes F35-0.5 and F35-1 showing cracks 1.25 and 2.25 hours later, respectively.

Furthermore, the largest average crack width recorded was 0.816mm for the Control Mix, while the smallest crack width was 0.274mm for Mix F35-1. These findings indicate that as the fibre percentage increases, a decrease in crack width was observed. This suggests that the addition of fibres in the mix provides restraint resulting in smaller plastic shrinkage crack widths.

An interesting observation was made when measuring the crack widths for Mix F35-0.5 using a USB microscope. In one instance, the presence of Agave fibres within the cracks was captured as shown in Figure 4-27. This image highlights that when the orientation of the fibre is perpendicular to the crack, more restraint is provided, resulting in narrower crack widths. Conversely, in Figure 4-28, since the orientation of the fibre is nearly parallel to the crack, larger crack widths are observed. These results from this test are provided in Appendix D.

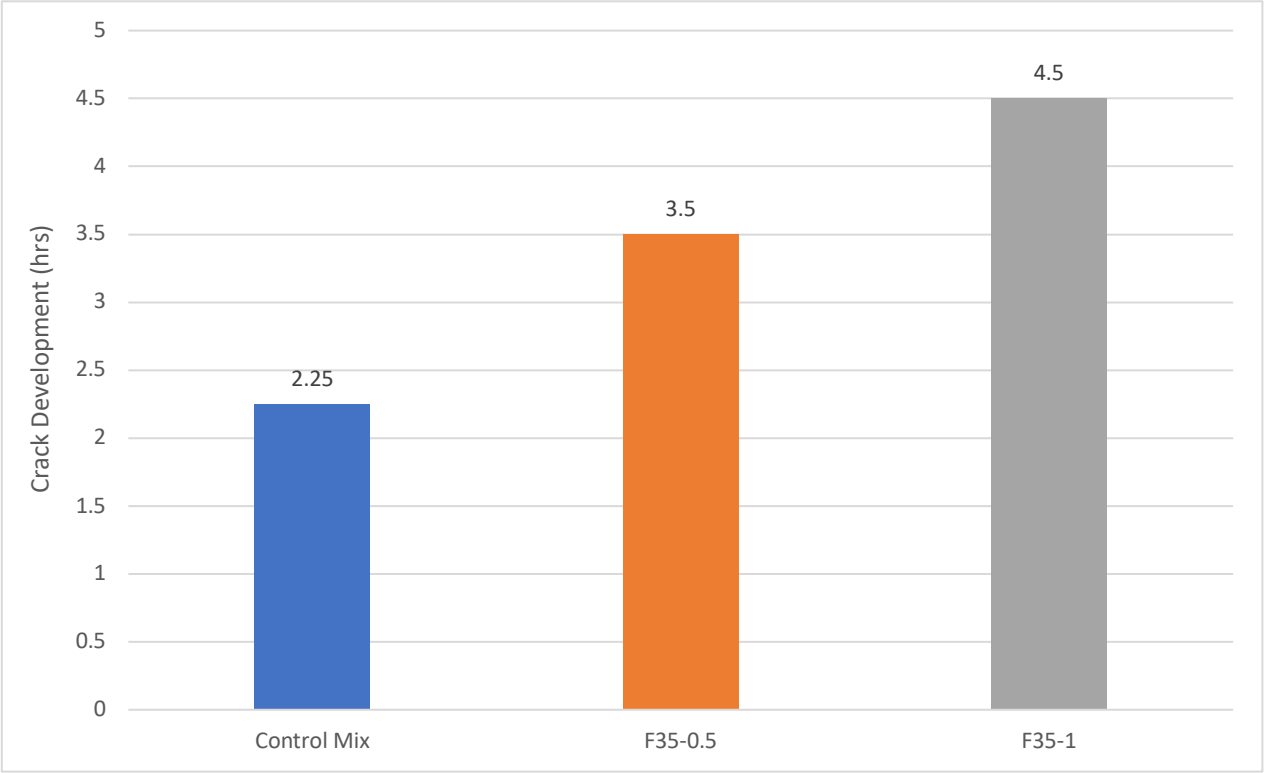

Fig 4-25: Crack development for different mixes

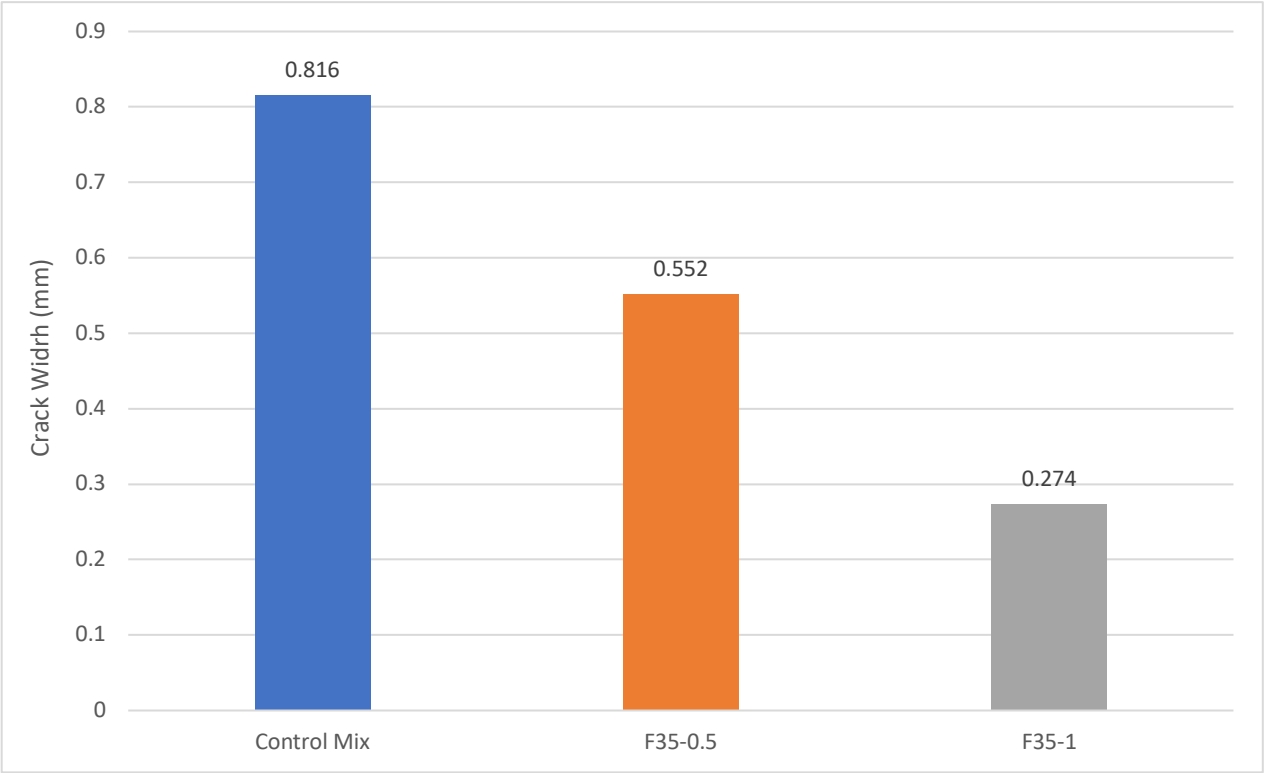

Fig 4-26: Crack widths for different mixes

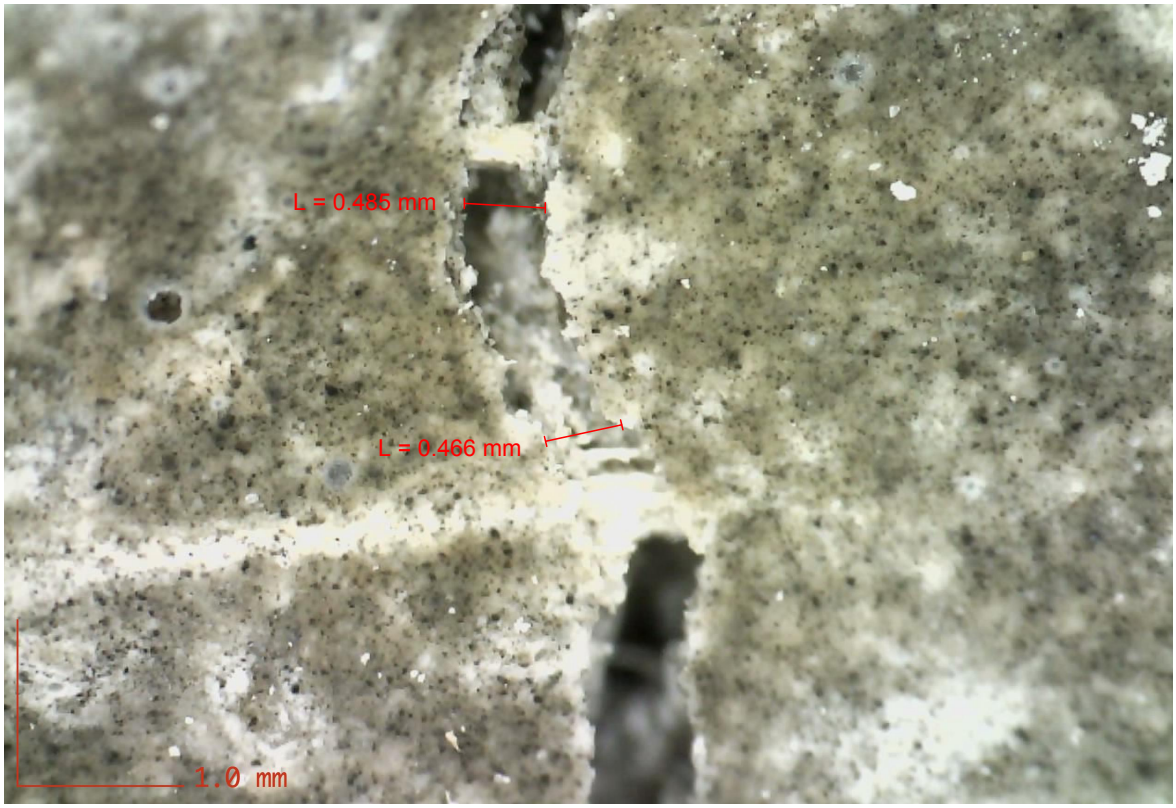

Fig 4-27: Agave fibres perpendicular to crack captured with USB microscope

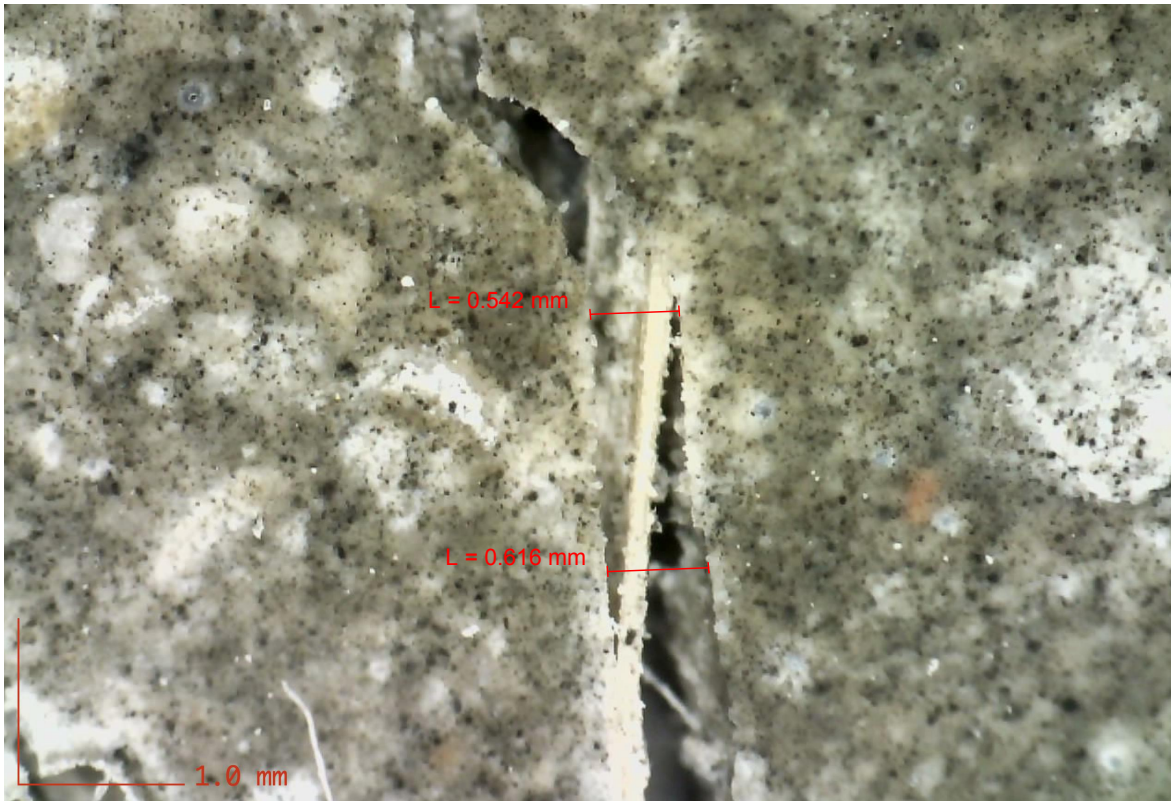

Fig 4-28: Agave fibres parallel to crack captured with USB microscope

Comparison with literature

Upon reviewing the existing literature, limited information was available regarding the evaluation of plastic shrinkage behaviour containing Agave Sisalana fibres. From research done by Toledo Filho et al. (2005) on cement mortars, it was observed that the addition of sisal fibres, with a length of 25mm and a volume fraction 0.2%, delayed the occurrence of initial cracking during plastic shrinkage. Moreover, when comparing the crack widths after 3.5 hours, it was observed that the cracks were narrower in the specimens reinforced with fibres compared to the plain mortar samples.

In this study, the longest fibre length (i.e., 35mm) was chosen to provide greater anchorage length embedded in the concrete. The findings demonstrated a similar trend, where an increase in the volume percentage of fibres in the SCC led to a reduction in crack widths. All the results related to this test are found in Appendix D.

4.4.2 Ring Test

The ring test was conducted to examine the impact of different concrete mixes containing Agave fibres on restrained shrinkage. To measure the strain caused by the concrete shrinkage, the inner steel ring was connected to a data logger. Figure 4-29 provides the results obtained, showing the change in strain over time.

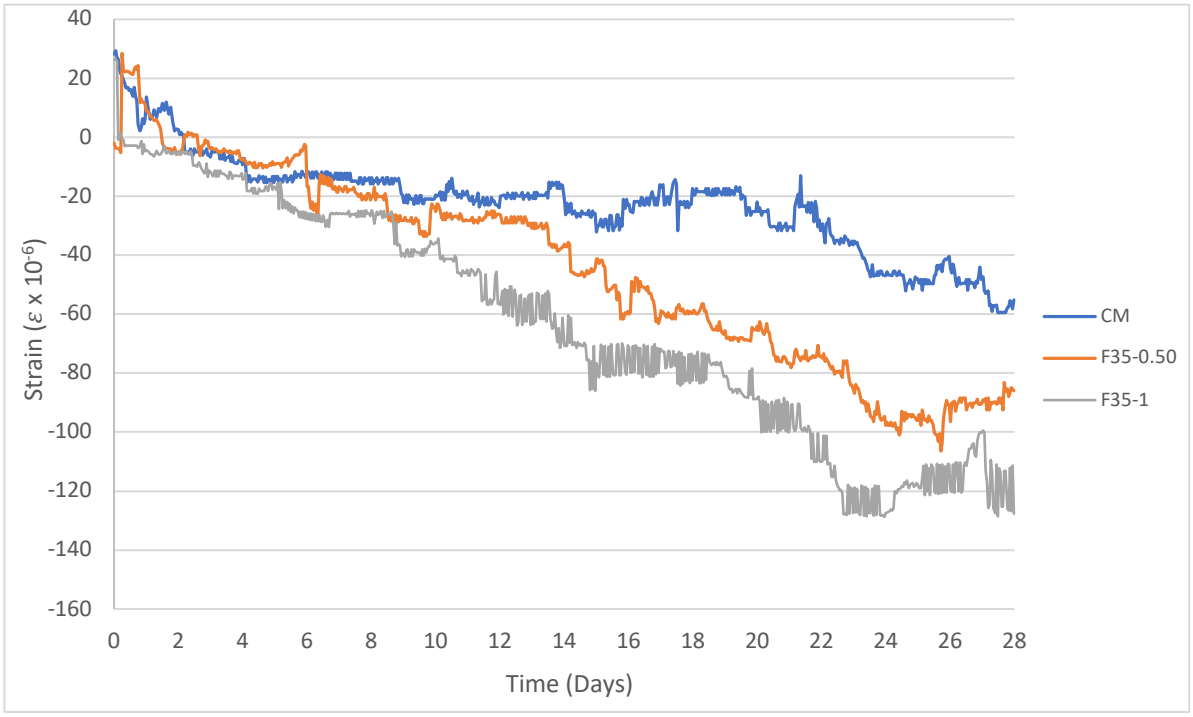

Fig 4-29: Strain imposed by the concrete on the steel ring over time

Although the Control Mix and Mix F35-0.50 experienced cracking, Figure 4-29 does not indicate any significant decrease in strain. As shown in Figure 4-30, the width of the crack on the outer surface of the specimen is narrower near the steel ring. This observation could be a possible explanation which suggests that the presence of Agave Fibres limited the crack width towards the inner steel ring, resulting in minimal differences in readings in the inner parts of the specimen. Furthermore, the formed cracks do not coincide with each other, which implies the material's ability to maintain its structural integrity.

Fig 4-30: Crack width on surface

The occurrence of cracking in each mix was observed through regular visual inspections, and the corresponding age at which cracking was observed was recorded. It was noted that the Control Mix and Mix F35-0.50 developed cracking at 9 days and 14 days, respectively, while Mix F35-1 did not develop any cracks. This can be further observed in Figure 4-29, which reveals an increase in strain with an increase in fibre dosage. This behaviour can be attributed to the addition of fibres, which allow the concrete to withstand higher tensile stresses when compared to the control mix. The control mix reached a maximum strain of -59.52 microstrains, whereas Mix F15-0.50 exhibited a maximum strain of -106.46 microstrains.

Fig 4-31: Ring Test, Control Mix crack

Fig 4-32: Ring Test, Mix F35-0.50 crack

Comparison with literature

Sanjuan and Toledo Filho (1998) conducted a similar research on the impact of sisal fibres on the restrained shrinkage of cement mortar. A similar setup was employed, involving a ring specimen with a central square core. The study revealed that while the unreinforced mortar did not exhibit any healing, the fibre reinforced specimens showed signs of healing. This observation indicates that the presence of sisal fibres acts as a bridging element allowing the closure of cracks.

Furthermore, similar tests were done by Vella (2018) and Abdilla (2021) using SWTF. Both studies observed that increasing the fibre dosage resulted in higher strains. This aligns with the findings of the current study, which also showed an increase in strain with an increase in fibre dosage. However, it is worth mentioning that Vella (2018) reported a different observation regarding the control mix. According to the study, the control mix specimens did not develop any cracks within 28 days. This contrasts with the results of the present research, where the control mix specimen did exhibit cracking.

4.5 Mortar Shrinkage Properties

4.5.1 Kraai Test

This test utilizes several test panels with different fibre volume percentages to assess the potential for cracking in mortar. To calculate the total crack area, the width of each crack is multiplied by its length. This measurement will indicate the crack control performance of the different mixes.

Figure 4-33 demonstrates a decrease in crack area as the percentage of fibres increases. In this test, fibre lengths of 35mm were chosen to provide better anchorage when compared to shorter fibres. It can be noted that the Control Mix had the highest number of cracks, whereas Mix F35-1 showed no cracks. Upon examining the crack patterns, it was observed that the Control Mix had several cracks with a width of 1mm and 2mm, while the mix containing 0.50% fibres only had a few hairline cracks. The reduction in crack area from the Control Mix to Mix F35-0.50 was 61.34%.

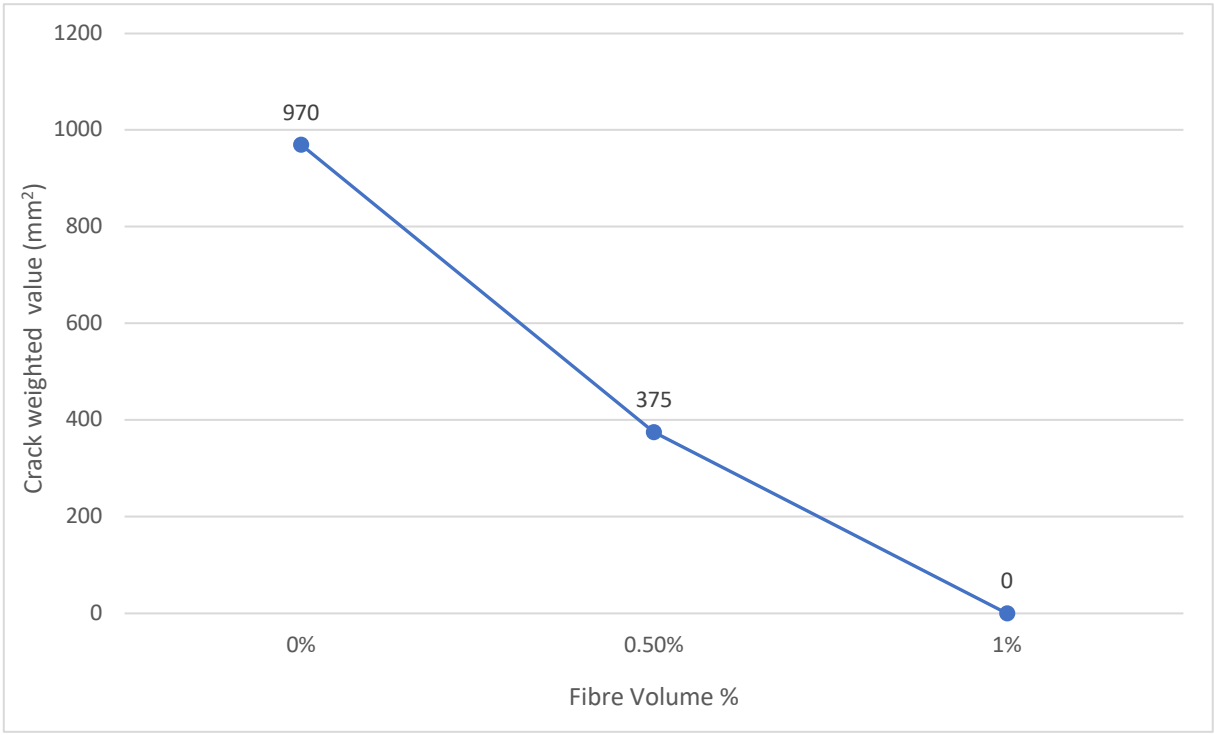

Fig 4-33: Relationship between crack area and fibre volume percentage

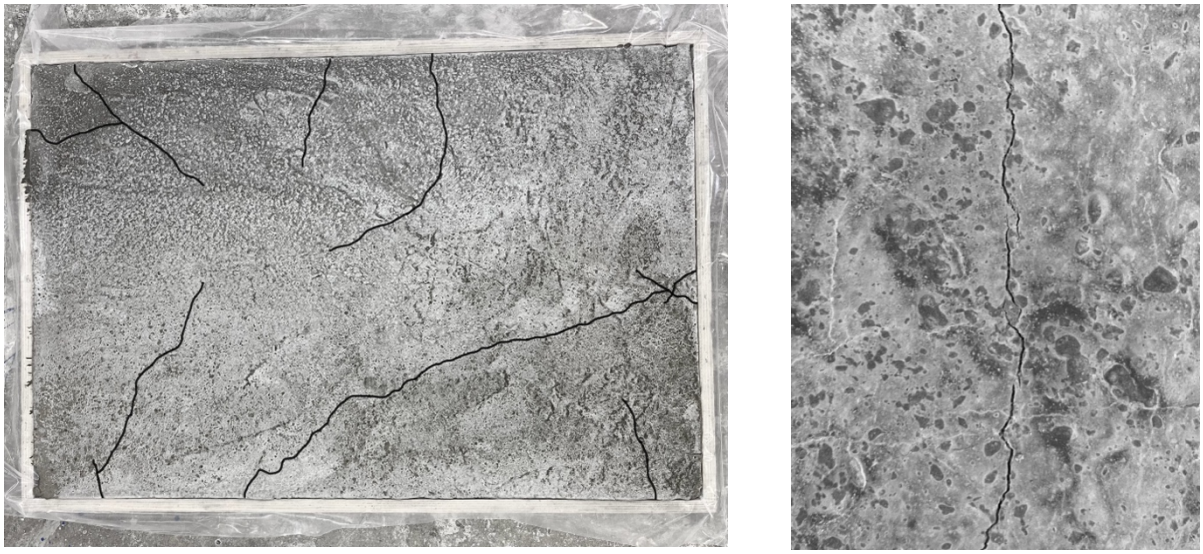

Fig 4-34: Kraai Test, Control Mix Panel

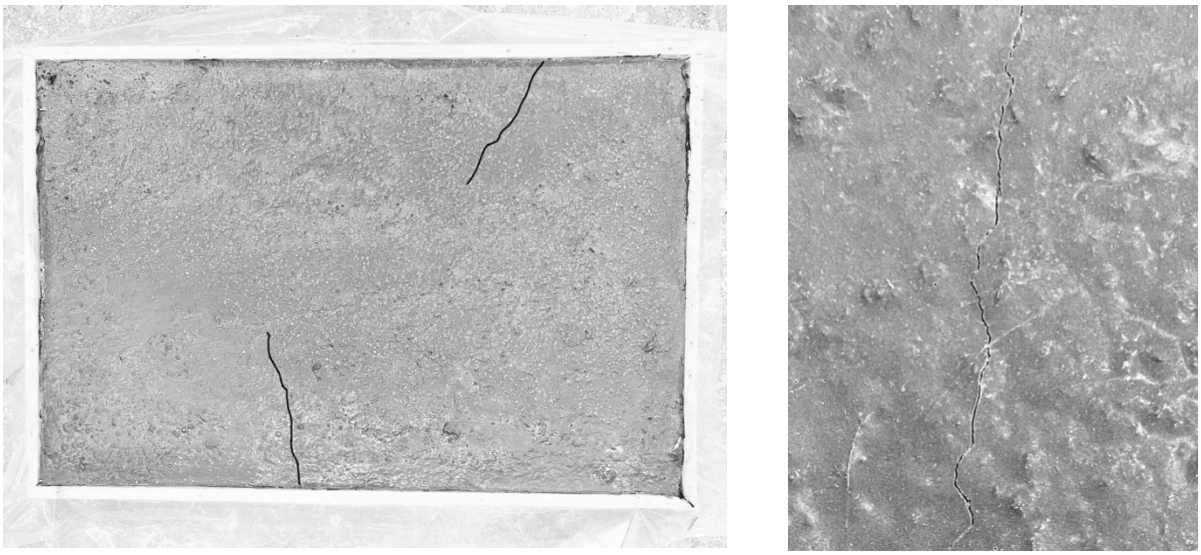

Fig 4-35: Kraai Test, Mix F35-0.50

Fig 4-36: Kraai Test, Mix F35-1

Comparison with literature

In a study conducted by Baldacchino (2014), the impact of Polyethylene Terephthalate (PET) fibres on the cracking restraint was investigated under similar conditions suggested by the Kraai paper. The results showed that increasing the fibre volume percentage led to a decrease in the crack area. Additionally, Baldacchino also investigated the effect of different fibre lengths, and concluded that the length of the fibres also affected the crack widths. It was observed that longer fibres exhibited better performance when compared to shorter fibres, due to their longer anchorage length within the mortar.

4.6 Treated and Untreated Fibres Properties

4.6.1 Slump Flow

The slump flow test was conducted to evaluate the flow of SCC mortar for each treated and untreated mix. As expected, the slump flow results indicated a decrease in diameter as the volume percentage or length of fibres increased. However, Figure 4-37 illustrates that the treated fibres exhibited a slight improvement in slump flow when compared to untreated fibres. Specifically, fibres treated with NaOH displayed an average increase of flowability of 3.47%, while for H_2O_2 was 1.35%.

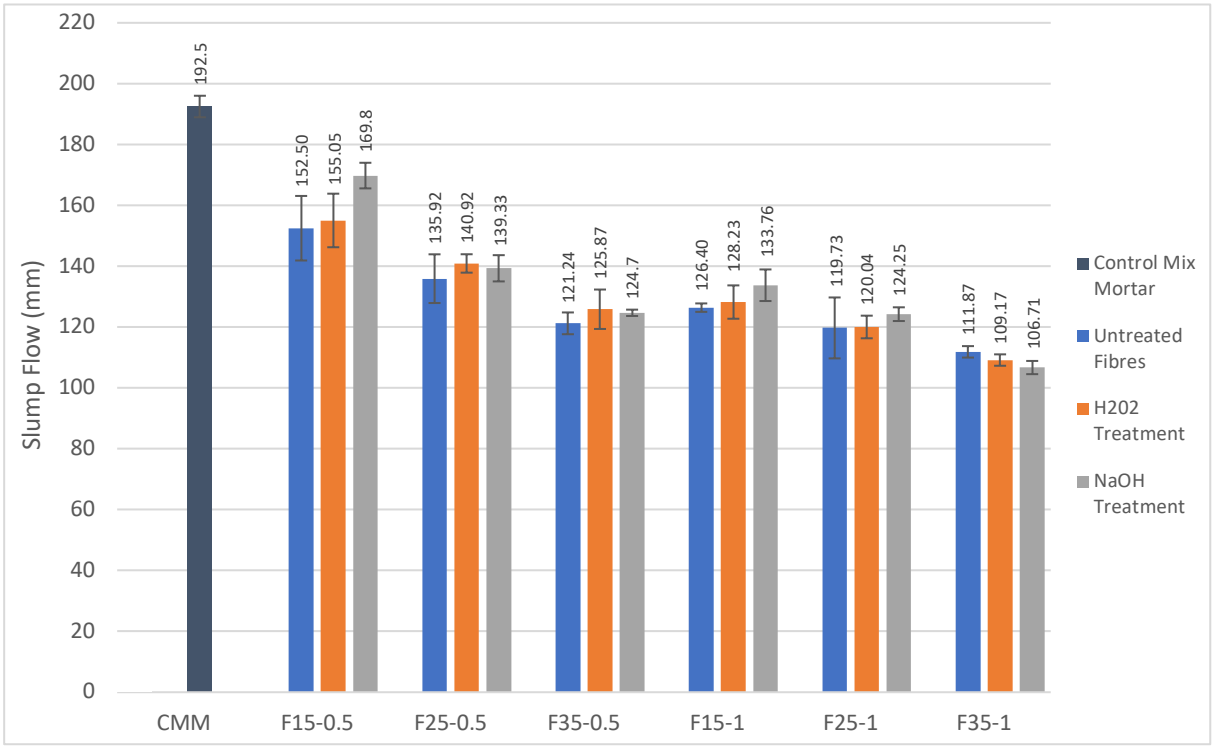

Fig 4-37: Slump flow diameter for treated and untreated fibres

Furthermore, this increase in flow can be clearly observed in Figure 4-38, particularly for Mix F15-0.5, where the effect of treatment for fibres is the most pronounced. The results of the slump flow tests for both treated and untreated fibres are all presented in Appendix E.

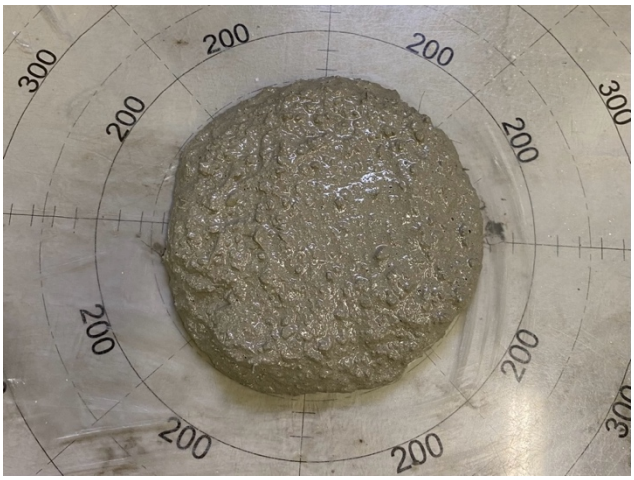

Untreated Fibres, F15-0.5 Mix

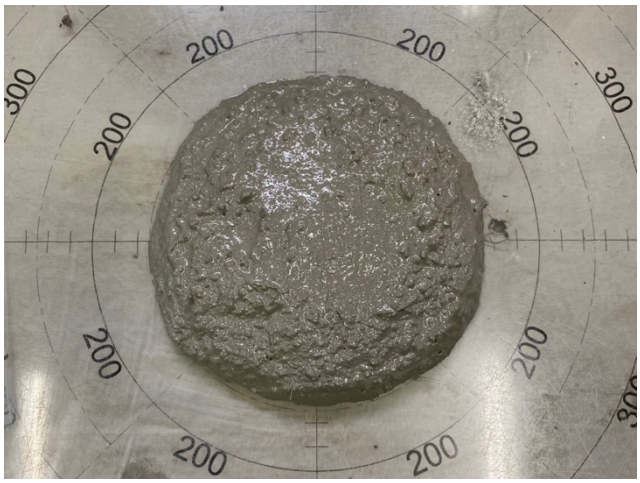

Treated Fibres with Hydrogen Peroxide, F15-0.5 Mix

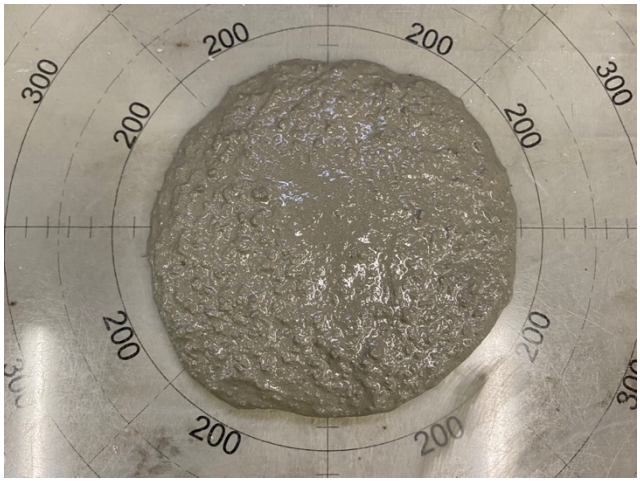

Treated Fibres with Sodium Hydroxide, F15-0.5 Mix

Fig 4-38: Slump flow treated and untreated fibres, F15-0.5 Mix

Comparison with literature

No literature was found that specifically addresses the impact of chemical treatments on the workability of concrete when applied to Agave fibres. However, a similar study by Hassan Nensok et al. (2021) on alkaline treatment on banana fibres was investigated. The fibres were treated to various concentrations of NaOH, including 2%, 4%, 6%, 8% and 10%. Their results demonstrated that the workability of untreated fibres was lower to that of all treated fibres. Notably, fibres treated with higher concentration of NaOH exhibited less water absorption, leading to improved workability.

4.6.2 Flexural Strength

The flexural strength test was performed to evaluate the maximum load for each mix variable using a three-point test on prisms after 7 days of casting. The results obtained in this test are consistent with the findings discussed in section 4.3.4 of this chapter, indicating a higher flexural strength with an increase in fibre length or volume. This was noted for both treated and untreated fibres. However, treated fibres demonstrated a higher maximum load when compared to the untreated fibres, indicating the potential enhancement achieved through the treatment process. Figure 4-40 provides a representation of the performance of the fibres under different treatments. Notably, the fibres treated with H_2O_2 exhibited the best performance. These fibres displayed an average increase of 10.70%, while the NaOH fibres showed an increase of 5.71%. Furthermore, the behaviour of the specimens after failure was observed. It was noted that all the specimens incorporating fibres exhibited a ductile failure mode. Figure 4-39 shows the contribution of fibres in crack bridging, allowing the sample to undergo plastic deformation before fracturing.

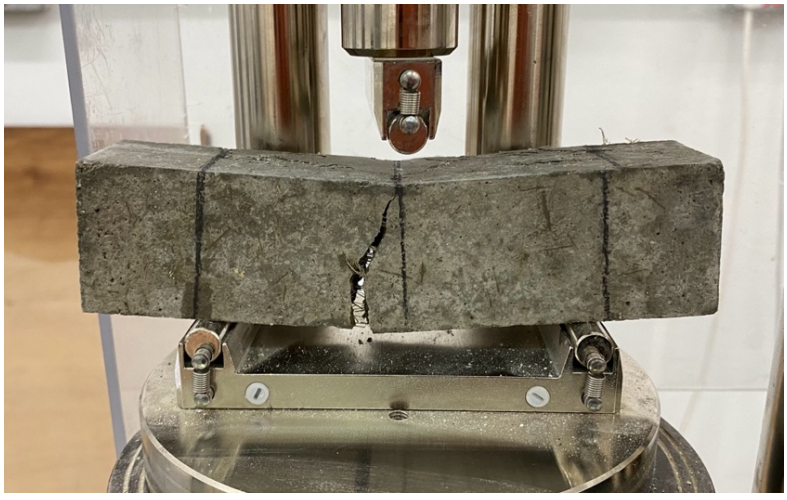

Fig 4-39: Flexural Strength after failure

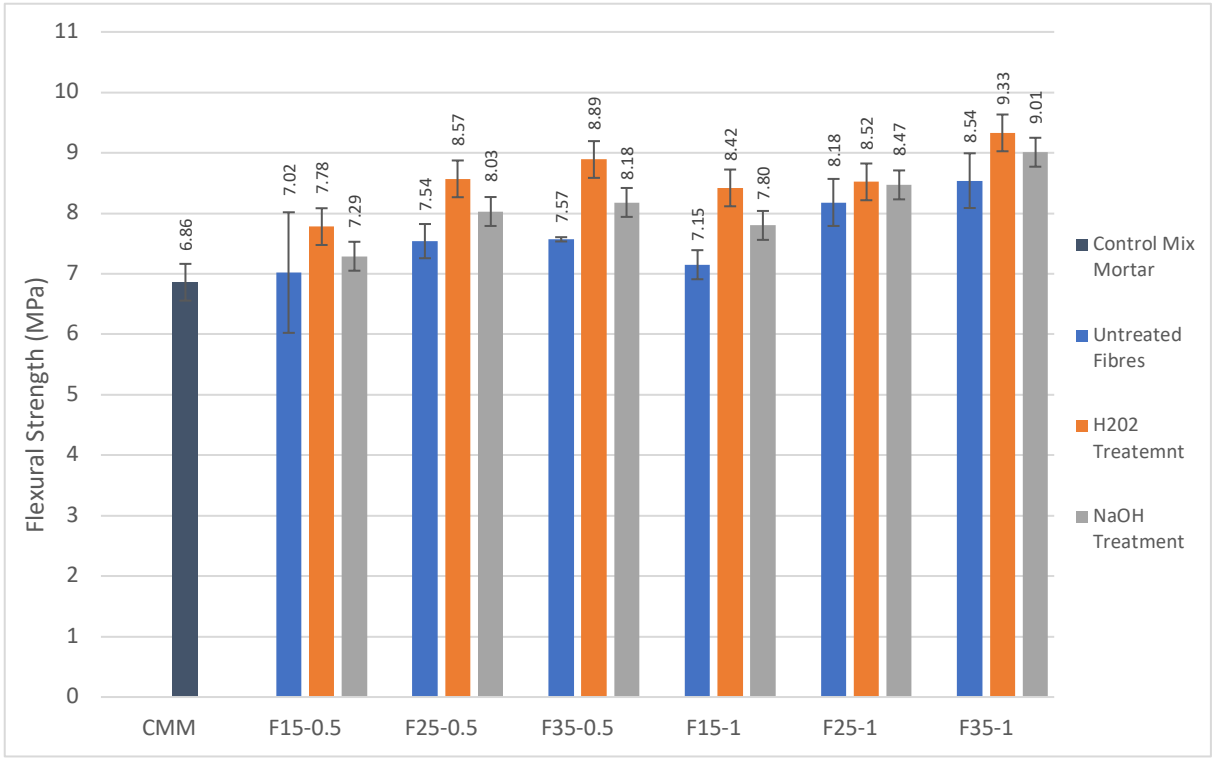

Fig 4-40: Flexural Strength for treated and untreated fibres

Comparison with literature

Limited data was available regarding sisal fibres treated with Hydrogen Peroxide; however, several studies were found using Sodium Hydroxide. In a study by de Klerk et al., (2020), the impact of NaOH treatment on sisal fibres was investigated. Different concentrations of NaOH, including 2%, 6%, 10%, 20% and 30% were studied. The findings indicated that the flexural peak strength increased with 2%, 6% and 10% NaOH treatment when compared to untreated fibres. However, higher concentrations of NaOH led to a decrease in the flexural peak load.

Additionally, in a similar study by Yimer and Gebre (2023), sisal fibres were treated with a NaOH concentration of 5% for 12 hours. The results demonstrated an increase in flexural strength of 13.59% when compared to the unreinforced concrete specimen.

4.6.3 Compressive Strength

The compressive strength test was performed to assess the strength characteristics of the mortar. The outcomes are shown in Figure 4-41, indicating the values obtained after 7 days. Comparing the results to those discussed in section 4.3.3, a decrease of 18.81% in compressive strength from the control mix was recorded. This reduction aligns with the earlier findings, which indicated a decrease of 23.12% in the concrete mix. However, consistent with similar trends observed in other tests, an increase in fibre length or volume percentage corresponded to an improvement in compressive strength. This observation is noted for both treated and untreated fibres.

Notably, the treated fibres, particularly those treated with H_2O_2 exhibited the highest compressive strength with an average increase of 4.33%. Similarly, fibres treated with NaOH demonstrated an increase of 1.71%. Another observation throughout the study was the optimal length and fibre dosage, beyond which the compressive strength of the mortar decreased. Based on the observations made in section 4.3.3, it was noted that for fibre dosages of 0.25%, 0.5% and 1% with fibre lengths up to 15mm, the compressive strength decreased. However, the present study provides additional insights, indicating that for a fibre percentage of 1% exceeding length of 25mm, an improvement in compressive strength can be noticed.

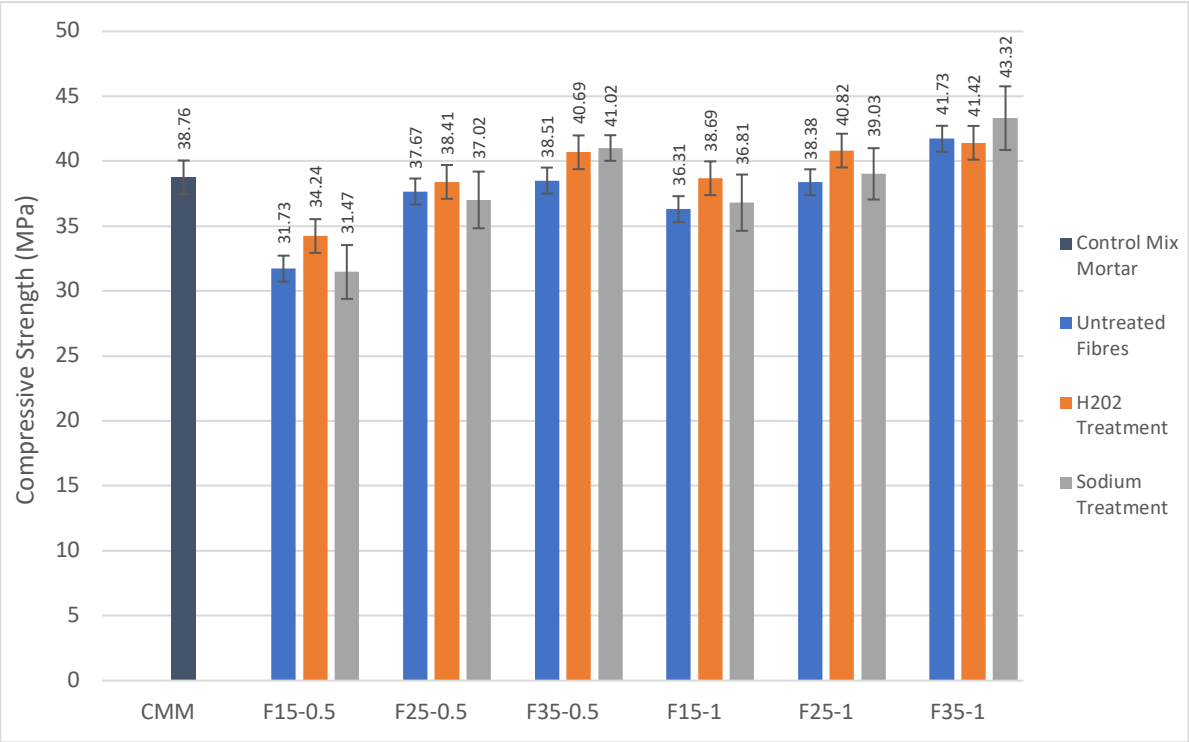

Fig 4-41: Compressive Strength for treated and untreated fibres

Fig 4-42: Compressive strength after failure

Comparison with literature

Data regarding the compressive strength of concrete with treated fibres was very limited. Yimer and Gebre (2023) investigated effects of Sodium Hydroxide treatment on sisal fibres. From their results it was found that the best performance was obtained when fibres were treated with a 5% concentration of alkali solution for 24 hours. This has shown a slight improvement in strength of 0.46% when compared to untreated fibres and a 13.12% with unreinforced concrete.

In a separate study by Hassan Nensok et al. (2021), Sodium Hydroxide treatment on banana fibres was investigated. Different concentrations of NaOH were examined, and it was observed that compressive strength increased at concentration of 2%, 4% and 6%. Specifically, the percentage increase in compressive strength was measured at 3.4% and 15.1% for concentrations of 2% and 4% respectively. Notably, fibres treated with 6% NaOH exhibited a progressive increase of 40.6% in compressive strength. These improvements can be attributed to the effective breakdown of hydrogen bonds between the hydroxyl groups of lignin and hemicellulose. Consequently, these changes also enhanced the surface area of the fibres within the cement matrix.

CHAPTER 5

Conclusion and Recommendations

5.1 Overview

The main aim of this research was to investigate the performance of Agave fibres in Self-compacting concrete (SCC). Eight different mixes with varying fibre lengths and volumes were evaluated to analyse the fresh properties and hardened properties of concrete. Furthermore, three mixes were considered to assess the shrinkage properties of concrete and mortar. The findings obtained from this research were compared with other relevant studies in the literature for further analysis.

5.2 Conclusion

The assessment of workability of various tests revealed that the addition of Agave fibres resulted in a decrease in workability of SCC. This reduction was evident across all the performed tests, including the Slump Flow, V-Funnel and L-Box tests. The findings from the Slump Flow test led to the conclusion that as the fibre volume percentage exceeded 0.50%, the mixes would not exhibit the characteristics of self-compacting concrete due to the increased stiffness of the mix. Furthermore, the V-Funnel test indicated a higher plastic viscosity with an increase of fibres. From the rheometer test a higher yield stress was observed with an increase in fibre length or fibre volume percentage.

Another test which provided additional insights on the fresh properties of the concrete, was the L-Box test. The inclusion of Agave fibres led to a notable decrease in passing ability. The results indicated that immediate clogging occurred when the fibre volume reached 1% at 0 minutes. As time progressed, there was a significant reduction in passing ability, with instances of clogging at 15 and 30 minutes.

In terms of the mechanical properties of Agave fibres in SCC, it was determined that the fibres affected the density and homogeneity of the concrete. The findings from the hardened concrete test and Ultrasonic Pulse Velocity (UPV) test highlight a similar behaviour. It can be seen that an increase in fibre dosage led to a reduction in the density and UPV.

The decrease in compressive strength was evident at both 7 and 28 days, with a decrease of 23.12%. It was noted that as the length of the fibres increase, the compressive strength of the concrete decreased. This decrease in strength can be attributed to the loss of workability, which resulted in the formation of air voids within the concrete.

The flexural strength results indicated that all the mixes, including those with Agave fibres, exhibited a brittle failure mode. However, it was observed that mixes containing longer fibres or higher volume percentages demonstrated a higher peak load compared to the Control Mix. In fact, Mix F35-0.50 showed the best performance with a notable increase of 37.65% in peak load. Furthermore, Mix F15-1 experienced a decrease of 9.03% in peak load. This can be attributed to the lower anchorage length and aspect ratio of the shorter fibres, leading to a decrease in strength. Notably, there also was a significant increase in the toughness factor of 85.06%, highlighting the positive affect of Agave fibres.

A similar observation was also made on the tensile strength of concrete, where mixes incorporating longer fibres or higher volumes exhibited a better performance. Mix F35-0.50 showed the highest tensile strength with an increase of 20.43% when compared to the Control Mix. In contrast to the flexural strength test, samples containing Agave fibres displayed a ductile failure mode.

To assess the impact of Agave fibres on the plastic shrinkage in concrete, an environmental chamber was setup exposed to controlled conditions. The results of this test concluded that the addition of fibres leads to a reduction in the width of the cracks. When comparing the Control Mix to Mix F35-1, a substantial reduction of 66.42% in crack width was observed. Moreover, higher fibre dosages resulted in a delay in crack development.

The restrained ring test was monitored for 28 days, during which data from strain gauges was collected to analyse the stress caused by concrete hardening. From regular inspections it was noticed that the specimens took longer to exhibit shrinkage cracking as the fibre dosage increased. Notably, Mix F35-1, which had the highest volume fraction, did not experience any cracks within 28 days. Furthermore, the specimens containing Agave fibres also demonstrated greater resistance subjected to higher tensile stresses when compared to the Control Mix.

Following the methodology described by Paul Kraai, mortar panels were used to investigate the effect of fibres in cement mortars. From similar observations, increase in the volume percentage of fibres resulted in a decrease in the total crack area. From the findings obtained, the Control Mix had several cracks of 1mm and 2mm, while the mix containing 0.50% fibres only a few hairline cracks were observed. This led to a reduction of 61.34% in the total crack area. Moreover, the panel containing 1% fibres developed no cracks.

Chemical treatments were applied to Agave fibres to explore their impact on the fresh properties and mechanical properties of mortars. Two chemicals used in the treatment process were Hydrogen Peroxide (H_2O_2) and Sodium Hydroxide (NaOH). The Slump flow, Flexural test and compressive strength test were conducted.

The results obtained from the Slump Flow test showed that the treated fibres exhibited only a slight improvement when compared to untreated fibres. The workability of fibres treated with H_2O_2 increased by 1.35%, while for NaOH fibres, the increase was of 3.47%.

From the flexural strength test, all specimens containing Agave fibres demonstrated a ductile mode of failure. From the findings obtained, treated fibres exhibited a higher maximum load compared to untreated fibres. An increase in load of 10.70% was obtained for fibres treated with H_2O_2, while for NaOH fibres an increase of 5.71% was observed.

The compressive strength results also indicated an improvement in strength with treatment of fibres. Fibres treated with H_2O_2 exhibited the highest compressive strength showing an increase of 4.33%. On the other hand, fibres treated with NaOH displayed an increase of 1.71%.

5.3 Limitations

One major limitation encountered in this study was the extensive time and effort required for the extraction of Agave fibres. Due to the degradation process, it took several weeks to obtain a sufficient quantity of fibres for experimentation. This limited the number of samples available for testing of the mechanical properties. With a larger number of samples, a more comprehensive assessment of the mechanical properties could have been conducted, leading to more precise and accurate results, minimizing the potential margin of error.

Another constraint in this research was the limited number of moulds for test repetitions. The environmental chamber used in the experiment could only accommodate one specimen at a time. This restriction resulted in a limited number of tests conducted within the available timeframe and only three mixes were chosen. Similarly, the ring test was also constrained by the availability of only three moulds, further limiting the number of samples that could be tested.

For the Kraai test, only one industrial fan was available in the laboratory. As a result, the same fan had to be shared between two panels, potentially impacting the number of cracks that developed in the mortar panels.

5.4 Recommendations for future studies

Based on the findings of this study, several recommendations for further research and areas of exploration can be suggested. Firstly, it is recommended to investigate the water absorption characteristics of Agave fibres. The fibres can potentially hinder the hydration process of the cement by reducing the available water in the mix. Thus, it is essential to gain a comprehensive understanding on the moisture absorption behaviour of the fibres and how it may impact the durability and mechanical properties of concrete.

In addition, further research on chemical treatments of Agave fibres can be conducted. The current study explored the impact of Hydrogen Peroxide and Sodium Hydroxide treatments on the fresh and mechanical properties of mortars. However, other chemical treatment combinations can be investigated to determine their effectiveness on the bonding with the cement matrix. Also, the effect of chemical treatments can be conducted on concrete mixes.

Furthermore, it is also recommended to perform pull-out tests to determine the bond strength between the Agave fibres and the matrix. By performing pull-out tests on Agave fibres under various conditions, such as different fibre lengths, an understanding of their reinforcing capabilities can be obtained.

BIBLIOGRAPHY

Abdilla, B. (2021). *Recycled concrete Aggregated and Steel Waste Tyre Fibres for High-Performance Self-Compacting Concrete. Dissertation Faculty for the Built Environment (Supervised by Prof. Ruben Paul Borg).*

Alshaya, N., Alhomidan, R., Alromizan, S., & Labib, W. (2018). The Use Of Plant-Based Natural Fibers In Reinforced Cement Composites. Vol. 12, No.5, pp. 11-21.

Arshad, A., Mansor, S., Shafie, E., & Hashim, W. (2016). PERFORMANCE OF STONE MASTIC ASPHALT MIX USING SELECTED FIBRES. *Jurnal teknologi. A, Pembuatan, bahan termaju, tenaga dan pengangkutan*, Vol. 78, No. 7-2, pp. 99-103.

ASTM C 1579 – 06. (2006). *Standard Test Method for Evaluating Plastic Shrinkage Cracking of Restrained Fiber Reinforced Concrete.*

ASTM C 1581-04. (2004). *Standard Test Method for Determining Age at Cracking and Induced Tensile Stress Characteristics of Mortar and Concrete under Restrained Shrinkage.*

Baldacchino, O. (2014). *Mechanical and shrinkage properties of recycled PET fibre-reinforced concrete. Dissertation Faculty for the Built Environment (Supervised by Prof. Ruben Paul Borg).*

Begum, H., Tanni, T., & Shahid, M. (2021). Analysis of Water Absorption of Different Natural Fibers. *Journal of Textile Science and Technology*, Vol.7, No.4, pp. 152-160.

Binici, H., Aksogan, O., & Shah, T. (2005). Investigation of fibre reinforced mud brick as a building material. *Construction & building materials*, Vol. 19, No.4, pp.313-318.

Binici, H., Aksogan, O., Bodur, M., Akca, E., & Kapur, S. (2007). Thermal isolation and mechanical properties of fibre reinforced mud bricks as wall materials. *Construction & building materials*, Vol. 21, No. 4, pp. 901-906.

Borg, R. P., Baldacchino, O., & Ferrara, L. (2016). Early age performance and mechanical

characteristics of recycled PET fibre reinforced concrete. Construction and Building Materials(108), 29-47.

BS 8500-2. (2006). Concrete - Complementary British Standard to BS EN 206 Part 2: Specification for Constituent Materials and Concrete.

BS EN 12350-2. (2009). Testing fresh concrete - Part 2: Slump-test. BSI Standards Publication.

BS EN 12390-3. {2002) Testing hardened concrete. Compressive strength of test specimens. BSI Standards Publication.

BS EN 12504-4. (2004). Testing concrete - Part 4: Determination of ultrasonic pulse velocity. BSI Standards Publication.

BS EN 12390-5. (2009). Testing hardened concrete - Part 6: Flexural strength of test specimens. BSI Standards Publication.

BS EN 12390-6. (2009). Testing hardened concrete - Part 6: Tensile splitting strength of test specimens. BSI Standards Publication.

BS EN 12390-7. (2019). Testing hardened concrete - Part 7: Density of Hardened Concrete BSI Standards Publication.

BS EN 12350-9. (2010). Testing fresh concrete - Part 9: Self-compacting concrete — V-funnel test. BSI Standards Publication.

BS EN 12350-10. (2010). Testing fresh concrete - Part 10: Self-compacting concrete — L box test. BSI Standards Publication.

Chand, N., & Fahim, M. (2020). *Tribology of Natural Fiber Polymer Composites.* San Diego: Elsevier Science.

Célino, A., Fréour, S., Jacquemin, F., & Casari, P. (2014). The hygroscopic behavior of plant fibers: a review. *Frontiers in Chemistry*, Vol. 1 No. 43 pp. 11-21.

de Klerk, M., Kayondo, M., Moelich, G., de Villiers, W., Combrinck, R., & Boshoff, W. (2020). Durability of chemically modified sisal fibre in cement-based composites. *Construction & building materials*, Vol. 241, pp. 117835.

E. Njoku, C., K. Alaneme, K., A. Omotoyinbo, J., & O. Daramola, M. (2019). Natural Fibers as Viable Sources for the Development of Structural, Semi-Structural, and Technological Materials – A Review. *Advanced Materials Letters*, Vol. 10, No. 10, pp. 682-694.

Fadhil, S., & Yaseen, M. (2015). The Effect of Adding Different Types of Natural Fibers on Mechanical Properties and Impact Resistance of Concrete. *Research journal of applied sciences, engineering and technology*, Vol.9, No.12, pp.1091-1096.

Fonseca, R., Rocha, J., & Cheriaf, M. (2021). Influence of Different Types of Treatments on Amazonian Vegetable Fibers on the Performance of Mortars Based on Portland Cement, Metakaolin and Fly Ash. *Materials research (São Carlos, São Paulo, Brazil)*, Vol.24, No.2, pp. 11-21.

Geremew, A., De Winne, P., De Backer, H., & Demissie, T. (2021). Treatment of Natural Fiber for Application in Concrete Pavement. *Advances in Civil Engineering*, 1-13.

Gholampour, A., & Ozbakkaloglu, T. (2019). A review of natural fiber composites: properties, modification and processing techniques, characterization, applications. *Journal of materials science*, Vol. 55, Issue 3, pp. 829-892.

Gholampour, A., & Ozbakkaloglu, T. (2020). A review of natural fiber composites: properties, modification and processing techniques, characterization, applications. *Journal of materials science*, Vol. 55, No. 3, pp. 829-892.

Hassan Nensok, M., Othuman Mydin, M., & Awang, H. (2021). Optimization of mechanical properties of cellular lightweight concrete with alkali treated banana fiber. *Revista de la construcción*, Vol. 20, No.3, pp.491-511.

ICAR Rheometer. (n.d.). ICAR Rheometer. Germann Instruments A/S.

Jawaid, M., & Thariq, M. (2018). Potential of natural/synthetic hybrid composites for aerospace applications. In *Sustainable Composites for Aerospace Applications.* Elsevier Science & Technology.

Jiao, L., Su, M., Chen, L., Wang, Y., Zhu, H., & Dai, H. (2016). Natural Cellulose Nanofibers As Sustainable Enhancers in Construction Cement. *PLOS ONE*, Vol 11, No. 12.

K Singh, V., Bansal, G., Gope, P., & Gupta, T. (2017). Application and Properties of Chicken Feather Fiber (CFF) a Livestock Waste in Composite Material Development. *Journal of Graphic Era University*, Vol.5, No.1, pp. 16-24.

Kaur, I., Kaith, B., & Kalia, S. (2011). *Cellulose Fibers: Bio- and Nano-Polymer Composites : Green Chemistry and Technology.* Springer Berlin Heidelberg.

Khedari, J., Watsanasathaporn, P., & Hirunlabh, J. (2005). Development of fibre-based soil–cement block with low thermal conductivity. *Cement & concrete composites*, Vol. 27, No.1, pp.111-116.

Kraai, P. (1985). A proposed test to determine the cracking potential due to drying shrinkage of concrete. San Jose State University.

Labib, W. (2022). Plant-based fibres in cement composites: A conceptual framework. *Journal of engineered fibers and fabrics*, Vol. 17.

Life Saving Buskett. (2018, February 1). *Action C4: Removal of Invasive Alien Species – Agave spp. (Century plants)*. From Life Saving Buskett:http://lifesavingbuskett.org.mt/ gallery/ action-c4-removal-of-invasive-alien-species-agave-spp-century-plants/1/

Lilargem Rocha, D., Tambara Júnior, L., Marvila, M., Pereira, E., Souza, D., & de Azevedo, A. (2022). A Review of the Use of Natural Fibers in Cement Composites: Concepts, Applications and Brazilian History. *Polymers*, Vol. 14, No. 10, pp. 2043.

Luhar, S., Suntharalingam, T., Navaratnam, S., Luhar, I., Thamboo, J., Poologanathan, K., & Gatheeshgar, P. (2020). Sustainable and Renewable Bio-Based Natural Fibres and Its Application for 3D Printed Concrete: A Review. *Sustainability*, Vol.12, No.24 pp.11-21.

Malta Today. (2020, May 16). *Over 200 tons of invasive alien species removed from Majjistral Park*. From Malta Today: https://www.maltatoday.com.mt/environment/environment/102377/over_200_tons_of_invasive_alien_species_removed_from_majjistral_park

Mehrez, I., Hachem, H., Gheith, R., & Jemni, A. (2022). Optimization of Mortar/Agave americana Fibers Composite Behavior Based on Experimental Design. *Journal of natural fibers*, Vol 20, No.1.

Mishra, S, Mohanty, A.K, Drzal, L.T, Misra, M, Parija, S, Nayak, S.K, & Tripathy, S.S. (2003). Studies on mechanical performance of biofibre/glass reinforced polyester hybrid composites. *Composites science and technology*, Vol. 63, No.10, pp. 1377-1385.

Mohajerani, A., Hui, S.-Q., Mirzababaei, M., Arulrajah, A., Horpibulsuk, S., Abdul Kadir, A., . . . Maghool, F. (2019). Amazing Types, Properties, and Applications of Fibres in Construction Materials. *Materials*, Vol. 12, No.6 pp.11-21.

MSA EN 12390-3. (2009). Testing hardened concrete - Part 3: Compressive strength of test specimens.

Mwaikambo, L. (2006). Review of the History, Properties and Application of Plant Fibres. *African Journal of Science and Technology (AJST)*, Vol 7, No.2 pp 120-133.

Ntenga, R., Saidjo, S., Wakata, A., Djoda, P., Tango, M., & Mfoumou, E. (2022). Extraction, Applications and Characterization of Plant Fibers. *Natural Fiber*, 11-21.

Okeola, A., Abuodha, S., & Mwero, J. (2018). The Effect of Specimen Shape on the Mechanical Properties of Sisal Fiber-Reinforced Concrete. *The open civil engineering journal*, Vol. 12, No.1, pp. 368-382.

Onuaguluchi, O., & Banthia, N. (2016). Plant-Based Natural Fibre Reinforced Cement Composites: A Review. *Cement and Concrete Composites*, vol. 68, pp. 96–108.

P., S., K.S, K., T.P, S., S., A., & A.S, A. (2021). Fiber extraction and mechanical properties of Agave Americana/Kenaf fiber reinforced hybrid epoxy composite. *Materials today : proceedings*, Vol. 46, pp.8594-8601.

Pérez-Zavala, M. d., Hernández-Arzaba, J. C., Bideshi, D., & Barboza-Corona, J. (2020). Agave: a natural renewable resource with multiple applications. *Journal of the science of food and agriculture*, Vol.100, No.15, pp.5324-5333.

Pickering, K. (2008). *Properties and Performance of Natural-Fibre Composites.* Woodhead Publishing Limited.

Ramamoorthy, S., Skrifvars, M., & Persson, A. (2015). A Review of Natural Fibers Used in Biocomposites: Plant, Animal and Regenerated Cellulose Fibers. 11-21.

Rashmi Nayak, J., Bochen, J., & Gołaszewska, M. (2022). Experimental studies on the effect of natural and synthetic fibers on properties of fresh and hardened mortar. *Construction & building materials*, Vol.347.

Rayung, M., Ibrahim, N., Zainuddin, N., Saad, W., Razak, N., & Chieng, B. (2014). The Effect of Fiber Bleaching Treatment on the Properties of Poly(lactic acid)/Oil Palm Empty Fruit Bunch Fiber Composites. *International Journal of Molecular Sciences*, Vol.15, No.8, pp.14728-14742.

Rong, M., Zhang, M., Liu, Y., Yang, G., & Zeng, H. (2001). The effect of fiber treatment on the mechanical properties of unidirectional sisal-reinforced epoxy composites.

Savastano Junior, H., Fiorelli, J., & Dos Santos, S. (2017). *Sustainable and Nonconventional Construction Materials Using Inorganic Bonded Fiber Composites.* Cambridge: Elsevier Science & Technology.

Savastano, H., Agopyan, V., Nolasco, A., & Pimentel, L. (1999). Plant fibre reinforced cement components for roofing. *Construction & building materials*, Vol. 13, No.8, pp. 433-438.

SCC European Project Group. (2005). The European Guidelines for Self-Compacting Concrete.

Solai Mathi, S. ,. (2021). *Experimental investigation on self compacting concrete with sisal fibre.*

Subaida, E., Chandrakaran, S., & Sankar, N. (2009). Laboratory performance of unpaved roads reinforced with woven coir geotextiles. *Geotextiles and geomembranes*, Vol. 27, No.3, pp. 204-210.

Sugathan, A. (2017). Self Compacting Concrete Reinforced with Sisal Fibres. *International Journal of Latest Technology in Engineering, Management & Applied Science (IJLTEMAS)*, Vol. 6, No.7 , pp.180-187.

Toledo Filho, R., Ghavami, K., Sanjuán, M., & England, G. (2005). Free, restrained and drying shrinkage of cement mortar composites reinforced with vegetable fibres. *Cement & concrete composites*, Vol. 27, No.5, pp. 537-546.

Vella, A. (2018). *The Fresh Properties and Early Age Performance of Waste-Tyre Fibre Reinforced Self- Compacting Concrete. Dissertation Faculty for the Built Environment (Supervised by Prof Ruben Paul Borg).*

Yimer, T., & Gebre, A. (2023). Effect of Fiber Treatments on the Mechanical Properties of Sisal Fiber-Reinforced Concrete Composites. *Advances in Civil Engineering*, pp.1-15.

Zhang, M., Rong, M., & Lu, X. (2005). Fully biodegradable natural fiber composites from renewable resources: All-plant fiber composites. *Composites science and technology*, Vol.65, No.15, pp.2514-2525.

APPENDIX A

Material Specifications

BASF
We create chemistry

MasterGlenium SKY 698

Total Performance Control™

Second generation high range water reducing polycarboxylate ether admixture primarily developed for ready-mix concrete industry where high slump retention and a low W/C are required. It is suitable for hot weather conditions.

DESCRIPTION AND WHERE TO USE

MasterGlenium SKY 698 is an innovative second generation superplasticizer of polycarboxylic ether (PCE) polymers. It is derived directly from the Total Performance Control™ concept.

MasterGlenium SKY 698 is specially engineered for ready-mix Rheoplastic concrete having fluid consistence and self-compacting concrete, having a very high workability retention (> 90 minutes), especially under hot weather conditions. The fresh concrete shows no segregation and at the same time has a low water cement ratio and, consequently, high early and long term strengths as per EN 206-1 and UNI 11104 standards.

MasterGlenium SKY 698 may be used also to produce Rheodynamic concrete, capable of self compaction, even in the presence of dense reinforcement, without the aid of vibration.

MasterGlenium SKY 698 is chloride free, meets UNI EN 934-2, UNI EN 480 (1-2), UNI 10765, ASTM C 494 requirements for Type F and it is also compatible with all cements meeting the EN 197 and ASTM C 150 standards.

TOTAL PERFORMANCE CONTROL ™

The Total Performance Control™ concept ensures that ready-mix producers, contractors and engineers get a concrete that is of the same high quality as originally specified; starting from production at the batching plant, to the delivery and placing into the formworks and followed by its hardening process. Utilizing Rheodynamic™ concrete technology it provides a concrete mix with exceptional placing characteristics and accelerated cement hydration for early strength development and high-quality concrete.

THE CHEMISTRY OF MASTERGLENIUM SKY

The Total Performance Control™ concept is the result of years of study of an in-house expertise in nanotechnology. This allows BASF Construction Chemicals to control the chemical and physical behaviour of polymers and their interactions with cement. MasterGlenium SKY 698 is an innovative second generation superplasticiser of polycarboxylic ether (PCE) polymers. The dispersion effect of superplasticizers is based on the adsorption of molecules on cement particles, imparting a negative charge that causes electrostatic repulsion and steric hindrance between them and, therefore, causing dispersion.

The hydration, and particularly the ettringite formation, works against the superplasticiser.

The molecules already adsorbed are covered by the ettringite lawn and thus are ineffective.

The particular configuration of the MasterGlenium SKY molecules allows its delayed adsorption onto the cement particles and disperses them efficiently over a long period of time. The molecular structure is essential for the early development of strength. With superplasticizers based on conventional polycarboxylate ether, the molecules cover the entire surface of the cement grain and build a barrier against contact with water. Therefore, the hydration process takes place slowly. The MasterGlenium SKY molecules on the other hand leave sufficient surface of the cement exposed to allow contact with water for a rapid hydration reaction which results in high early strength development.

BENEFITS FOR READY-MIX PRODUCER

Total Performance Control and the use of MasterGlenium SKY 698 offers the following benefit to the ready-mix concrete producer:

- Reduction the water content with respect to the state of the art polycarboxylate based superplasticisers.
- Production of Rheoplastic and Rheodynamic concrete having a very low W/C.
- Workability retention for a longer period especially in hot weather conditions avoiding the problem of re-tempering with water before the pouring operation.
- Improvement of the rheology even in concrete mixes having a low fines content.
- Optimization of the production of durable concrete as per the EN 206-1 and UNI 11104 standards.
- As compared to the traditional superplasticisers, the engineering properties such as early and ultimate compressive and flexural strengths, bond to steel, and modulus of elasticity, shrinkage, creep, and impermeability are improved.

MASTER® BUILDERS SOLUTIONS

We create chemistry

MasterGlenium SKY 698

Total Performance Control™

COMPATIBILITY

In order to optimise some special properties of the concrete, use of the following complementary admixtures is suggested:

- air entraining agent **MasterAir** to improve freeze thaw resistance (exposure class XF1 to XF4, EN 206-1);
- silica fume, **MasterRoc MS 610**, for high performance concrete and to improve the durability in chemical aggressive environments (exposure class XA1 to XA3, EN 206-1)
- synthetic micro-fibres **MasterFiber 24** to prevent cracks due to plastic shrinkage;
- curing agent **MasterKure** for sealing the surface of freshly finished concrete against rapid evaporation of water which may cause plastic shrinkage cracking.
- demoulding agent MasterFinish for good surface appearance.

DIRECTIONS FOR USE

MasterGlenium SKY 698 is a liquid admixture to be added to the concrete during the mixing process:

- mix cement and secondary binders, sand, coarse aggregates and the mix water until a stiff, yet homogeneous, mixture is obtained;
- optimal mixing water reduction is obtained if MasterGlenium SKY 698 is mixed into the concrete right after the addition of the initial 80-90% of the total water;
- avoid adding the admixture to the dry aggregates;
- add MasterGlenium SKY 698 admixture and mix again for to 60 seconds in order to disperse it homogeneously;
- continue mixing until required workability is obtained, with addition of the remaining water.

MasterGlenium SKY 698 is not compatible with all admixtures of MasterRheobuild series.

Technical Information	
Form	Liquid
Relative density (g/cc at 20°C)	1.059 – 1.099

DOSAGE

MasterGlenium SKY 698 The recommended dosage rate range is 1.2 to 1.6 litres per 100 kg of binder.

Other dosages may be recommended in special cases according to specific job site conditions.
In such cases please consult our Technical Service Department for advice.

PACKAGING AND STORAGE

MasterGlenium SKY 698 is available in 10 litre cans, 1000 litre container or in bulk.
MasterGlenium SKY 698 must be stored in a place where the temperature does not drop below 5 °C. In case of freezing, warm up and homogenise the admixture solution before using.

BASF Construction Chemicals Italia Spa
Via Vicinale delle Corti, 21 – 31100 Treviso – Italy
T +39 0422 429200 F +39 0422 421802
http:// www.master-builders-solutions.basf.it e-mail: infomac@basf.com

CE

Supersedes all prior issues on this product.
December 2016

MASTER® BUILDERS SOLUTIONS

COLACEM
forte • sostenibile
Ragusa Cementi S.p.A. - Gruppo Colacem

Technical data sheet CEMENT

26/04/2023

CEM II/A-LL 42,5 R
Portland-limestone cement
Ragusa Plant (Italy)
Cement loaded: *MT 2600*
Vessel's name: *M/V NS Holland – v.313*
Loading port: *Pozzallo Italy*
B/L date: *23/03/2023*
Discharge port: *La Valletta - Malta*

Cement provided with:
- Certificate of constancy of performance 0970-CPR-0243/CE/0202 in accordance with EN 197-1 Standard
- Evaluation Document 0011/CR/19 in compliance with the Ministerial Decrees dated 10/05/2004 and 17/02/2005 (water-soluble chromium (VI) content of cement ≤ 2 ppm)

Chemical features

	unit	average ship	requirement in EN 197-1	method
Sulfate content (as SO_3)	%	**3,08**	≤ 4,00	EN 196-2
Chloride content (Cl^-)	%	**0,05**	≤ 0,10	EN 196-2

Physical features

	unit	average ship	requirement in EN 197-1	method
Initial setting time	min	**141**	≥ 60	EN 196-3
Soundness (expansion)	min	**0**	≤ 10	EN 196-3
Fineness (as Blaine specific surface)	cm^2/g	**3819**	n.a.	EN 196-6
Residue on 63 µm	%	**2,3**	n.a.	EN 196-3

Mechanical compressive strength

	unit	average ship	requirement in EN 197-1	method
Early strength at 2 days	MPa	**29,0**	≥ 20,0	EN 196-1
Std strength at 28 days	MPa	**51,7**	≥ 42,5 e ≤ 62,5 MPa	EN 196-1

Notes

1) Data sheet issued by the Quality Assurance Department in accordance with the company procedures and using the test results carried out by the Factory Laboratory.
2) For technical-commercial information: +39 075 924 00 24 assistenzaclienti@colacem.it

Plant Manager
(Mr. Nunzio TUMINO)
.....
(Signature)

www.colacem.it

solidbase LABORATORY LTD.

ISO 17025 ACCREDITED TESTING NAB- MALTA Nº 008

Test for the Determination of Cement Strength to MSA EN 196-1:2016

Client Information

Client	Central Cement Ltd	Client tel. No.	21232282	Certificate date	2023-04-25
Client Address	Cem House	Client fax No.	21221659	Certificate No.	2881
	National Road	Client ref No.	138239	Logbook ID	23/00642523/006425
	Blata-l-Bajda HMR 9011	Attn.	Sammut John Mr	Project	Central Cement Ltd - J064 - Cement: 23/006425

General Information

Shipment ID / Location	Holland 313	Shipment date	2023-03-27	Country of origin	N.A.
Truck No.	JBW 451	Delivery note No.	138239	Cement type	CEM II / A-LL 42.5R
Date received sample	2023-03-27	Date / time prisms cast	2023-03-28 07:00	Quantity of prisms	9
Compressive strength pace rate (N/s)	2400	Flexural pace rate (N/s)	50	Mix Ratio (H_2O : Cement : Sand)	0.5:1:3
No. of layers	2	Jolts per layer	60	Laboratory temp. (°C)	20

Test Results

	Prisms Pre-Test Data					Flexural Strength Test					Compressive Strength Test				
Sample No.	L (mm)	B (mm)	H (mm)	Weight (g)	Flatness	Test Date / Time	Age (Days)	Ft (N)	l (mm)	Rt (N/mm²)	Plattens (mm²)	F_C Part A (N)	R_C Part A (N/mm²)	F_C Part B (N)	R_C Part B (N/mm²)
M23/00549	160	40	40	602	good	2023-04-25 07:00	28	3850	100	9.0	1600	83360	52.1	83300	52.1
M23/00548	160	40	40	600	good	2023-04-25 07:00	28	3940	100	9.2	1600	83790	52.4	84940	53.1
M23/00547	160	40	40	601	good	2023-04-25 07:00	28	3960	100	9.3	1600	83730	52.3	85180	53.2
M23/00546	160	40	40	599	good	2023-04-04 07:00	7	3360	100	7.9	1600	63240	39.5	61370	38.4
M23/00545	160	40	40	601	good	2023-04-04 07:00	7	3160	100	7.4	1600	61760	38.6	62680	39.2
M23/00544	160	40	40	601	good	2023-04-04 07:00	7	3160	100	7.4	1600	63970	40.0	61270	38.3
M23/00543	160	40	40	595	good	2023-03-30 07:00	2	2970	100	7.0	1600	48420	30.3	49070	30.7
M23/00542	160	40	40	598	good	2023-03-30 07:00	2	2780	100	6.5	1600	44810	28.0	47050	29.4
M23/00541	160	40	40	597	good	2023-03-30 07:00	2	2730	100	6.4	1600	48010	30.0	45690	28.6

F_t	Load applied to the middle of the prism at fracture
l	Span-rods
R_t	Flexural strength
F_C - Part A	Failure load for compression test of first part of prism
R_C - Part A	Compressive strength of first part of prism
F_C - Part B	Failure load for compression test of second part of prism
R_C - Part B	Compressive strength of second part of prism

Blaine Fineness Test (cm^2/g): 4491.48

Initial setting time: Final setting time:

NB: An NAB-MALTA accredited Testing Laboratory Reg. No. 008
Accreditation applies to the Compressive and Machine operations.

Deviations from standard None

Comments None

Darmanin Gilbert
Laboratory Manager

Tal-Handaq Industrial Estate, N/S in Handaq Road, Qormi, QRM 4000, Malta.
T: (356) 2149 2807/8
F: (356) 2149 2810
E: info@solidbasemalta.com
W: www.solidbasemalta.com
Co. No.: C 33162
VAT No.: MT 1695 3537

The expanded level of uncertainty is less than 0.1%. The uncertainty evaluation has been carried out in accordance with NAB-Malta requirements.

solidbase LABORATORY LTD.

ISO/IEC 17025 ACCREDITED TESTING N° 008 NAB- MALTA

Aggregate Test Report

Client Name:	Central Cement Ltd		
Client Address:	Cem House	Certificate Date:	2023-02-24
	National Road	Certificate No:	2869
	Blata-l-Bajda HMR 9011	Client Ref:	
Client Tel No:	21232282	Logbook ID	23/003228
Client Fax No:	21221659	Project:	Central Cement Ltd - J064
Attn:	Sammut John Mr		

Sampling

Test carried out to EN 932-1:1997

Supplier	Central Cement Ltd	Location of sampling	Moon 3
Date sampled	2023-02-21	Sampled by	
Material type	0-4mm	Date received	2023-02-21
Material description	Dolomite Sand		
Comments	Receipt No.: 138226, Truck No.: JBW 451		
Deviations	Sampled by client		

Particle Size Distribution

Test carried out to EN 933-1:2012

Sieve Size (mm)	Passing %	Upper Limit	Lower Limit
8.0	100.0	0.0	0.0
6.3	100.0	0.0	0.0
4.0	94.0	0.0	0.0
2.0	66.0	0.0	0.0
1.0	41.0	0.0	0.0
0.25	18.0	0.0	0.0
0.063	10.0	0.0	0.0

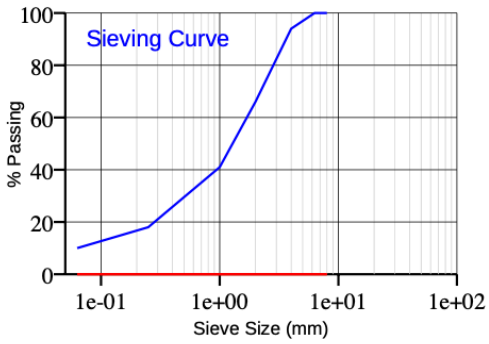

Fines content	10.3%
Fineness modulus	2.7
Method of analysis	wet sieving
Comment	None
Deviation	None

Moisture Content

Test carried out to EN 1097-5:2008

Moisture content	0.83%		
Technician	Camilleri Nathan	Date tested	2023-02-23
Comments	None		
Deviation	None		

Tal-Handaq Industrial Estate,
N/S in Handaq Road,
Qormi, QRM 4000, Malta.
T: (356) 2149 2807/8
F: (356) 2149 2810
E: info@solidbasemalta.com
W: www.solidbasemalta.com
Co. No.: C 33162
VAT No.: MT 1695 3537

solidbase LABORATORY LTD.

ISO/IEC 17025 ACCREDITED TESTING N° 008 NAB- MALTA

Relative Density

Test carried out to EN 1097-6:2022

Method used		Pyknometer method pass 4mm, retain 63µm	
Mass of dry portion (g)		390.21	
Apparent particle density (ρ_{a}) (Mg/m^3)*		2.77	
Oven dry particle density (ρ_{rd}) (Mg/m^3)*		2.75	
Saturated surface-dried particle density (ρ_{ssd}) (Mg/m^3)*		2.76	
Water absorption (WA_{24}) (%)		0.3	
Technician	Atif Hanif	Date tested	2023-02-24
Comments	None		
Deviation	None		

Darmanin Gilbert
Laboratory Manager

Tal-Handaq Industrial Estate,
N/S in Handaq Road,
Qormi, QRM 4000, Malta.

T: (356) 2149 2807/8
F: (356) 2149 2810
E: info@solidbasemalta.com
W: www.solidbasemalta.com

Co. No.: C 33162
VAT No.: MT 1695 3537

solidbase LABORATORY LTD.

ISO/IEC 17025 ACCREDITED TESTING NAB- MALTA N° 008

Aggregate Test Report

Client Name:	Central Cement Ltd		
Client Address:	Cem House	Certificate Date:	2023-02-24
	National Road	Certificate No:	2870
	Blata-l-Bajda HMR 9011	Client Ref:	
Client Tel No:	21232282	Logbook ID	23/003229
Client Fax No:	21221659	Project:	Central Cement Ltd - J064
Attn:	Sammut John Mr		

Sampling

Test carried out to EN 932-1:1997

Supplier	Central Cement Ltd	Location of sampling	Moon 3
Date sampled	2023-02-21	Sampled by	
Material type	4-10mm	Date received	2023-02-21
Material description	Dolomite Gravel		
Comments	Receipt No.: 138227, Truck No.: JBW 451		
Deviations	Sampled by client		

Particle Size Distribution

Test carried out to EN 933-1:2012

Sieve Size (mm)	Passing %	Upper Limit	Lower Limit
20.0	100.0	0.0	0.0
14.0	100.0	0.0	0.0
10.0	100.0	0.0	0.0
8.0	65.0	0.0	0.0
4.0	10.0	0.0	0.0
2.0	4.0	0.0	0.0
0.063	2.0	0.0	0.0

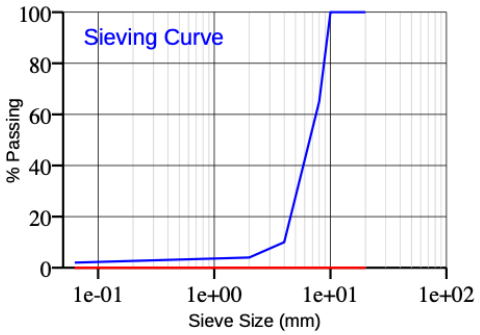

Fines content	2.3%
Fineness modulus	3.2
Method of analysis	wet sieving
Comment	None
Deviation	None

Moisture Content

Test carried out to EN 1097-5:2008

Moisture content	0.66%		
Technician	Camilleri Nathan	Date tested	2023-02-23
Comments	None		
Deviation	None		

Tal-Handaq Industrial Estate,
N/S in Handaq Road,
Qormi, QRM 4000, Malta.
T: (356) 2149 2807/8
F: (356) 2149 2810
E: info@solidbasemalta.com
W: www.solidbasemalta.com
Co. No.: C 33162
VAT No.: MT 1695 3537

solidbase LABORATORY LTD.

ISO/IEC 17025 ACCREDITED TESTING NAB- MALTA N° 008

Relative Density

Test carried out to EN 1097-6:2022

Method used		Pyknometer method pass 31.5mm, retain 4mm	
Mass of dry portion (g)		1444.57	
Apparent particle density (ρno_a) (Mg/m^3)*		2.84	
Oven dry particle density (ρ_{rd}) (Mg/m^3)*		2.83	
Saturated surface-dried particle density (ρ_{ssd}) (Mg/m^3)*		2.83	
Water absorption (WA_{24}) (%)		0.2	
Technician	Atif Hanif	Date tested	2023-02-24
Comments	None		
Deviation	None		

Aggregate Abrasion Value by Los Angeles

Test carried out to EN 1097-2:2020

No. of balls used in charge		9	
Size fraction of test portions		6.3 - 10mm : 100.0%	
Los Angeles Coefficient (LA)		17.8	
Technician	Atif Hanif	Date tested	2023-02-24
Comments	None		
Deviation	None		

Darmanin Gilbert
Laboratory Manager

Tal-Handaq Industrial Estate,
N/S in Handaq Road,
Qormi, QRM 4000, Malta.
T: (356) 2149 2807/8
F: (356) 2149 2810
E: info@solidbasemalta.com
W: www.solidbasemalta.com
Co. No.: C 33162
VAT No.: MT 1695 3537

Safety data sheet

according to Regulation (EC) No. 1907/2006 (REACH)

Hydrogen peroxide 5 %

article number: **1YT3**
Version: **1.0 en**

date of compilation: 18.01.2023

SECTION 1: Identification of the substance/mixture and of the company/ undertaking

1.1 Product identifier

Identification of the substance	**Hydrogen peroxide** 5 %
Article number	1YT3
Registration number (REACH)	not relevant (mixture)

1.2 Relevant identified uses of the substance or mixture and uses advised against

Relevant identified uses:	Laboratory and analytical use Laboratory chemical
Uses advised against:	Do not use for products which come into contact with foodstuffs. Do not use for private purposes (household).

1.3 Details of the supplier of the safety data sheet

Carl Roth GmbH + Co KG
Schoemperlenstr. 3-5
D-76185 Karlsruhe
Germany

Telephone:+49 (0) 721 - 56 06 0
Telefax: +49 (0) 721 - 56 06 149
e-mail: sicherheit@carlroth.de
Website: www.carlroth.de

Competent person responsible for the safety data sheet:	:Department Health, Safety and Environment
e-mail (competent person):	**sicherheit@carlroth.de**

1.4 Emergency telephone number

SECTION 2: Hazards identification

2.1 Classification of the substance or mixture

Classification according to Regulation (EC) No 1272/2008 (CLP)

Section	Hazard class	Cat-egory	Hazard class and category	Hazard statement
3.3	Serious eye damage/eye irritation	2	Eye Irrit. 2	H319

For full text of abbreviations: see SECTION 16

2.2 Label elements

Labelling according to Regulation (EC) No 1272/2008 (CLP)

Signal word **Warning**

Pictograms

GHS07

Hazard statements

H319 Causes serious eye irritation

Precautionary statements

Precautionary statements - prevention

P280 Wear protective gloves/eye protection

Precautionary statements - response

P305+P351+P338 IF IN EYES: Rinse cautiously with water for several minutes. Remove contact lenses, if present and easy to do. Continue rinsing

P337+P313 If eye irritation persists: Get medical advice/attention

Labelling of packages where the contents do not exceed 125 ml

Signal word: **Warning**

Symbol(s)

2.3 Other hazards

Results of PBT and vPvB assessment

This mixture does not contain any substances that are assessed to be a PBT or a vPvB.

SECTION 3: Composition/information on ingredients

3.1 Substances

not relevant (mixture)

3.2 Mixtures

Description of the mixture

Name of sub-stance	Identifier	Wt%	Classification acc. to GHS	Pictograms	Notes
Hydrogen peroxide solution ... %	CAS No 7722-84-1 EC No 231-765-0 Index No 008-003-00-9 REACH Reg. No 01-2119485845-22-xxxx	5	Ox. Liq. 1 / H271 Acute Tox. 4 / H302 Acute Tox. 4 / H332 Skin Corr. 1A / H314 Eye Dam. 1 / H318 STOT SE 3 / H335 Aquatic Chronic 3 / H412		B(a) GHS-HC

Notes

B(a): The classification refers to an aqueous solution
GHS-HC: Harmonised classification (the classification of the substance corresponds to the entry in the list according to 1272/2008/EC, Annex VI)

Name of substance	Identifier	Specific Conc. Limits	M-Factors	ATE	Exposure route
Hydrogen peroxide solution ... %	CAS No 7722-84-1 EC No 231-765-0 Index No 008-003-00-9	Ox. Liq. 1; H271: C ≥ 70 % Ox. Liq. 2; H272: 50 % ≤ C < 70 % Skin Corr. 1A; H314: C ≥ 70 % Skin Corr. 1B; H314: 50 % ≤ C < 70 % Skin Irrit. 2; H315: 35 % ≤ C < 50 % Eye Dam. 1; H318: C ≥ 8 % Eye Irrit. 2; H319: 5 % ≤ C < 8 % STOT SE 3; H335: C ≥ 35 %	-	500 $^{mg}/_{kg}$ 11 $^{mg}/_{l}$/4h	oral inhalation: vapour

For full text of abbreviations: see SECTION 16

SECTION 4: First aid measures

4.1 Description of first aid measures

General notes

Take off contaminated clothing.

Following inhalation

Provide fresh air. In all cases of doubt, or when symptoms persist, seek medical advice.

Following skin contact

Rinse skin with water/shower. In all cases of doubt, or when symptoms persist, seek medical advice.

Following eye contact

Irrigate copiously with clean, fresh water for at least 10 minutes, holding the eyelids apart. In case of eye irritation consult an ophthalmologist.

Following ingestion

Rinse mouth. Call a doctor if you feel unwell.

4.2 Most important symptoms and effects, both acute and delayed

Irritation

4.3 Indication of any immediate medical attention and special treatment needed

none

SECTION 5: Firefighting measures

5.1 Extinguishing media

Suitable extinguishing media

co-ordinate firefighting measures to the fire surroundings
water spray, alcohol resistant foam, dry extinguishing powder, BC-powder, carbon dioxide (CO_2)

Unsuitable extinguishing media

water jet

5.2 Special hazards arising from the substance or mixture

Non-combustible.

5.3 Advice for firefighters

In case of fire and/or explosion do not breathe fumes. Fight fire with normal precautions from a reasonable distance. Wear self-contained breathing apparatus.

SECTION 6: Accidental release measures

6.1 Personal precautions, protective equipment and emergency procedures

For non-emergency personnel

Avoid contact with skin, eyes and clothes. Do not breathe vapour/spray.

6.2 Environmental precautions

Keep away from drains, surface and ground water.

6.3 Methods and material for containment and cleaning up

Advice on how to contain a spill

Covering of drains.

Advice on how to clean up a spill

Absorb with liquid-binding material (sand, diatomaceous earth, acid- or universal binding agents).

Other information relating to spills and releases

Place in appropriate containers for disposal. Ventilate affected area.

6.4 Reference to other sections

Hazardous combustion products: see section 5. Personal protective equipment: see section 8. Incompatible materials: see section 10. Disposal considerations: see section 13.

SECTION 7: Handling and storage

7.1 Precautions for safe handling

No special measures are necessary.

Advice on general occupational hygiene

Wash hands before breaks and after work. Keep away from food, drink and animal feedingstuffs.

7.2 Conditions for safe storage, including any incompatibilities

Keep container tightly closed. May cause decomposition by long-term light influence.

Incompatible substances or mixtures

Observe hints for combined storage.

Protect against external exposure, such as

UV-radiation/sunlight

Consideration of other advice:

Specific designs for storage rooms or vessels

Do not keep the container sealed.
Recommended storage temperature: 15 – 25 °C

7.3 Specific end use(s)

No information available.

SECTION 8: Exposure controls/personal protection

8.1 Control parameters

National limit values

Occupational exposure limit values (Workplace Exposure Limits)

This information is not available.

Relevant DNELs of components of the mixture

Name of substance	CAS No	End-point	Threshold level	Protection goal, route of exposure	Used in	Exposure time
Hydrogen peroxide solution ... %	7722-84-1	DNEL	1,4 mg/m³	human, inhalatory	worker (industry)	chronic - local effects
Hydrogen peroxide solution ... %	7722-84-1	DNEL	3 mg/m³	human, inhalatory	worker (industry)	acute - local effects

Relevant PNECs of components of the mixture

Name of substance	CAS No	End-point	Threshold level	Organism	Environmental compartment	Exposure time
Hydrogen peroxide solution ... %	7722-84-1	PNEC	0,0138 mg/l	aquatic organisms	water	intermittent release
Hydrogen peroxide solution ... %	7722-84-1	PNEC	0,013 mg/l	aquatic organisms	freshwater	short-term (single instance)
Hydrogen peroxide solution ... %	7722-84-1	PNEC	0,013 mg/l	aquatic organisms	marine water	short-term (single instance)
Hydrogen peroxide solution ... %	7722-84-1	PNEC	4,66 mg/l	aquatic organisms	sewage treatment plant (STP)	short-term (single instance)
Hydrogen peroxide solution ... %	7722-84-1	PNEC	0,047 mg/kg	aquatic organisms	freshwater sediment	short-term (single instance)
Hydrogen peroxide solution ... %	7722-84-1	PNEC	0,047 mg/kg	aquatic organisms	marine sediment	short-term (single instance)
Hydrogen peroxide solution ... %	7722-84-1	PNEC	0,002 mg/kg	terrestrial organisms	soil	short-term (single instance)

8.2 Exposure controls

Individual protection measures (personal protective equipment)

Eye/face protection

Use safety goggle with side protection.

Skin protection

• hand protection

Wear suitable gloves. Chemical protection gloves are suitable, which are tested according to EN 374. For special purposes, it is recommended to check the resistance to chemicals of the protective gloves mentioned above together with the supplier of these gloves. The times are approximate values from measurements at 22 ° C and permanent contact. Increased temperatures due to heated substances, body heat etc. and a reduction of the effective layer thickness by stretching can lead to a considerable reduction of the breakthrough time. If in doubt, contact manufacturer. At an approx. 1.5 times larger / smaller layer thickness, the respective breakthrough time is doubled / halved. The data apply only to the pure substance. When transferred to substance mixtures, they may only be considered as a guide.

• type of material

NBR (Nitrile rubber)

• material thickness

>0,11 mm

• breakthrough times of the glove material

>480 minutes (permeation: level 6)

• other protection measures

Take recovery periods for skin regeneration. Preventive skin protection (barrier creams/ointments) is recommended.

Respiratory protection

Respiratory protection necessary at: Aerosol or mist formation. P1 (filters at least 80 % of airborne particles, colour code: White).

Environmental exposure controls

Keep away from drains, surface and ground water.

SECTION 9: Physical and chemical properties

9.1 Information on basic physical and chemical properties

Physical state	liquid
Colour	colourless
Odour	characteristic
Melting point/freezing point	~0 °C
Boiling point or initial boiling point and boiling range	~100 °C at 1.013 hPa
Flammability	non-combustible
Lower and upper explosion limit	not determined
Flash point	not determined

Auto-ignition temperature	not determined
Decomposition temperature	not relevant
pH (value)	not determined
Kinematic viscosity	not determined
Solubility(ies)	
Water solubility	miscible in any proportion
Partition coefficient	
Partition coefficient n-octanol/water (log value):	not relevant (inorganic)
Vapour pressure	23 hPa at 20 °C
Density and/or relative density	
Density	1,01 $^{g}/_{cm^3}$ at 20 °C
Relative vapour density	information on this property is not available
Particle characteristics	not relevant (liquid)
Other safety parameters	
Oxidising properties	none

9.2 Other information

Information with regard to physical hazard classes:	hazard classes acc. to GHS (physical hazards): not relevant
Other safety characteristics:	
Miscibility	completely miscible with water

SECTION 10: Stability and reactivity

10.1 Reactivity

This material is not reactive under normal ambient conditions.

10.2 Chemical stability

The material is stable under normal ambient and anticipated storage and handling conditions of temperature and pressure.

10.3 Possibility of hazardous reactions

Violent reaction with: Alkali metals

10.4 Conditions to avoid

There are no specific conditions known which have to be avoided.

10.5 Incompatible materials

There is no additional information.

10.6 Hazardous decomposition products

Hazardous combustion products: see section 5.

SECTION 11: Toxicological information

11.1 Information on hazard classes as defined in Regulation (EC) No 1272/2008

Test data are not available for the complete mixture.

Classification procedure

The method for classification of the mixture is based on ingredients of the mixture (additivity formula).

Classification according to GHS (1272/2008/EC, CLP)

Acute toxicity

Shall not be classified as acutely toxic.

Acute toxicity estimate (ATE) of components of the mixture

Name of substance	CAS No	Exposure route	ATE
Hydrogen peroxide solution ... %	7722-84-1	oral	500 $^{mg}/_{kg}$
Hydrogen peroxide solution ... %	7722-84-1	inhalation: vapour	11 $^{mg}/_{l}$/4h

Acute toxicity of components of the mixture

Name of substance	CAS No	Exposure route	Endpoint	Value	Species
Hydrogen peroxide solution ... %	7722-84-1	oral	LD50	693,7 $^{mg}/_{kg}$	rat
Hydrogen peroxide solution ... %	7722-84-1	oral	LD50	1.026 $^{mg}/_{kg}$	rat
Hydrogen peroxide solution ... %	7722-84-1	dermal	LD50	>2.000 $^{mg}/_{kg}$	rabbit

Skin corrosion/irritation

Shall not be classified as corrosive/irritant to skin.

Serious eye damage/eye irritation

Causes serious eye irritation.

Respiratory or skin sensitisation

Shall not be classified as a respiratory or skin sensitiser.

Germ cell mutagenicity

Shall not be classified as germ cell mutagenic.

Carcinogenicity

Shall not be classified as carcinogenic.

Reproductive toxicity

Shall not be classified as a reproductive toxicant.

Specific target organ toxicity - single exposure

Shall not be classified as a specific target organ toxicant (single exposure).

Specific target organ toxicity - repeated exposure

Shall not be classified as a specific target organ toxicant (repeated exposure).

Aspiration hazard

Shall not be classified as presenting an aspiration hazard.

Symptoms related to the physical, chemical and toxicological characteristics

• If swallowed

Data are not available.

• If in eyes

Causes serious eye irritation

• If inhaled

Data are not available.

• If on skin

Frequently or prolonged contact with skin may cause dermal irritation

• Other information

none

11.2 Endocrine disrupting properties

None of the ingredients are listed.

11.3 Information on other hazards

There is no additional information.

SECTION 12: Ecological information

12.1 Toxicity

Shall not be classified as hazardous to the aquatic environment.

Aquatic toxicity (acute) of components of the mixture

Name of substance	CAS No	Endpoint	Value	Species	Exposure time
Hydrogen peroxide solution ... %	7722-84-1	LC50	16,4 $^{mg}/_{l}$	fish	96 h
Hydrogen peroxide solution ... %	7722-84-1	ErC50	1,38 $^{mg}/_{l}$	algae	72 h

Aquatic toxicity (chronic) of components of the mixture

Name of substance	CAS No	Endpoint	Value	Species	Exposure time
Hydrogen peroxide solution ... %	7722-84-1	EC50	466 $^{mg}/_{l}$	microorganisms	30 min

12.2 Persistence and degradability

Data are not available.

12.3 Bioaccumulative potential

Data are not available.

12.4 Mobility in soil

Data are not available.

12.5 Results of PBT and vPvB assessment

Data are not available.

12.6 Endocrine disrupting properties

None of the ingredients are listed.

12.7 Other adverse effects

Data are not available.

SECTION 13: Disposal considerations

13.1 Waste treatment methods

This material and its container must be disposed of as hazardous waste. Dispose of contents/container in accordance with local/regional/national/international regulations.

Sewage disposal-relevant information

Do not empty into drains.

13.2 Relevant provisions relating to waste

The allocation of waste identity numbers/waste descriptions must be carried out according to the EEC, specific to the industry and process.

Properties of waste which render it hazardous

HP 8 corrosive

13.3 Remarks

Waste shall be separated into the categories that can be handled separately by the local or national waste management facilities. Please consider the relevant national or regional provisions.

SECTION 14: Transport information

14.1	**UN number or ID number**	not subject to transport regulations
14.2	**UN proper shipping name**	not assigned
14.3	**Transport hazard class(es)**	none
14.4	**Packing group**	not assigned
14.5	**Environmental hazards**	non-environmentally hazardous acc. to the dangerous goods regulations

14.6 Special precautions for user

There is no additional information.

14.7 Maritime transport in bulk according to IMO instruments

The cargo is not intended to be carried in bulk.

14.8 Information for each of the UN Model Regulations

International Maritime Dangerous Goods Code (IMDG) - Additional information

Not subject to IMDG.

International Civil Aviation Organization (ICAO-IATA/DGR) - Additional information

Not subject to ICAO-IATA.

SECTION 15: Regulatory information

15.1 Safety, health and environmental regulations/legislation specific for the substance or mixture

Relevant provisions of the European Union (EU)

Restrictions according to REACH, Annex XVII

Dangerous substances with restrictions (REACH, Annex XVII)

Name of substance	Name acc. to inventory	CAS No	Restriction	No
Hydrogen peroxide	this product meets the criteria for classification in accordance with Regulation No 1272/2008/EC		R3	3
Hydrogen peroxide solution ... %	substances in tattoo inks and permanent make-up		R75	75

Legend

R3 1. Shall not be used in:
- ornamental articles intended to produce light or colour effects by means of different phases, for example in ornamental lamps and ashtrays,
- tricks and jokes,
- games for one or more participants, or any article intended to be used as such, even with ornamental aspects,
2. Articles not complying with paragraph 1 shall not be placed on the market.
3. Shall not be placed on the market if they contain a colouring agent, unless required for fiscal reasons, or perfume, or both, if they:
— can be used as fuel in decorative oil lamps for supply to the general public, and
— present an aspiration hazard and are labelled with H304.
4. Decorative oil lamps for supply to the general public shall not be placed on the market unless they conform to the European Standard on Decorative oil lamps (EN 14059) adopted by the European Committee for Standardisation (CEN).
5. Without prejudice to the implementation of other Union provisions relating to the classification, labelling and packaging of substances and mixtures, suppliers shall ensure, before the placing on the market, that the following requirements are met:
(a) lamp oils, labelled with H304, intended for supply to the general public are visibly, legibly and indelibly marked as follows: "Keep lamps filled with this liquid out of the reach of children"; and, by 1 December 2010, "Just a sip of lamp oil – or even sucking the wick of lamps – may lead to life-threatening lung damage";
(b) grill lighter fluids, labelled with H304, intended for supply to the general public are legibly and indelibly marked by 1 December 2010 as follows: 'Just a sip of grill lighter fluid may lead to life threatening lung damage';
(c) lamps oils and grill lighters, labelled with H304, intended for supply to the general public are packaged in black opaque containers not exceeding 1 litre by 1 December 2010.';

Legend

R75 1. Shall not be placed on the market in mixtures for use for tattooing purposes, and mixtures containing any such substances shall not be used for tattooing purposes, after 4 January 2022 if the substance or substances in question is or are present in the following circumstances:
(a) in the case of a substance classified in Part 3 of Annex VI to Regulation (EC) No 1272/2008 as carcinogen category 1A, 1B or 2, or germ cell mutagen category 1A, 1B or 2, the substance is present in the mixture in a concentration equal to or greater than 0,00005 % by weight;
(b) in the case of a substance classified in Part 3 of Annex VI to Regulation (EC) No 1272/2008 as reproductive toxicant category 1A, 1B or 2, the substance is present in the mixture in a concentration equal to or greater than 0,001 % by weight;
(c) in the case of a substance classified in Part 3 of Annex VI to Regulation (EC) No 1272/2008 as skin sensitiser category 1, 1A or 1B, the substance is present in the mixture in a concentration equal to or greater than 0,001 % by weight;
(d) in the case of a substance classified in Part 3 of Annex VI to Regulation (EC) No 1272/2008 as skin corrosive category 1, 1A, 1B or 1C or skin irritant category 2, or as serious eye damage category 1 or eye irritant category 2, the substance is present in the mixture in a concentration equal to or greater than:
(i) 0,1 % by weight, if the substance is used solely as a pH regulator;
(ii) 0,01 % by weight, in all other cases;
(e) in the case of a substance listed in Annex II to Regulation (EC) No 1223/2009 (*1), the substance is present in the mixture in a concentration equal to or greater than 0,00005 % by weight;
(f) in the case of a substance for which a condition of one or more of the following kinds is specified in column g (Product type, Body parts) of the table in Annex IV to Regulation (EC) No 1223/2009, the substance is present in the mixture in a concentration equal to or greater than 0,00005 % by weight:
(i) “Rinse-off products”;
(ii) “Not to be used in products applied on mucous membranes”;
(iii) “Not to be used in eye products”;
(g) in the case of a substance for which a condition is specified in column h (Maximum concentration in ready for use preparation) or column i (Other) of the table in Annex IV to Regulation (EC) No 1223/2009, the substance is present in the mixture in a concentration, or in some other way, that does not accord with the condition specified in that column;
(h) in the case of a substance listed in Appendix 13 to this Annex, the substance is present in the mixture in a concentration equal to or greater than the concentration limit specified for that substance in that Appendix.
2. For the purposes of this entry use of a mixture “for tattooing purposes” means injection or introduction of the mixture into a person’s skin, mucous membrane or eyeball, by any process or procedure (including procedures commonly referred to as permanent make-up, cosmetic tattooing, micro-blading and micro-pigmentation), with the aim of making a mark or design on his or her body.
3. If a substance not listed in Appendix 13 falls within more than one of points (a) to (g) of paragraph 1, the strictest concentration limit laid down in the points in question shall apply to that substance. If a substance listed in Appendix 13 also falls within one or more of points (a) to (g) of paragraph 1, the concentration limit laid down in point (h) of paragraph 1 shall apply to that substance.
4. By way of derogation, paragraph 1 shall not apply to the following substances until 4 January 2023:
(a) Pigment Blue 15:3 (CI 74160, EC No 205-685-1, CAS No 147-14-8);
(b) Pigment Green 7 (CI 74260, EC No 215-524-7, CAS No 1328-53-6).
5. If Part 3 of Annex VI to Regulation (EC) No 1272/2008 is amended after 4 January 2021 to classify or re-classify a substance such that the substance then becomes caught by point (a), (b), (c) or (d) of paragraph 1 of this entry, or such that it then falls within a different one of those points from the one within which it fell previously, and the date of application of that new or revised classification is after the date referred to in paragraph 1 or, as the case may be, paragraph 4 of this entry, that amendment shall, for the purposes of applying this entry to that substance, be treated as taking effect on the date of application of that new or revised classification.
6. If Annex II or Annex IV to Regulation (EC) No 1223/2009 is amended after 4 January 2021 to list or change the listing of a substance such that the substance then becomes caught by point (e), (f) or (g) of paragraph 1 of this entry, or such that it then falls within a different one of those points from the one within which it fell previously, and the amendment takes effect after the date referred to in paragraph 1 or, as the case may be, paragraph 4 of this entry, that amendment shall, for the purposes of applying this entry to that substance, be treated as taking effect from the date falling 18 months after entry into force of the act by which that amendment was made.
7. Suppliers placing a mixture on the market for use for tattooing purposes shall ensure that, after 4 January 2022, the mixture is marked with the following information:
(a) the statement “Mixture for use in tattoos or permanent make-up”;
(b) a reference number to uniquely identify the batch;
(c) the list of ingredients in accordance with the nomenclature established in the glossary of common ingredient names pursuant to Article 33 of Regulation (EC) No 1223/2009, or in the absence of a common ingredient name, the IUPAC name. In the absence of a common ingredient name or IUPAC name, the CAS and EC number. Ingredients shall be listed in descending order by weight or volume of the ingredients at the time of formulation. “Ingredient” means any substance added during the process of formulation and present in the mixture for use for tattooing purposes. Impurities shall not be regarded as ingredients. If the name of a substance, used as ingredient within the meaning of this entry, is already required to be stated on the label in accordance with Regulation (EC) No 1272/2008, that ingredient does not need to be marked in accordance with this Regulation;
(d) the additional statement “pH regulator” for substances falling under point (d)(i) of paragraph 1;
(e) the statement "Contains nickel. Can cause allergic reactions." if the mixture contains nickel below the concentration limit specified in Appendix 13;
(f) the statement "Contains chromium (VI). Can cause allergic reactions." if the mixture contains chromium (VI) below the concentration limit specified in Appendix 13;
(g) safety instructions for use insofar as they are not already required to be stated on the label by Regulation (EC) No 1272/2008.
The information shall be clearly visible, easily legible and marked in a way that is indelible.
The information shall be written in the official language(s) of the Member State(s) where the mixture is placed on the market, unless the Member State(s) concerned provide(s) otherwise.
Where necessary because of the size of the package, the information listed in the first subparagraph, except for point (a), shall be included instead in the instructions for use.
Before using a mixture for tattooing purposes, the person using the mixture shall provide the person undergoing the procedure with the information marked on the package or included in the instructions for use pursuant to this paragraph.
8. Mixtures that do not contain the statement “Mixture for use in tattoos or permanent make-up” shall not be used for tattooing purposes.

Legend

9. This entry does not apply to substances that are gases at temperature of 20 °C and pressure of 101,3 kPa, or generate a vapour pressure of more than 300 kPa at temperature of 50 °C, with the exception of formaldehyde (CAS No 50-00-0, EC No 200-001-8).
10. This entry does not apply to the placing on the market of a mixture for use for tattooing purposes, or to the use of a mixture for tattooing purposes, when placed on the market exclusively as a medical device or an accessory to a medical device, within the meaning of Regulation (EU) 2017/745, or when used exclusively as a medical device or an accessory to a medical device, within the same meaning. Where the placing on the market or use may not be exclusively as a medical device or an accessory to a medical device, the requirements of Regulation (EU) 2017/745 and of this Regulation shall apply cumulatively.

List of substances subject to authorisation (REACH, Annex XIV)/SVHC - candidate list

None of the ingredients are listed.

Seveso Directive

2012/18/EU (Seveso III)			
No	**Dangerous substance/hazard categories**	**Qualifying quantity (tonnes) for the application of lower and upper-tier requirements**	**Notes**
	not assigned		

Deco-Paint Directive

VOC content	0 % 0 $^{g}/_{l}$

Industrial Emissions Directive (IED)

VOC content	0 %
VOC content (Water content was discounted)	0 $^{g}/_{l}$

Directive on the restriction of the use of certain hazardous substances in electrical and electronic equipment (RoHS)

none of the ingredients are listed

Regulation concerning the establishment of a European Pollutant Release and Transfer Register (PRTR)

none of the ingredients are listed

Water Framework Directive (WFD)

List of pollutants (WFD)				
Name of substance	**Name acc. to inventory**	**CAS No**	**Listed in**	**Remarks**
Hydrogen peroxide solution ... %	Substances and preparations, or the breakdown products of such, which have been proved to possess carcinogenic or mutagenic properties or properties which may affect steroidogenic, thyroid, reproduction or other endocrine-related functions in or via the aquatic environment		a)	

Legend

A) Indicative list of the main pollutants

Regulation on the marketing and use of explosives precursors

Explosives precursors which are subject to restrictions						
Name of substance	**CAS No**	**Wt%**	**Type of registration**	**Re-marks**	**Limit value**	**Upper limit value for the pur-pose of licens-ing un-der Art-icle 5(3)**
Hydrogen peroxide solution ... %	7722-84-1	5	Annex I		12 % w/w	35 % w/w

Legend

annex I Substances which shall not be made available to members of the general public on their own, or in mixtures or substances including them, except if the concentration is equal to or lower than the limit values set out below

Additional statements

If the product is passed on to third parties, in accordance with Article 7 "Notification of the supply chain" of Regulation EU 2019/1148, the information obligation is subject to the entire supply chain and all other provisions mentioned in Article 7 on restricted and regulated raw materials.

Regulation on drug precursors

none of the ingredients are listed

Regulation on substances that deplete the ozone layer (ODS)

none of the ingredients are listed

Regulation concerning the export and import of hazardous chemicals (PIC)

none of the ingredients are listed

Regulation on persistent organic pollutants (POP)

none of the ingredients are listed

Other information

Directive 94/33/EC on the protection of young people at work. Observe employment restrictions under the Maternity Protection Directive (92/85/EEC) for expectant or nursing mothers.

National inventories

Country	Inventory	Status
AU	AIIC	all ingredients are listed
CA	DSL	all ingredients are listed
CN	IECSC	all ingredients are listed
EU	ECSI	all ingredients are listed
EU	REACH Reg.	all ingredients are listed
JP	CSCL-ENCS	all ingredients are listed
KR	KECI	all ingredients are listed
MX	INSQ	all ingredients are listed
NZ	NZIoC	all ingredients are listed
PH	PICCS	all ingredients are listed

Country	Inventory	Status
TR	CICR	not all ingredients are listed
TW	TCSI	all ingredients are listed
US	TSCA	all ingredients are listed as "ACTIVE"

Legend

AIIC	Australian Inventory of Industrial Chemicals
CICR	Chemical Inventory and Control Regulation
CSCL-ENCS	List of Existing and New Chemical Substances (CSCL-ENCS)
DSL	Domestic Substances List (DSL)
ECSI	EC Substance Inventory (EINECS, ELINCS, NLP)
IECSC	Inventory of Existing Chemical Substances Produced or Imported in China
INSQ	National Inventory of Chemical Substances
KECI	Korea Existing Chemicals Inventory
NZIoC	New Zealand Inventory of Chemicals
PICCS	Philippine Inventory of Chemicals and Chemical Substances (PICCS)
REACH Reg.	REACH registered substances
TCSI	Taiwan Chemical Substance Inventory
TSCA	Toxic Substance Control Act

15.2 Chemical Safety Assessment

Chemical safety assessments for substances in this mixture were not carried out.

SECTION 16: Other information

Abbreviations and acronyms

Abbr.	Descriptions of used abbreviations
Acute Tox.	Acute toxicity
ADR	Accord relatif au transport international des marchandises dangereuses par route (Agreement concerning the International Carriage of Dangerous Goods by Road)
Aquatic Chronic	Hazardous to the aquatic environment - chronic hazard
ATE	Acute Toxicity Estimate
CAS	Chemical Abstracts Service (service that maintains the most comprehensive list of chemical substances)
CLP	Regulation (EC) No 1272/2008 on classification, labelling and packaging of substances and mixtures
DGR	Dangerous Goods Regulations (see IATA/DGR)
DNEL	Derived No-Effect Level
EC50	Effective Concentration 50 %. The EC50 corresponds to the concentration of a tested substance causing 50 % changes in response (e.g. on growth) during a specified time interval
EC No	The EC Inventory (EINECS, ELINCS and the NLP-list) is the source for the seven-digit EC number, an identifier of substances commercially available within the EU (European Union)
EINECS	European Inventory of Existing Commercial Chemical Substances
ELINCS	European List of Notified Chemical Substances
ErC50	≡ EC50: in this method, that concentration of test substance which results in a 50 % reduction in either growth (EbC50) or growth rate (ErC50) relative to the control
Eye Dam.	Seriously damaging to the eye
Eye Irrit.	Irritant to the eye
GHS	"Globally Harmonized System of Classification and Labelling of Chemicals" developed by the United Nations
IATA	International Air Transport Association

Abbr.	Descriptions of used abbreviations
IATA/DGR	Dangerous Goods Regulations (DGR) for the air transport (IATA)
ICAO	International Civil Aviation Organization
IMDG	International Maritime Dangerous Goods Code
index No	The Index number is the identification code given to the substance in Part 3 of Annex VI to Regulation (EC) No 1272/2008
LC50	Lethal Concentration 50%: the LC50 corresponds to the concentration of a tested substance causing 50 % lethality during a specified time interval
LD50	Lethal Dose 50 %: the LD50 corresponds to the dose of a tested substance causing 50 % lethality during a specified time interval
NLP	No-Longer Polymer
Ox. Liq.	Oxidising liquid
PBT	Persistent, Bioaccumulative and Toxic
PNEC	Predicted No-Effect Concentration
REACH	Registration, Evaluation, Authorisation and Restriction of Chemicals
Skin Corr.	Corrosive to skin
Skin Irrit.	Irritant to skin
STOT SE	Specific target organ toxicity - single exposure
SVHC	Substance of Very High Concern
VOC	Volatile Organic Compounds
vPvB	Very Persistent and very Bioaccumulative

Key literature references and sources for data

Regulation (EC) No 1272/2008 on classification, labelling and packaging of substances and mixtures. Regulation (EC) No. 1907/2006 (REACH), amended by 2020/878/EU.

Agreement concerning the International Carriage of Dangerous Goods by Road (ADR). International Maritime Dangerous Goods Code (IMDG). Dangerous Goods Regulations (DGR) for the air transport (IATA).

Classification procedure

Physical and chemical properties. The classification is based on tested mixture.
Health hazards. Environmental hazards. The method for classification of the mixture is based on ingredients of the mixture (additivity formula).

List of relevant phrases (code and full text as stated in section 2 and 3)

Code	Text
H271	May cause fire or explosion; strong oxidiser.
H302	Harmful if swallowed.
H314	Causes severe skin burns and eye damage.
H318	Causes serious eye damage.
H319	Causes serious eye irritation.
H332	Harmful if inhaled.
H335	May cause respiratory irritation.

Code	Text
H412	Harmful to aquatic life with long lasting effects.

Disclaimer

This information is based upon the present state of our knowledge. This SDS has been compiled and is solely intended for this product.

APPENDIX B

Fresh Properties Results

Slump Flow

Mix Code	Date of Test	Time	t_{500}	Diameter d_1	Diameter d_2	Slump Flow	Classification EFNARC	
			s	mm	mm	mm	Viscosity	Flow
Control Mix	09/05/2023	t_0	1.27	690	700	695	VS1	SF2
		t_{15}	1.35	680	690	685	VS1	SF2
		t_{30}	1.58	650	670	660	VS1	SF2
F15-0.25	16/05/2023	t_0	2.10	610	620	615	VS2	SF1
		t_{15}	3.29	580	590	585	VS2	SF1
		t_{30}	5.08	560	580	570	VS2	SF1
F25-0.25	18/05/2023	t_0	3.40	590	595	592.5	VS2	SF1
		t_{15}	4.04	580	570	575	VS2	SF1
		t_{30}	6.22	570	560	565	VS2	SF1
F35-0.25	22/05/2023	t_0	4.30	600	580	590	VS2	SF1
		t_{15}	5.87	560	570	565	VS2	SF1
		t_{30}	7.18	560	550	555	VS2	SF1
F15-0.50	12/05/2023	t_0	3.50	570	590	580	VS2	SF1
		t_{15}	4.46	540	550	545	VS2	-
		t_{30}	6.31	540	545	542.5	VS2	-
F25-0.50	15/05/2023	t_0	4.40	565	560	562.5	VS2	SF1
		t_{15}	5.24	560	550	555	VS2	SF1
		t_{30}	6.90	530	545	537.5	VS2	-
F35-0.50	17/05/2023	t_0	5.47	550	530	540	VS2	-
		t_{15}	6.84	530	510	520	VS2	-
		t_{30}	7.15	510	520	515	VS2	-
F15-1	11/05/2023	t_0	0	360	340	350	-	-
		t_{15}	0	345	350	347.5	-	-
		t_{30}	0	350	330	340	-	-

(-) Not within EFNARC Classifications

V-Funnel

Mix Code	Date of Test	Time	Time	Classification EFNARC
			s	
Control Mix	09/05/2023	t_0	5	VF1
		t_{15}	6	VF1
		t_{30}	7	VF1
F15-0.25	16/05/2023	t_0	5	VF1
		t_{15}	6	VF1
		t_{30}	7	VF1
F25-0.25	18/05/2023	t_0	6	VF1
		t_{15}	7	VF1
		t_{30}	12	VF2
F35-0.25	22/05/2023	t_0	8	VF1
		t_{15}	9	VF2
		t_{30}	15	VF2
F15-0.50	12/05/2023	t_0	6	VF1
		t_{15}	7	VF1
		t_{30}	14	VF2
F25-0.50	15/05/2023	t_0	11	VF2
		t_{15}	14	VF2
		t_{30}	21	VF2
F35-0.50	17/05/2023	t_0	12	VF2
		t_{15}	17	VF2
		t_{30}	26	-
F15-1	11/05/2023	t_0	31	-
		t_{15}	41	-
		t_{30}	45	-

(-) Not within EFNARC Classifications

L-Box Test

Mix Code	Date of Test	Time	H_1			H_1 Avg	H_2			H_2 Avg	PL Ratio	Distance Travelled in L-Box (mm)	Classification EFNARC
			mm			mm	mm			mm			Passing Ability
Control Mix	09/05/2023	t_0	76	77	76	76.33	63	63	62	62.67	0.82	*530	PA2
		t_{15}	76	76	78	76.67	61	60	62	61	0.80	*530	PA2
		t_{30}	75	76	76	75.67	60	59	59	59.33	0.78	*530	-
F15-0.25	16/05/2023	t_0	88	88	89	88.33	60	61	61	60.67	0.69	*530	-
		t_{15}	106	105	107	106	71	72	72	71.67	0.67	*530	-
		t_{30}	114	115	112	113.67	74	75	76	75	0.66	*530	-
F25-0.25	18/05/2023	t_0	90	92	89	90.33	146	144	145	145	0.63	*530	-
		t_{15}	72	71	73	72	126	125	126	125.67	0.57	*530	-
		t_{30}	82	80	83	81.67	148	145	144	145.67	0.56	*530	-
F35-0.25	22/05/2023	t_0	65	66	65	65.33	105	105	106	105.33	0.62	*530	-
		t_{15}	66	67	65	66	112	112	115	113	0.58	*530	-
		t_{30}	79	80	80	79.67	145	144	147	145.33	0.54	*530	-
F15-0.50	12/05/2023	t_0	75	77	76	76	137	136	134	135.57	0.56	*530	-
		t_{15}	59	60	60	59.67	112	113	111	112	0.53	*530	-
		t_{30}	59	59	58	58.67	120	119	119	119.33	0.49	*530	-
F25-0.50	15/05/2023	t_0	60	59	62	60.33	102	101	99	100.67	0.59	*530	-
		t_{15}	71	72	70	71	141	140	141	140.67	0.50	*530	-
		t_{30}	75	78	77	76.67	/	/	/	/	/	500	-
F35-0.50	17/05/2023	t_0	75	75	76	75.33	139	140	138	139	0.54	*530	-
		t_{15}	69	71	72	70.67	/	/	/	/	/	480	-
		t_{30}	/	/	/	/	/	/	/	/	/	/	-
F15-1	11/05/2023	t_0	/	/	/	/	/	/	/	/	/	/	-
		t_{15}	/	/	/	/	/	/	/	/	/	/	-
		t_{30}	/	/	/	/	/	/	/	/	/	/	-

Stress Growth Test

Test Parameters			
Test Speed (rps)		0.025	
Mix Code	Date of Test	Peak Torque (Nm)	Yield Stress (Pa)
Control Mix	09/05/2023	0.505	117.615
F15-0.25	16/05/2023	0.709	165.376
F25-0.25	18/05/2023	0.774	180.319
F35-0.25	22/05/2023	1.490	347.252
F15-0.50	12/05/2023	0.844	196.72
F25-0.50	15/05/2023	1.156	269.460
F35-0.50	17/05/2023	1.819	423.981
F15-1	11/05/2023	-	-

Flow Curve Test

Test Parameters							
Breakdown Time (s)		20					
Breakdown Speed (rps)		0.500					
Number of Points		7					
Time per Point (s)		5.0					
Initial Speed (rps)		0.500					
Final Speed (rps)		0.050					
Mix Code	**Date of Test**	**Relative Parameters**			**Bingham Parameters**		
		Y (Nm)	**V (Nm)**	**R^2**	**T_o (Pa)**	**μ (Pa.s)**	**(mse)**
Control Mix	09/05/2023	0.276	1.862	0.99	49.10	34.73	0.001
F15-0.25	16/05/2023	0.357	1.238	1.00	68.64	20.72	0.003
F25-0.25	18/05/2023	0.269	1.352	1.00	45.51	25.57	0.005
F35-0.25	22/05/2023	0.603	1.151	1.00	136.71	14.80	0.003
F15-0.50	12/05/2023	0.478	1.612	1.00	94.63	26.14	0.003
F25-0.50	15/05/2023	0.639	1.262	0.98	150.51	15.08	0.004
F35-0.50	17/05/2023	0.548	1.675	0.99	112.36	25.97	0.008
F15-1	11/05/2023	-	-	-	-	-	-

APPENDIX C

Mechanical Properties Results

Hardened Density at 28 days

Mix Code	Date of Test	Sample	Weight in air (kg)	Weight in Water (kg)	Volume (m^3)	Density (kg/m^3)	Average Density (kg/m^3)
Control Mix	06/06/2023	A	2.387	1.139	1.035	2.306	2.299
		B	2.96	1.118	1.045	2.292	
F15-1	08/06/2023	A	2.260	1.015	1.032	2.189	2.168
		B	2.286	1.008	1.065	2.146	
F15-0.25	13/06/2023	A	2.481	1.186	1.082	2.292	2.265
		B	2.454	1.145	1.096	2.238	
F25-0.25	15/06/2023	A	2.389	1.117	1.059	2.255	2.258
		B	2.358	1.102	1.043	2.260	
F35-0.25	19/06/2023	A	2.398	1.112	1.073	2.234	2.238
		B	2.435	1.136	1.086	2.241	
F15-0.5	09/06/2023	A	2.365	1.096	1.056	2.239	2.249
		B	2.321	1.081	1.027	2.259	
F25-0.5	12/06/23	A	2.341	1.092	1.036	2.259	2.210
		B	2.379	1.066	1.100	2.162	
F35-0.5	14/06/23	A	2.275	1.049	1.013	2.245	2.171
		B	2.340	1.011	1.116	2.096	

Ultrasonic Pulse Velocity at 28 days

Mix Code	Date of Test	Sample	Dimensions Readings (mm)			Average Path Length (mm)	Time (μs)	Pulse Velocity (km/s)	Average Pulse Velocity (km/s)
			1st	2nd	3rd				
Control Mix	06/06/2023	A	100.83	100.52	100.49	100.61	20.6	4.88	4.76
			100.69	100.67	100.70	100.69	19.8	5.09	
		B	101.91	101.87	103.51	102.43	21.6	4.74	
			101.85	102.00	102.21	102.02	23.5	4.34	
F15-1	08/06/2023	A	99.50	99.41	99.61	99.51	20.8	4.78	4.39
			100.71	100.10	99.89	100.23	25.7	3.90	
		B	100.53	100.46	100.37	100.45	20.9	4.81	
			100.83	100.66	100.01	100.50	24.6	4.08	
F15-0.25	13/06/2023	A	100.70	100.65	100.52	100.62	20.6	4.88	4.72
			101.68	100.85	101.04	101.07	20.4	4.95	
		B	100.86	100.51	100.75	100.71	22.9	4.40	
			100.83	101.09	101.56	101.16	21.8	4.64	
F25-0.25	15/06/2023	A	100.25	100.10	100.07	100.14	20.8	4.81	4.65
			100.68	100.78	100.32	100.59	21.6	4.66	
		B	100.20	100.11	100.49	100.27	21.2	4.73	
			100.14	100.61	100.20	100.32	22.8	4.40	
F35-0.25	19/06/2023	A	100.62	101.32	100.63	100.86	22.1	4.56	4.57
			100.81	100.68	101.48	100.99	23.4	4.32	
		B	101.29	101.69	100.83	101.27	21.7	4.67	
			101.20	100.04	100.85	100.58	21.3	4.72	
F15-0.5	09/06/2023	A	100.59	100.91	100.59	100.70	21.6	4.66	4.63
			101.00	100.41	100.61	100.67	21.4	4.70	
		B	100.48	100.78	100.60	100.62	22.1	4.55	
			100.59	100.43	100.54	100.52	21.8	4.61	
F25-0.5	12/06/2023	A	100.69	100.80	100.46	100.65	21.1	4.77	4.54
			100.13	100.40	100.66	100.40	22.7	4.42	
		B	100.44	100.50	100.65	100.53	23.4	4.30	
			100.53	100.49	100.56	100.53	21.6	4.65	
F35-0.5	14/06/2023	A	100.26	100.72	100.27	100.42	22.7	4.42	4.52
			100.40	100.13	100.19	100.24	21.9	4.58	
		B	100.57	100.99	100.52	100.69	22.1	4.56	
			101.70	100.83	100.33	100.95	22.4	4.51	

Compressive Strength at 7 days

Mix Code	Date of Test	Sample	Dimensions Readings (mm)				Average (mm)	Volume (cm^3)	Mass (g)	Density (g/cm^3)	Max. Load (kN)	Compressive Strength (Mpa)	Average Density (g/cm^3)	Average Compressive Strength (Mpa)
				1st	2nd	3rd								
Control Mix	16/05/2023	A	L	100.28	100.26	100.23	100.26	1009.33	2461	2.44	522.2	52.22	2.44	53.92
			B	100.47	100.51	100.46	100.48							
			H	100.15	100.18	100.23	100.19							
		B	L	100.64	100.56	100.62	100.61	1009.42	2466	2.44	556.62	55.62		
			B	100.32	100.28	100.35	100.32							
			H	99.98	100.1	99.95	100.01							

Compressive Strength at 7 days

Mix Code	Date of Test	Sample	Dimensions Readings (mm)				Average (mm)	Volume (cm^3)	Mass (g)	Density (g/cm^3)	Max. Load (kN)	Compressive Strength (Mpa)	Average Density (g/cm^3)	Average Compressive Strength (Mpa)
				1st	2nd	3rd								
F15-0.25	23/05/2023	A	L	100.55	100.58	100.52	100.55	1013.86	2394.5	2.36	433.9	43.39	2.38	44.07
			B	100.41	100.45	100.46	100.44							
			H	100.39	100.42	100.37	100.39							
		B	L	100.58	100.56	100.53	100.56	998.2	2400	2.40	447.5	44.75		
			B	100.49	100.51	100.44	100.48							
			H	98.74	98.85	98.77	98.79							

Compressive Strength at 7 days

Mix Code	Date of Test	Sample	Dimensions Readings (mm)				Average (mm)	Volume (cm^3)	Mass (g)	Density (g/cm^3)	Max. Load (kN)	Compressive Strength (Mpa)	Average Density (g/cm^3)	Average Compressive Strength (Mpa)
				1st	2nd	3rd								
F25-0.25	25/05/2023	A	L	100.82	100.71	100.67	100.73	1011.92	2323.5	2.30	389.4	38.94	2.29	41.3
			B	100.60	100.56	100.78	100.65							
			H	98.91	100.05	100.48	99.81							
		B	L	100.45	100.51	100.66	100.54	1002.94	2285.5	2.28	436.6	43.66		
			B	100.50	100.53	100.59	100.54							
			H	99.53	98.85	99.32	99.22							

Compressive Strength at 7 days

Mix Code	Date of Test	Sample	Dimensions Readings (mm)				Average (mm)	Volume (cm^3)	Mass (g)	Density (g/cm^3)	Max. Load (kN)	Compressive Strength (Mpa)	Average Density (g/cm^3)	Average Compressive Strength (Mpa)
				1st	2nd	3rd								
F35-0.25	29/05/2023	A	L	100.95	101.14	100.74	100.94	1030.81	2378.5	2.31	390.9	39.09	2.3	41.61
			B	101.31	100.55	100.94	100.93							
			H	101.05	101.61	100.89	101.18							
		B	L	104.41	101.95	101.66	102.67	1063.23	2436	2.29	441.2	44.12		
			B	100.36	100.75	100.75	100.62							
			H	102.74	103.61	102.43	102.92							

Compressive Strength at 7 days

Mix Code	Date of Test	Sample		Dimensions Readings (mm)			Average (mm)	Volume (cm^3)	Mass (g)	Density (g/cm^3)	Max. Load (kN)	Compressive Strength (Mpa)	Average Density (g/cm^3)	Average Compressive Strength (Mpa)
				1st	2nd	3rd								
F15-0.5	19/05/2023	A	L	100.54	100.61	100.58	100.58	1018.51	2352.5	2.31	431.9	43.19	2.315	42.63
			B	100.62	100.65	100.55	100.61							
			H	100.65	100.59	100.72	100.65							
		B	L	100.63	100.74	100.55	100.64	1016.79	2360.5	2.32	420.7	42.07		
			B	100.67	100.69	100.61	100.66							
			H	100.41	100.34	100.46	100.37							

Compressive Strength at 7 days

Mix Code	Date of Test	Sample		Dimensions Readings (mm)			Average (mm)	Volume (cm^3)	Mass (g)	Density (g/cm^3)	Max. Load (kN)	Compressive Strength (Mpa)	Average Density (g/cm^3)	Average Compressive Strength (Mpa)
				1st	2nd	3rd								
F25-0.5	22/05/2023	A	L	100.62	100.44	100.49	100.52	1015.07	2420	2.38	442.7	44.27	2.375	42.21
			B	100.73	100.54	100.76	100.68							
			H	100.38	100.85	99.68	100.30							
		B	L	100.84	100.88	100.98	100.90	1003.74	2374	2.37	401.5	40.15		
			B	100.89	100.56	101.01	100.82							
			H	97.77	99.19	99.06	98.67							

Compressive Strength at 7 days

Mix Code	Date of Test	Sample	Dimensions Readings (mm)				Average (mm)	Volume (cm^3)	Mass (g)	Density (g/cm^3)	Max. Load (kN)	Compressive Strength (Mpa)	Average Density (g/cm^3)	Average Compressive Strength (Mpa)
				1st	2nd	3rd								
F35-0.5	24/05/2023	A	L	100.34	100.44	100.37	100.38	1014.06	2379.5	2.34	432.1	43.21	2.31	40.32
			B	100.21	100.32	100.26	100.26							
			H	100.71	100.75	100.83	100.76							
		B	L	101.45	101.23	100.94	101.20	1053.75	2394.5	2.27	374.3	37.43		
			B	100.76	100.80	100.68	100.75							
			H	103.63	102.98	103.45	103.35							

Compressive Strength at 7 days

Mix Code	Date of Test	Sample	Dimensions Readings (mm)				Average (mm)	Volume (cm^3)	Mass (g)	Density (g/cm^3)	Max. Load (kN)	Compressive Strength (Mpa)	Average Density (g/cm^3)	Average Compressive Strength (Mpa)
				1st	2nd	3rd								
F15-1	18/05/2023	A	L	100.77	100.68	100.82	100.76	1021.25	2319.5	2.27	391.7	39.17	2.27	39.975
			B	100.56	100.59	100.44	100.53							
			H	100.82	100.75	100.88	100.82							
		B	L	100.73	100.64	100.81	100.73	1003.03	2265.5	2.26	407.8	40.78		
			B	100.42	100.45	100.41	100.43							
			H	98.53	99.26	99.65	99.15							

Compressive Strength at 28 days

Mix Code	Date of Test	Sample	Dimensions Readings (mm)				Average (mm)	Volume (cm^3)	Mass (g)	Density (g/cm^3)	Max. Load (kN)	Compressive Strength (Mpa)	Average Density (g/cm^3)	Average Compressive Strength (Mpa)
				1st	2nd	3rd								
Control Mix	06/06/2023	A	L	100.48	100.04	99.85	100.12	1003.90	2387.66	2.38	592.3	59.23	2.375	59.68
			B	100.30	100.23	100.01	100.18							
			H	100.36	100.04	99.89	100.09							
		B	L	100.19	100.10	100.06	100.12	1012.53	2396.34	2.37	601.2	60.12		
			B	100.24	100.21	100.16	100.20							
			H	101.35	100.98	100.46	100.93							

Compressive Strength at 28 days

Mix Code	Date of Test	Sample	Dimensions Readings (mm)				Average (mm)	Volume (cm^3)	Mass (g)	Density (g/cm^3)	Max. Load (kN)	Compressive Strength (Mpa)	Average Density (g/cm^3)	Average Compressive Strength (Mpa)
				1st	2nd	3rd								
F15-0.25	13/06/2023	A	L	100.70	100.65	100.52	100.62	1038.93	2480.74	2.39	527.4	52.74	2.365	51.85
			B	101.68	100.85	101.04	101.07							
			H	102.23	102.82	101.43	102.16							
		B	L	100.86	100.51	100.75	100.71	1048.23	2453.99	2.34	509.6	50.96		
			B	100.83	101.09	101.56	101.16							
			H	102.99	103.12	102.55	102.89							

Compressive Strength at 28 days

Mix Code	Date of Test	Sample	Dimensions Readings (mm)				Average (mm)	Volume (cm^3)	Mass (g)	Density (g/cm^3)	Max. Load (kN)	Compressive Strength (Mpa)	Average Density (g/cm^3)	Average Compressive Strength (Mpa)
				1st	2nd	3rd								
F25-0.25	14/06/2023	A	L	100.25	100.10	100.07	100.14	1014.46	2389.95	2.35	495.2	49.52	2.355	50.10
			B	100.68	100.78	100.32	100.59							
			H	100.82	100.69	100.61	100.71							
		B	L	100.20	100.11	100.49	100.27	998.77	2358.52	2.36	506.8	50.68		
			B	100.14	100.61	100.20	100.32							
			H	99.72	99.28	98.88	99.29							

Compressive Strength at 28 days

Mix Code	Date of Test	Sample	Dimensions Readings (mm)				Average (mm)	Volume (cm^3)	Mass (g)	Density (g/cm^3)	Max. Load (kN)	Compressive Strength (Mpa)	Average Density (g/cm^3)	Average Compressive Strength (Mpa)
				1st	2nd	3rd								
F35-0.25	19/06/2023	A	L	100.62	101.32	100.63	100.86	1038.45	2398.33	2.31	461.2	46.12	2.355	47.03
			B	100.81	100.68	101.48	100.99							
			H	101.96	102.07	101.87	101.95							
		B	L	101.29	101.69	100.83	101.27	1034.06	2435.44	2.36	479.3	47.93		
			B	101.20	100.04	100.85	100.58							
			H	101.16	102.42	100.99	101.52							

Compressive Strength at 28 days

Mix Code	Date of Test	Sample	Dimensions Readings (mm)				Average (mm)	Volume (cm^3)	Mass (g)	Density (g/cm^3)	Max. Load (kN)	Compressive Strength (Mpa)	Average Density (g/cm^3)	Average Compressive Strength (Mpa)
				1st	2nd	3rd								
F15-0.5	09/06/2023	A	L	100.59	100.91	100.59	100.70	1015.77	2365.02	2.33	493.6	49.36	2.32	48.65
			B	101.00	100.41	100.61	100.67							
			H	99.59	99.58	101.42	100.20							
		B	L	100.48	100.78	100.60	100.62	1005.36	2321.39	2.31	479.4	47.94		
			B	100.59	100.43	100.54	100.52							
			H	100.39	98.50	99.30	99.40							

Compressive Strength at 28 days

Mix Code	Date of Test	Sample	Dimensions Readings (mm)				Average (mm)	Volume (cm^3)	Mass (g)	Density (g/cm^3)	Max. Load (kN)	Compressive Strength (Mpa)	Average Density (g/cm^3)	Average Compressive Strength (Mpa)
				1st	2nd	3rd								
F25-0.5	12/06/2023	A	L	100.69	100.80	100.46	100.65	1017.50	2341.92	2.30	486.2	48.62	2.32	47.58
			B	100.13	100.40	100.66	100.40							
			H	100.72	100.58	100.77	100.69							
		B	L	100.44	100.50	100.65	100.53	1021.44	2379.24	2.33	465.4	46.54		
			B	100.53	100.49	100.56	100.53							
			H	100.67	100.74	101.81	101.07							

Compressive Strength at 28 days

Mix Code	Date of Test	Sample		Dimensions Readings (mm)			Average (mm)	Volume (cm^3)	Mass (g)	Density (g/cm^3)	Max. Load (kN)	Compressive Strength (Mpa)	Average Density (g/cm^3)	Average Compressive Strength (Mpa)
				1st	2nd	3rd								
F35-0.5	14/06/2023	A	L	100.26	100.72	100.27	100.42	989.19	2275.95	2.28	472.1	47.21	2.30	46.92
			B	100.40	100.13	100.19	100.24							
			H	98.20	97.84	98.78	98.27							
		B	L	100.57	100.99	100.52	100.69	1012.40	2340.02	2.31	466.2	46.62		
			B	101.70	100.83	100.33	100.95							
			H	99.47	99.59	99.73	99.60							

Compressive Strength at 28 days

Mix Code	Date of Test	Sample		Dimensions Readings (mm)			Average (mm)	Volume (cm^3)	Mass (g)	Density (g/cm^3)	Max. Load (kN)	Compressive Strength (Mpa)	Average Density (g/cm^3)	Average Compressive Strength (Mpa)
				1st	2nd	3rd								
F15-1	08/06/2023	A	L	99.50	99.41	99.61	99.51	984.32	2260.84	2.296	451.8	45.18	2.273	45.88
			B	100.71	100.10	99.89	100.23							
			H	99.32	98.12	98.62	98.69							
		B	L	100.53	100.46	100.80	100.60	1016.29	2286.01	2.249	465.7	46.57		
			B	100.89	100.30	100.37	100.52							
			H	100.83	100.66	100.01	100.50							

Tensile Splitting Test at 28 days

Mix Code	Date of Test	Sample	Specimen Length (mm)			Specimen Radius (mm)		Mass (kg)	Density (kg/m^3)	Max. Load (kN)	Tensile Splitting Strength (Mpa)	Average Density (g/cm^3)	Average Tensile Splitting Strength (Mpa)
					Avg		Avg						
Control Mix	06/06/2023	A	1st	302.80	301.20	149.85	150.37	12.64	2.36	209	2.96	2.38	3.56
			2nd	300.70		150.46							
			3rd	300.10		150.80							
		B	1st	298.20	297.90	150.30	150.52	12.68	2.39	294.8	4.17		
			2nd	297.60		150.62							
			3rd	297.90		150.66							

Tensile Splitting Test at 28 days

Mix Code	Date of Test	Sample	Specimen Length (mm)			Specimen Radius (mm)		Mass (kg)	Density (kg/m^3)	Max. Load (kN)	Tensile Splitting Strength (Mpa)	Average Density (g/cm^3)	Average Tensile Splitting Strength (Mpa)
					Avg		Avg						
F15-1	08/06/2023	A	1st	295.50	296.10	150.16	150.02	12.45	2.38	298.9	4.23	2.325	4.45
			2nd	294.50		149.81							
			3rd	298.30		150.08							
		B	1st	301.50	301.77	152.10	151.87	13.04	2.27	332.4	4.70		
			2nd	301.30		152.39							
			3rd	302.50		151.11							

Tensile Splitting Test at 28 days

Mix Code	Date of Test	Sample	Specimen Length (mm)			Specimen Radius (mm)		Mass (kg)	Density (kg/m^3)	Max. Load (kN)	Tensile Splitting Strength (Mpa)	Average Density (g/cm^3)	Average Tensile Splitting Strength (Mpa)
					Avg		Avg						
F15-0.25	13/06/2023	A	1st	298.50	298.80	150.67	150.54	12.835	2.42	222.8	3.15	2.41	3.76
			2nd	297.50		150.71							
			3rd	300.40		150.24							
		B	1st	298.50	299.80	150.02	150.23	12.705	2.39	309.6	4.38		
			2nd	299.70		150.54							
			3rd	301.20		150.14							

Tensile Splitting Test at 28 days

Mix Code	Date of Test	Sample	Specimen Length (mm)			Specimen Radius (mm)		Mass (kg)	Density (kg/m^3)	Max. Load (kN)	Tensile Splitting Strength (Mpa)	Average Density (g/cm^3)	Average Tensile Splitting Strength (Mpa)
					Avg		Avg						
F25-0.25	15/06/2023	A	1st	295.20	295.27	150.16	150.21	12.65	2.40	273.6	3.93	2.39	4.03
			2nd	295.80		149.48							
			3rd	294.80		150.99							
		B	1st	294.70	295.30	150.98	151.06	12.51	2.37	289.1	4.13		
			2nd	295.80		151.17							
			3rd	295.40		151.04							

Tensile Splitting Test at 28 days

Mix Code	Date of Test	Sample	Specimen Length (mm)			Specimen Radius (mm)		Mass (kg)	Density (kg/m^3)	Max. Load (kN)	Tensile Splitting Strength (Mpa)	Average Density (g/cm^3)	Average Tensile Splitting Strength (Mpa)
					Avg		Avg						
F35-0.25	19/06/2023	A	1st	300.80	300.87	150.54	150.44	12.595	2.34	302.4	4.28	2.36	4.18
			2nd	300.60		150.27							
			3rd	301.20		150.51							
		B	1st	303.10	303.27	152.22	152.26	12.065	2.37	297.4	4.21		
			2nd	303.90		152.29							
			3rd	302.80		152.28							

Tensile Splitting Test at 28 days

Mix Code	Date of Test	Sample	Specimen Length (mm)			Specimen Radius (mm)		Mass (kg)	Density (kg/m^3)	Max. Load (kN)	Tensile Splitting Strength (Mpa)	Average Density (g/cm^3)	Average Tensile Splitting Strength (Mpa)
					Avg		Avg						
F15-0.5	09/06/2023	A	1st	301	300.67	149.63	149.87	13.14	2.48	291.9	4.13	2.37	4.04
			2nd	301.50		149.95							
			3rd	299.50		150.05							
		B	1st	297.50	298	152.85	152.89	12.34	2.26	282.5	3.95		
			2nd	297		152.69							
			3rd	299.50		153.12							

Tensile Splitting Test at 28 days

Mix Code	Date of Test	Sample	Specimen Length (mm)			Specimen Radius (mm)		Mass (kg)	Density (kg/m^3)	Max. Load (kN)	Tensile Splitting Strength (Mpa)	Average Density (g/cm^3)	Average Tensile Splitting Strength (Mpa)
					Avg		Avg						
F25-0.5	12/06/2023	A	1st	292.50	293.40	150.89	150.64	12.25	2.34	246.3	3.49	2.36	4.20
			2nd	293.20		150.38							
			3rd	294.50		150.66							
		B	1st	302.50	302.07	152.79	152.68	13.18	2.38	351.7	4.98		
			2nd	302.20		152.27							
			3rd	301.50		152.99							

Tensile Splitting Test at 28 days

Mix Code	Date of Test	Sample	Specimen Length (mm)			Specimen Radius (mm)		Mass (kg)	Density (kg/m^3)	Max. Load (kN)	Tensile Splitting Strength (Mpa)	Average Density (g/cm^3)	Average Tensile Splitting Strength (Mpa)
					Avg		Avg						
F35-0.5	14/06/2023	A	1st	300.80	300.70	152.60	152.85	13.06	2.37	322	4.46	2.37	4.47
			2nd	300.60		153.32							
			3rd	300.70		152.62							
		B	1st	300.30	299.87	150.37	150.28	12.63	2.37	317.1	4.48		
			2nd	300.10		150.20							
			3rd	299.20		150.26							

Toughness Factor for Flexural Beams at 28 days

Mix Code	Date of Test	Dimensions Readings (mm)				Average (mm)	Area under Load Displacement graph (kN)	Toughness Index (Mpa)
			1st	2nd	3rd			
Control Mix	06/06/2023	L	557.60	559.50	558.50	558.53	7.51	0.27
		B	154.42	154.89	153.64	154.32		
		H	154.64	155.00	154.50	154.71		
F15-0.25	13/06/2023	L	551.30	551.90	551.80	551.67	25.13	0.98
		B	153.15	152.59	152.85	152.86		
		H	152.43	151.98	149.30	151.24		
F25-0.25	15/06/2023	L	554.80	554.60	554.60	554.67	38.86	1.49
		B	155.32	154.80	154.98	155.03		
		H	153.04	150.78	149.30	151.04		
F35-0.25	19/06/2023	L	554.40	555.80	553.70	554.63	45.10	1.79
		B	154.49	155.71	154.67	154.97		
		H	148.06	147.10	149.16	148.11		
F15-0.50	09/06/2023	L	556.10	556.20	556.90	556.40	30.58	1.17
		B	153.24	153.70	154.71	153.88		
		H	146.95	150.80	155.24	150.99		
F25-0.50	12/06/2023	L	556.10	556.60	554.70	556.10	41.08	1.50
		B	153.22	152.73	153.28	153.08		
		H	158.05	153.83	153.51	155.13		
F35-0.50	14/06/2023	L	551.90	551.80	550.60	551.43	48.86	1.83
		B	152.75	153.59	153.67	153.34		
		H	153.85	153.97	154.19	154.00		
F15-1	08/06/2023	L	554.40	554.30	554.90	554.53	29.36	1.11
		B	152.85	152.31	153.56	152.91		
		H	153.88	154.77	151.06	153.24		

APPENDIX D

Shrinkage Test Results

Environmental Chamber Test

Date of Test		31/05/2023			
Mix Code		Control Mix			
Area of water container (m^2)		0.06			
Crack Developed at (hrs)		2.25			
Time (hrs)	**Ambient Temp. (°C)**	**Concrete Temp. (°C)**	**Mass of Water (g)**	**Mass of water evaporated (g)**	**Rate of evaporation ($kg/m^2/hr$)**
0	32.58	23.72	1839.5	0	-
0.5	37.51	25.62	1833	6.5	0.22
1	39.16	26.13	1825.5	7.5	0.25
1.5	39.47	26.75	1816	9.5	0.32
2	39.91	26.95	1803	13	0.43
2.5	40.63	27.57	1787.5	15.5	0.52
3	40.91	28.25	1768.5	19	0.63
4	39.90	29.67	1717.5	51	0.85
5	42.40	30.71	1660	57.5	0.96
6	43.39	31.55	1597.5	62.5	1.04

Environmental Chamber Test

Date of Test		05/06/2023			
Mix Code		F35-0.5			
Area of water container (m^2)		0.06			
Crack Developed at (hrs)		3.5			
Time (hrs)	**Ambient Temp. (°C)**	**Concrete Temp. (°C)**	**Mass of Water (g)**	**Mass of water evaporated (g)**	**Rate of evaporation ($kg/m^2/hr$)**
0	32.91	24.05	2141	0	-
0.5	36.36	25.16	2136.5	4.5	0.15
1	36.67	25.98	2127.5	9	0.32
1.5	37.23	26.86	2114.5	13	0.43
2	38.01	27.59	2097	17.5	0.58
2.5	38.68	28.42	2076.5	20.5	0.68
3	39.02	29.15	2054.5	24	0.80
4	39.51	30.36	2001	53.5	0.89
5	41.01	31.62	1943.5	57.5	0.96
6	41.86	32.67	1884.5	59	0.98

Environmental Chamber Test

Date of Test		08/06/2023			
Mix Code		F35-0.5			
Area of water container (m^2)		0.06			
Crack Developed at (hrs)		4.5			
Time (hrs)	**Ambient Temp. (°C)**	**Concrete Temp. (°C)**	**Mass of Water (g)**	**Mass of water evaporated (g)**	**Rate of evaporation ($kg/m^2/hr$)**
0	31.62	23.18	1717.5	0	-
0.5	34.46	24.96	1710.5	7	0.23
1	34.64	26.12	1699.5	11	0.37
1.5	35.72	26.92	1687	12.5	0.42
2	36.29	27.49	1671	16	0.53
2.5	36.85	28.38	1651.5	19.5	0.65
3	37.34	29.43	1628	23.5	0.78
4	38.12	30.98	1576	52	0.87
5	39.23	32.37	1517.5	58.5	0.98
6	40.15	33.74	1456	61.5	1.03

Control Mix

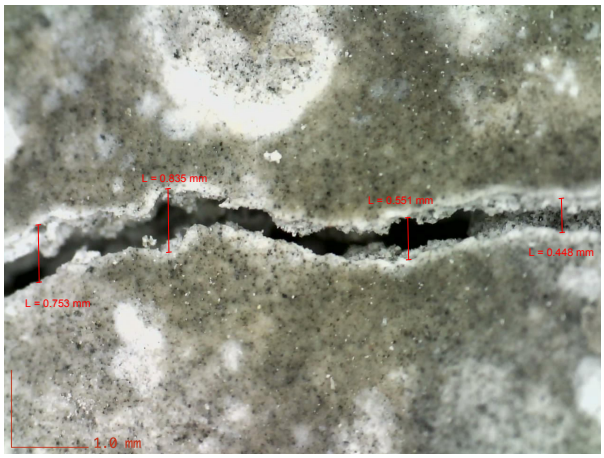
L = 0.535 mm
L = 0.551 mm
L = 0.448 mm
L = 0.753 mm
1.0 mm

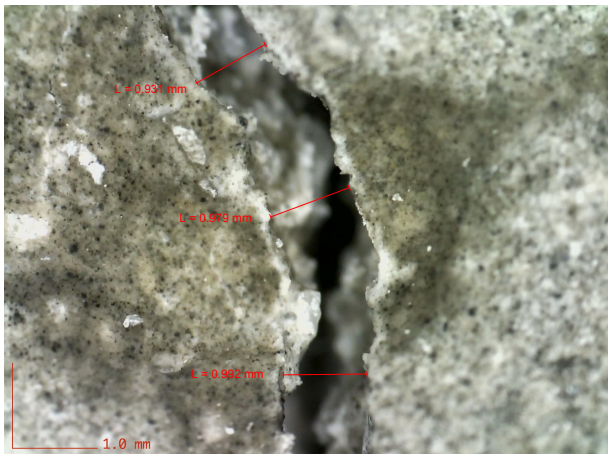
L = 0.931 mm
L = 0.579 mm
L = 0.992 mm
1.0 mm

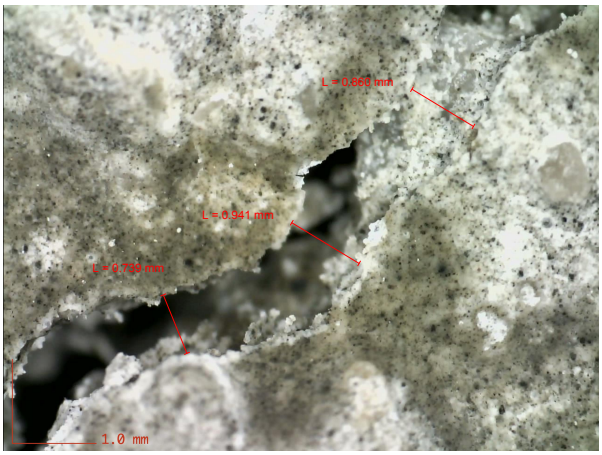
L = 0.868 mm
L = 0.941 mm
L = 0.734 mm
1.0 mm

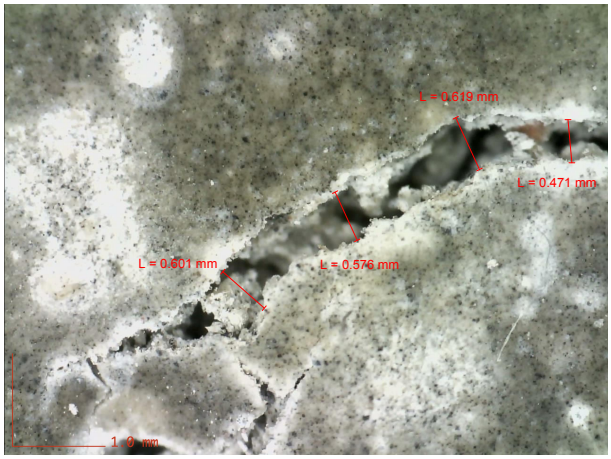
L = 0.619 mm
L = 0.471 mm
L = 0.601 mm
L = 0.576 mm
1.0 mm

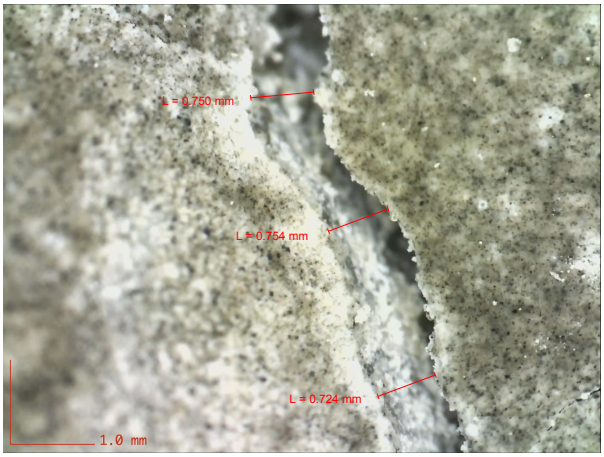
L = 0.750 mm
L = 0.754 mm
L = 0.724 mm
1.0 mm

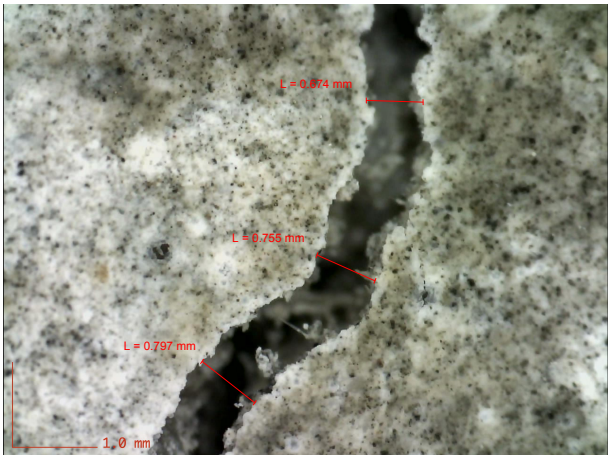
L = 0.874 mm
L = 0.755 mm
L = 0.797 mm
1.0 mm

F35-0.50

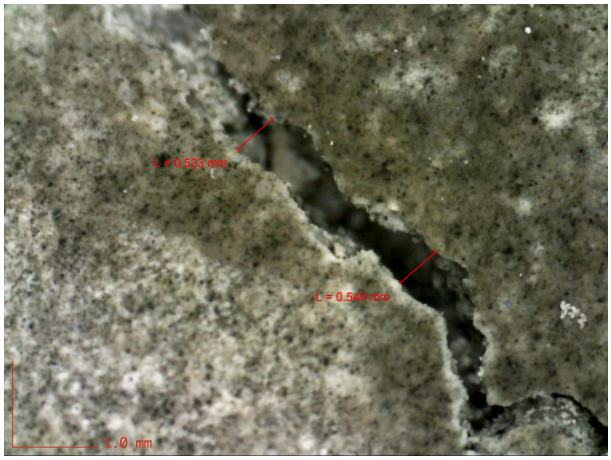
L = 0.533 mm
L = 0.543 mm
1.0 mm

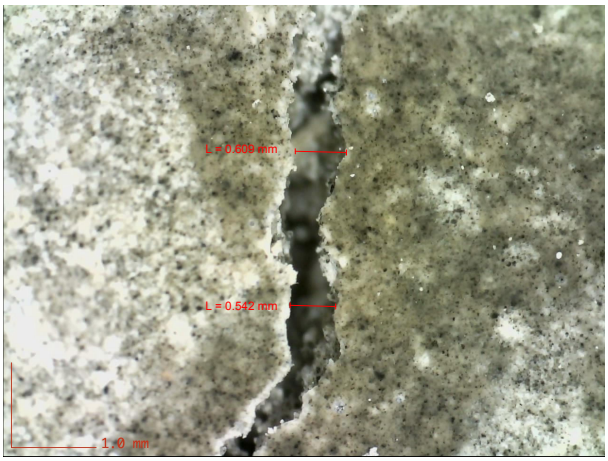
L = 0.609 mm
L = 0.542 mm
1.0 mm

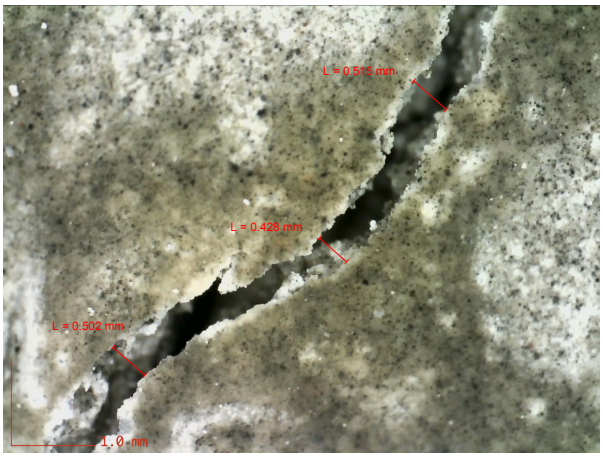
L = 0.515 mm
L = 0.428 mm
L = 0.502 mm
1.0 mm

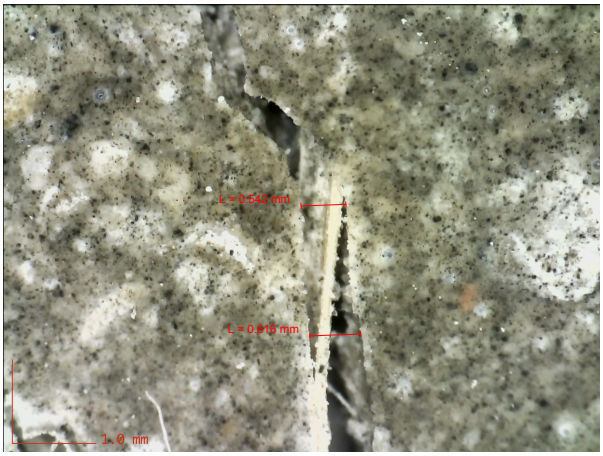
L = 0.542 mm
L = 0.613 mm
1.0 mm

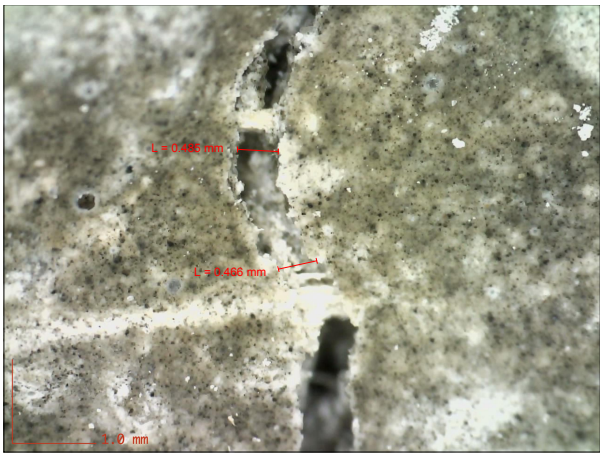
L = 0.486 mm
L = 0.466 mm
1.0 mm

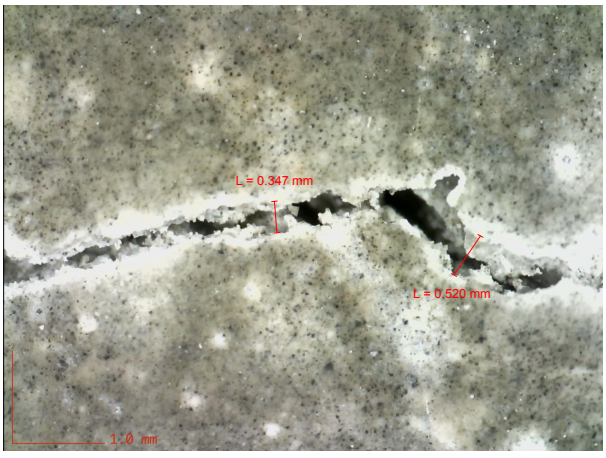
L = 0.347 mm
L = 0.520 mm
1.0 mm

F35-1

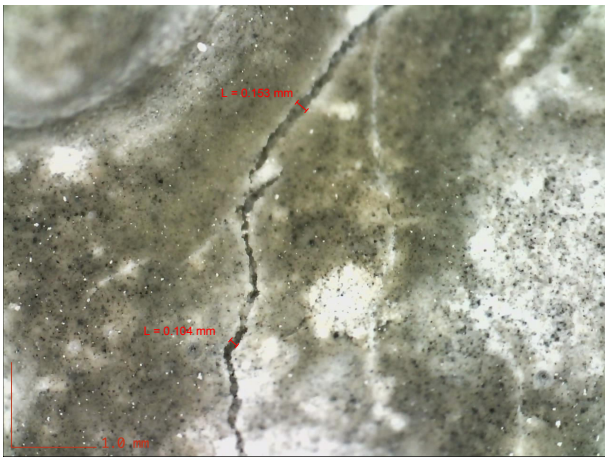
L = 0.194 mm
1.0 mm

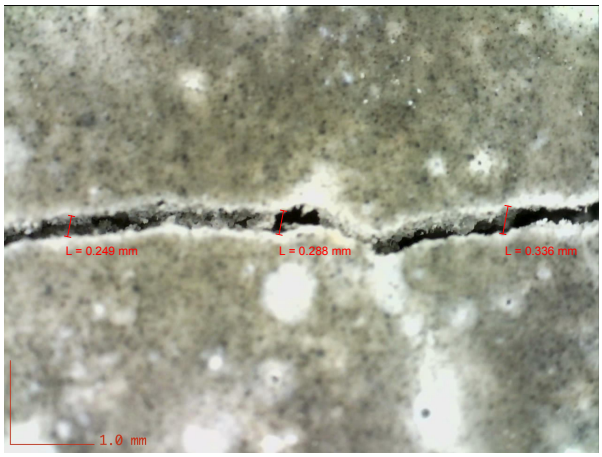
L = 0.249 mm
L = 0.288 mm
L = 0.336 mm
1.0 mm

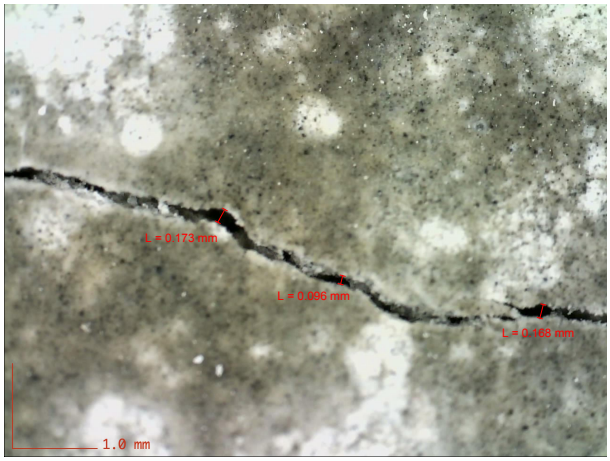
L = 0.173 mm
L = 0.096 mm
L = 0.168 mm
1.0 mm

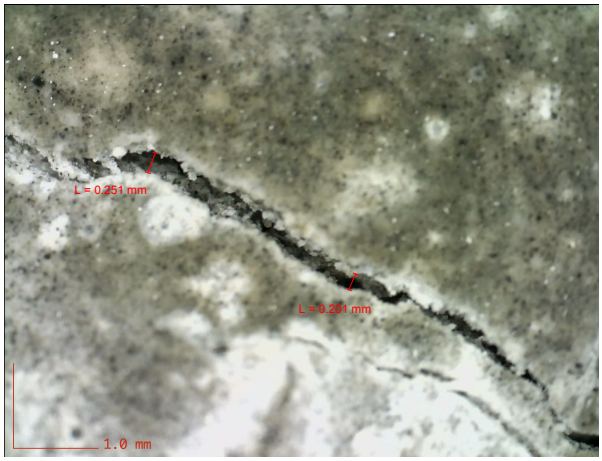
L = 0.251 mm
L = 0.251 mm
1.0 mm

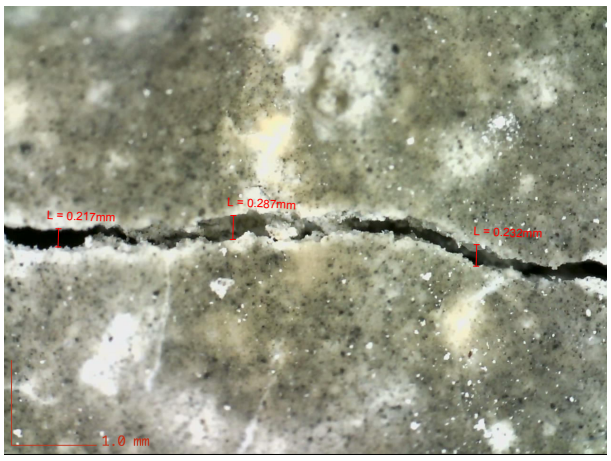
L = 0.217mm
L = 0.287mm
L = 0.233mm
1.0 mm

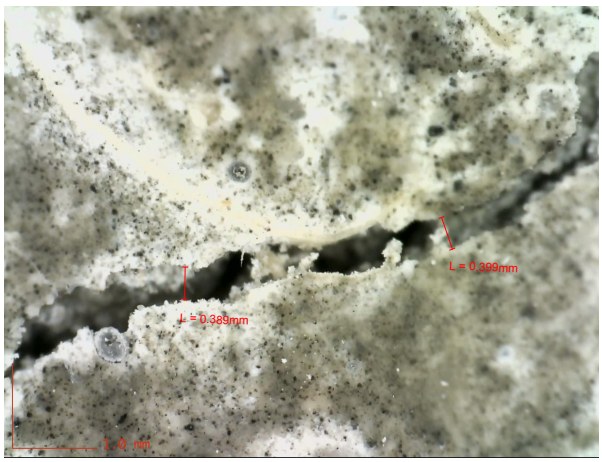
L = 0.389mm
L = 0.389mm
1.0 mm

Crack Width (mm)

Mix Code	Date	d_1	d_2	d_3	d_4	d_5	d_6	d_7	d_8	d_9	d_{10}	Avg. Crack Width
Control Mix	31/05/2023	0.931	0.992	0.739	0.860	0.941	0.797	0.674	0.724	0.750	0.754	0.816
F35-0.5	05/06/2023	0.533	0.549	0.542	0.609	0.502	0.519	0.520	0.616	0.535	0.591	0.552
F35-1	08/06/2023	0.399	0.389	0.249	0.288	0.336	0.232	0.217	0.201	0.251	0.173	0.274

APPENDIX E

Fresh Properties of Treated Fibres Results

Slump Flow

Mix Code	Date of Test	Diameter d_1	Diameter d_2	Slump Flow
		mm	mm	mm
Control Mix				
CMM	29/05/2023	190.00	195.00	192.50
Untreated Fibres				
UF15-0.5	30/05/2023	145.00	160.00	152.50
UF25-0.5	30/05/2023	130.26	141.58	135.92
UF35-0.5	29/05/2023	118.71	123.77	121.24
UF15-1	30/05/2023	127.38	125.42	126.40
UF25-1	30/05/2023	112.65	126.81	119.73
UF35-1	29/05/2023	110.54	113.20	111.87
Treated Fibres Hydrogen Peroxide 5%				
HPF15-0.5	02/06/2023	148.82	161.27	155.05
HPF25-0.5	09/06/2023	138.78	143.06	140.92
HPF35-0.5	09/06/2023	121.29	130.45	125.87
HPF15-1	02/06/2023	124.36	132.11	128.23
HPF25-1	09/06/2023	117.41	122.67	120.04
HPF35-1	09/06/2023	107.84	110.49	109.17
Treated Fibres Sodium Hydroxide 5%				
SHF15-0.5	16/09/2023	169.80	163.85	166.82
SHF25-0.5	16/09/2023	139.33	145.43	142.38
SHF35-0.5	16/09/2023	124.70	126.17	125.43
SHF15-1	16/09/2023	133.76	126.42	130.09
SHF25-1	16/09/2023	124.25	127.44	125.85
SHF35-1	16/09/2023	106.71	109.78	108.25

APPENDIX F

Mechanical Properties of Treated Fibres Results

Flexural Strength at 7 days

Mix Code	Date of Test	Sample	Dimensions Readings (mm)				Average (mm)	Volume (cm^3)	Mass (g)	Density (g/cm^3)	Max. Load (kN)	Flexural Strength (Mpa)	Average Density (g/cm^3)	Average Flexural Strength (Mpa)
				1st	2nd	3rd								
Control Mix	05/06/2023	A	L	160.20	160.30	159.40	159.97	261.60	560.08	2.14	3.137	7.07	2.12	6.86
			B	40.46	40.07	40.05	40.19							
			H	40.94	40.32	40.80	40.69							
		B	L	160.36	160.16	160.03	160.18	254.30	532.21	2.09	2.791	6.65		
			B	39.93	40.01	40.16	40.03							
			H	39.77	38.84	40.37	39.66							

Flexural Strength at 7 days

Mix Code	Date of Test	Sample	Dimensions Readings (mm)				Average (mm)	Volume (cm^3)	Mass (g)	Density (g/cm^3)	Max. Load (kN)	Flexural Strength (Mpa)	Average Density (g/cm^3)	Average Flexural Strength (Mpa)
				1st	2nd	3rd								
UF15-0.5	06/06/2023	A	L	159.24	159.27	159.06	159.19	251.15	530.76	2.11	2.646	6.31	2.12	7.02
			B	39.60	39.54	39.64	39.59							
			H	39.75	39.92	39.87	39.85							
		B	L	160.64	161.01	160.29	160.65	258.71	551.53	2.13	3.34	7.72		
			B	39.89	39.92	40.11	39.97							
			H	39.83	40.26	40.79	40.29							

Flexural Strength at 7 days

Mix Code	Date of Test	Sample	Dimensions Readings (mm)				Average (mm)	Volume (cm^3)	Mass (g)	Density (g/cm^3)	Max. Load (kN)	Flexural Strength (Mpa)	Average Density (g/cm^3)	Average Flexural Strength (Mpa)
				1st	2nd	3rd								
UF25-0.5	06/06/2023	A	L	160.28	160.35	160.14	160.26	252.83	563.02	2.23	3.056	7.34	2.235	7.54
			B	39.86	39.81	39.98	39.88							
			H	39.33	39.94	39.42	39.56							
		B	L	159.93	160.04	159.21	159.73	250.39	561.29	2.25	3.171	7.74		
			B	39.81	40.13	40.04	39.99							
			H	39.13	39.15	39.33	39.20							

Flexural Strength at 7 days

Mix Code	Date of Test	Sample	Dimensions Readings (mm)				Average (mm)	Volume (cm^3)	Mass (g)	Density (g/cm^3)	Max. Load (kN)	Flexural Strength (Mpa)	Average Density (g/cm^3)	Average Flexural Strength (Mpa)
				1st	2nd	3rd								
UF35-0.5	05/06/2023	A	L	161.02	160.29	161.37	160.89	259.92	585.31	2.25	3.112	7.58	2.22	7.57
			B	39.87	39.77	39.93	39.86							
			H	40.82	40.83	39.95	40.53							
		B	L	160.33	160.62	160.25	160.40	259.27	568.59	2.19	3.076	7.53		
			B	40.58	39.76	39.84	40.06							
			H	39.50	41.09	40.47	40.35							

Flexural Strength at 7 days

Mix Code	Date of Test	Sample	Dimensions Readings (mm)				Average (mm)	Volume (cm^3)	Mass (g)	Density (g/cm^3)	Max. Load (kN)	Flexural Strength (Mpa)	Average Density (g/cm^3)	Average Flexural Strength (Mpa)
				1st	2nd	3rd								
UF15-1	06/06/2023	A	L	160.15	160.19	159.65	159.99	256.75	560.75	2.18	2.995	6.98	2.125	7.15
			B	39.86	40.05	40.17	40.03							
			H	39.98	39.95	40.34	40.09							
		B	L	160.66	160.93	160.99	160.86	253.44	542.17	2.14	3.021	7.32		
			B	40.25	40.11	39.97	40.11							
			H	38.88	39.74	39.22	39.28							

Flexural Strength at 7 days

Mix Code	Date of Test	Sample	Dimensions Readings (mm)				Average (mm)	Volume (cm^3)	Mass (g)	Density (g/cm^3)	Max. Load (kN)	Flexural Strength (Mpa)	Average Density (g/cm^3)	Average Flexural Strength (Mpa)
				1st	2nd	3rd								
UF25-1	06/06/2023	A	L	162.19	161.50	161.54	161.74	254.21	540.23	2.13	3.497	8.45	2.16	8.18
			B	40.17	39.50	39.66	39.78							
			H	39.85	39.51	39.17	39.51							
		B	L	160.55	161.35	160.98	160.96	251.77	532.51	2.12	3.242	7.90		
			B	39.86	39.71	39.74	39.77							
			H	39.41	39.41	39.17	39.33							

Flexural Strength at 7 days

Mix Code	Date of Test	Sample	Dimensions Readings (mm)				Average (mm)	Volume (cm^3)	Mass (g)	Density (g/cm^3)	Max. Load (kN)	Flexural Strength (Mpa)	Average Density (g/cm^3)	Average Flexural Strength (Mpa)
				1st	2nd	3rd								
UF35-1	06/06/2023	A	L	160.19	160.47	160.44	160.37	253.83	542.30	2.14	3.747	8.86	2.125	8.54
			B	39.55	39.60	39.27	39.47							
			H	40.22	40.03	40.06	40.10							
		B	L	161.17	160.76	159.90	160.61	253.17	535.38	2.11	3.389	8.22		
			B	40.09	40.13	40.27	40.16							
			H	39.39	39.26	39.10	39.25							

Flexural Strength at 7 days

Mix Code	Date of Test	Sample	Dimensions Readings (mm)				Average (mm)	Volume (cm^3)	Mass (g)	Density (g/cm^3)	Max. Load (kN)	Flexural Strength (Mpa)	Average Density (g/cm^3)	Average Flexural Strength (Mpa)
				1st	2nd	3rd								
HPF15-0.5	09/06/2023	A	L	160.03	159.59	158.94	159.52	250.19	509.5	2.04	3.060	7.46	2.03	7.78
			B	39.88	40.24	39.81	39.98							
			H	39.19	39.15	39.36	39.23							
		B	L	160.32	159.86	159.06	159.75	251.52	508	2.02	3.352	8.10		
			B	40.06	39.75	39.93	39.91							
			H	39.33	39.37	39.64	39.45							

Flexural Strength at 7 days

Mix Code	Date of Test	Sample	Dimensions Readings (mm)			Average (mm)	Volume (cm^3)	Mass (g)	Density (g/cm^3)	Max. Load (kN)	Flexural Strength (Mpa)	Average Density (g/cm^3)	Average Flexural Strength (Mpa)
				1st	2nd	3rd								
HPF25-0.5	16/06/2023	A	L	161.60	160.86	160.27	160.91	253.00	570.50	2.25	3.618	8.81	2.29	8.57
			B	39.93	40.11	40.22	40.09							
			H	39.07	39.44	39.14	39.22							
		B	L	160.29	160.37	160.18	160.28	248.09	576.50	2.32	3.350	8.33		
			B	39.92	39.69	39.67	39.76							
			H	38.68	39.48	38.62	38.93							

Flexural Strength at 7 days

Mix Code	Date of Test	Sample	Dimensions Readings (mm)			Average (mm)	Volume (cm^3)	Mass (g)	Density (g/cm^3)	Max. Load (kN)	Flexural Strength (Mpa)	Average Density (g/cm^3)	Average Flexural Strength (Mpa)
				1st	2nd	3rd								
HPF35-0.5	16/06/2023	A	L	160.80	160.62	160.49	160.64	253.18	528.50	2.09	3.378	8.11	2.11	8.89
			B	39.88	39.75	39.68	39.77							
			H	39.42	39.30	40.17	39.63							
		B	L	160.91	160.67	160.52	160.70	247.95	529.00	` 2.13	3.849	9.67		
			B	40.01	39.83	39.84	39.89							
			H	39.26	39.69	40.08	38.68							

Flexural Strength at 7 days

Mix Code	Date of Test	Sample	Dimensions Readings (mm)				Average (mm)	Volume (cm^3)	Mass (g)	Density (g/cm^3)	Max. Load (kN)	Flexural Strength (Mpa)	Average Density (g/cm^3)	Average Flexural Strength (Mpa)
				1st	2nd	3rd								
HPF15-1	09/06/2023	A	L	159.70	159.59	158.81	159.37	251.74	548	2.18	3.525	8.47	2.16	8.42
			B	39.91	40.22	39.80	39.98							
			H	40.16	39.12	39.24	39.51							
		B	L	160.65	160.26	160.03	160.31	253.11	542.5	2.14	3.486	8.36		
			B	39.95	39.71	39.95	39.87							
			H	39.58	39.62	39.59	39.60							

Flexural Strength at 7 days

Mix Code	Date of Test	Sample	Dimensions Readings (mm)				Average (mm)	Volume (cm^3)	Mass (g)	Density (g/cm^3)	Max. Load (kN)	Flexural Strength (Mpa)	Average Density (g/cm^3)	Average Flexural Strength (Mpa)
				1st	2nd	3rd								
HPF25-1	16/06/2023	A	L	160.68	160.80	160.11	160.53	253.58	575	2.27	3.202	7.69	2.27	8.52
			B	39.94	40.19	39.67	39.93							
			H	39.25	39.41	40.01	39.56							
		B	L	160.01	160.47	160.04	160.17	254.54	577.5	2.27	3.970	9.36		
			B	39.79	39.48	39.81	39.69							
			H	40.35	39.50	40.28	40.04							

Flexural Strength at 7 days

Mix Code	Date of Test	Sample	Dimensions Readings (mm)				Average (mm)	Volume (cm^3)	Mass (g)	Density (g/cm^3)	Max. Load (kN)	Flexural Strength (Mpa)	Average Density (g/cm^3)	Average Flexural Strength (Mpa)
				1st	2nd	3rd								
HPF35-1	16/06/2023	A	L	160.54	160.10	159.87	160.17	258.90	588.5	2.27	3.982	9.15	2.26	9.33
			B	40.14	39.92	39.97	40.01							
			H	40.49	40.62	40.08	40.40							
		B	L	160.49	160.32	159.59	160.13	255.70	574.5	2.25	4.046	9.52		
			B	39.88	39.96	40.10	39.98							
			H	39.66	39.84	40.33	39.94							

Flexural Strength at 7 days

Mix Code	Date of Test	Sample	Dimensions Readings (mm)				Average (mm)	Volume (cm^3)	Mass (g)	Density (g/cm^3)	Max. Load (kN)	Flexural Strength (Mpa)	Average Density (g/cm^3)	Average Flexural Strength (Mpa)
				1st	2nd	3rd								
SHF15-0.5	23/06/2023	A	L	160.14	161.68	160.95	160.99	265.82	566	2.13	3.023	6.72	2.135	7.29
			B	40.20	40.04	41.05	40.43							
			H	40.95	40.82	40.75	40.84							
		B	L	160.95	159.23	159.89	160.02	259.18	553.5	2.14	3.406	7.85		
			B	40.32	39.71	40.93	40.32							
			H	40.37	39.46	40.69	40.17							

Flexural Strength at 7 days

Mix Code	Date of Test	Sample		Dimensions Readings (mm)			Average (mm)	Volume (cm^3)	Mass (g)	Density (g/cm^3)	Max. Load (kN)	Flexural Strength (Mpa)	Average Density (g/cm^3)	Average Flexural Strength (Mpa)
				1st	2nd	3rd								
SHF25-0.5	23/06/2023	A	L	159.86	160.80	160.20	160.29	244.76	509.5	2.08	2.821	7.19	2.06	8.03
			B	39.69	39.57	39.61	39.62							
			H	39.10	38.45	38.06	38.54							
		B	L	160.49	159.89	159.90	160.09	250.16	511	2.04	3.592	8.86		
			B	40.10	40.77	39.61	40.16							
			H	38.62	38.99	39.11	38.91							

Flexural Strength at 7 days

Mix Code	Date of Test	Sample		Dimensions Readings (mm)			Average (mm)	Volume (cm^3)	Mass (g)	Density (g/cm^3)	Max. Load (kN)	Flexural Strength (Mpa)	Average Density (g/cm^3)	Average Flexural Strength (Mpa)
				1st	2nd	3rd								
SHF35-0.5	23/06/2023	A	L	160.01	160.54	159.39	159.98	262.58	587.5	2.24	3.979	8.90	2.215	8.18
			B	40.01	39.91	40.56	40.16							
			H	41.33	40.51	40.77	40.87							
		B	L	160.35	160.43	159.56	160.11	257.39	562.5	2.19	3.208	7.47		
			B	40.54	39.95	39.83	40.11							
			H	40.10	39.79	40.34	40.08							

Flexural Strength at 7 days

Mix Code	Date of Test	Sample	Dimensions Readings (mm)				Average (mm)	Volume (cm^3)	Mass (g)	Density (g/cm^3)	Max. Load (kN)	Flexural Strength (Mpa)	Average Density (g/cm^3)	Average Flexural Strength (Mpa)
				1st	2nd	3rd								
SHF15-1	23/06/2023	A	L	160.80	161.49	160.40	160.90	256.03	555	2.17	3.206	7.58	2.23	7.80
			B	39.99	39.90	39.79	39.89							
			H	39.70	40.90	39.08	39.89							
		B	L	161.22	161.75	160.85	161.27	257.00	588.5	2.29	3.398	8.02		
			B	39.78	39.80	40.35	39.98							
			H	39.71	39.45	40.32	39.86							

Flexural Strength at 7 days

Mix Code	Date of Test	Sample	Dimensions Readings (mm)				Average (mm)	Volume (cm^3)	Mass (g)	Density (g/cm^3)	Max. Load (kN)	Flexural Strength (Mpa)	Average Density (g/cm^3)	Average Flexural Strength (Mpa)
				1st	2nd	3rd								
SHF25-1	23/06/2023	A	L	160.13	160.39	160.19	160.24	257.92	586.5	2.28	3.783	8.83	2.16	8.47
			B	40.47	40.30	40.27	40.35							
			H	39.93	39.98	39.75	39.89							
		B	L	160.32	160.50	160.07	160.30	256.80	526.5	2.04	3.458	8.11		
			B	39.97	40.02	40.37	40.12							
			H	40.72	39.73	39.33	39.93							

Flexural Strength at 7 days

Mix Code	Date of Test	Sample	Dimensions Readings (mm)				Average (mm)	Volume (cm^3)	Mass (g)	Density (g/cm^3)	Max. Load (kN)	Flexural Strength (Mpa)	Average Density (g/cm^3)	Average Flexural Strength (Mpa)
				1st	2nd	3rd								
SHF15-1	23/06/2023	A	L	160.80	161.49	160.40	160.90	256.03	555	2.17	3.206	7.58	2.23	7.80
			B	39.99	39.90	39.79	39.89							
			H	39.70	40.90	39.08	39.89							
		B	L	161.22	161.75	160.85	161.27	257.00	588.5	2.29	3.398	8.02		
			B	39.78	39.80	40.35	39.98							
			H	39.71	39.45	40.32	39.86							

Flexural Strength at 7 days

Mix Code	Date of Test	Sample	Dimensions Readings (mm)				Average (mm)	Volume (cm^3)	Mass (g)	Density (g/cm^3)	Max. Load (kN)	Flexural Strength (Mpa)	Average Density (g/cm^3)	Average Flexural Strength (Mpa)
				1st	2nd	3rd								
SHF25-1	23/06/2023	A	L	160.13	160.39	160.19	160.24	257.92	586.5	2.28	3.783	8.83	2.16	8.47
			B	40.47	40.30	40.27	40.35							
			H	39.93	39.98	39.75	39.89							
		B	L	160.32	160.50	160.07	160.30	256.80	526.5	2.04	3.458	8.11		
			B	39.97	40.02	40.37	40.12							
			H	40.72	39.73	39.33	39.93							

Compressive Strength at 7 days

Mix Code	Date of Test	Sample	Dimensions Readings (mm)				Average (mm)	Volume (cm^3)	Mass (g)	Density (g/cm^3)	Max. Load (kN)	Compressive Strength (Mpa)	Average Density (g/cm^3)	Average Compressive Strength (Mpa)
				1st	2nd	3rd								
UF15-0.5	06/06/2023	A	L	159.24	159.27	159.06	159.19	251.15	530.76	2.11	44.86	28.43	2.12	31.74
			B	39.60	39.54	39.64	39.59				48.72	30.88		
			H	39.75	39.92	39.87	39.85							
		B	L	160.64	161.01	160.29	160.65	258.71	551.53	2.13	55.38	34.39		
			B	39.89	39.92	40.11	39.97				53.53	33.24		
			H	39.83	40.26	40.79	40.29							

Compressive Strength at 7 days

Mix Code	Date of Test	Sample	Dimensions Readings (mm)				Average (mm)	Volume (cm^3)	Mass (g)	Density (g/cm^3)	Max. Load (kN)	Compressive Strength (Mpa)	Average Density (g/cm^3)	Average Compressive Strength (Mpa)
				1st	2nd	3rd								
UF25-0.5	06/06/2023	A	L	160.28	160.35	160.14	160.26	252.83	563.02	2.23	58.74	37.23	2.235	37.67
			B	39.86	39.81	39.98	39.88				59.03	37.42		
			H	39.33	39.94	39.42	39.56							
		B	L	159.93	160.04	159.21	159.73	250.39	561.29	2.24	57.65	36.78		
			B	39.81	40.13	40.04	39.99				61.53	39.25		
			H	39.13	39.15	39.33	39.20							

Compressive Strength at 7 days

Mix Code	Date of Test	Sample	Dimensions Readings (mm)				Average (mm)	Volume (cm^3)	Mass (g)	Density (g/cm^3)	Max. Load (kN)	Compressive Strength (Mpa)	Average Density (g/cm^3)	Average Compressive Strength (Mpa)
				1st	2nd	3rd								
UF35-0.5	05/06/2023	A	L	160.2	160.3	159.4	159.97	261.60	560.08	2.14	64.45	39.42	2.125	38.51
			B	40.46	40.07	40.05	40.19				60.39	36.93		
			H	40.94	40.32	40.80	40.69							
		B	L	160.36	160.16	160.03	160.18	254.3	532.21	2.09	61.07	38.47		
			B	39.93	40.01	40.16	40.03				62.30	39.24		
			H	39.83	40.26	40.79	40.29							

Compressive Strength at 7 days

Mix Code	Date of Test	Sample	Dimensions Readings (mm)				Average (mm)	Volume (cm^3)	Mass (g)	Density (g/cm^3)	Max. Load (kN)	Compressive Strength (Mpa)	Average Density (g/cm^3)	Average Compressive Strength (Mpa)
				1st	2nd	3rd								
UF15-1	06/06/2023	A	L	160.15	160.19	159.65	159.99	256.75	560.75	2.18	63.42	39.52	2.16	36.31
			B	39.86	40.05	40.17	40.03				60.95	37.98		
			H	39.98	39.95	40.34	40.09							
		B	L	160.66	160.93	160.99	160.86	253.44	542.17	2.14	59.69	37.89		
			B	40.25	40.11	39.97	40.11				47.06	29.87		
			H	38.88	39.74	39.22	39.28							

Compressive Strength at 7 days

Mix Code	Date of Test	Sample	Dimensions Readings (mm)				Average (mm)	Volume (cm^3)	Mass (g)	Density (g/cm^3)	Max. Load (kN)	Compressive Strength (Mpa)	Average Density (g/cm^3)	Average Compressive Strength (Mpa)
				1st	2nd	3rd								
UF25-1	06/06/2023	A	L	162.19	161.50	161.54	161.74	254.21	540.23	2.13	62.82	39.97	2.125	38.38
			B	40.17	39.50	39.66	39.78				57.44	36.55		
			H	39.85	39.51	39.17	39.51							
		B	L	160.55	161.35	160.98	160.96	251.77	532.51	2.12	61.72	39.46		
			B	39.86	39.71	39.74	39.77				58.71	37.53		
			H	39.41	39.41	39.17	39.33							

Compressive Strength at 7 days

Mix Code	Date of Test	Sample	Dimensions Readings (mm)				Average (mm)	Volume (cm^3)	Mass (g)	Density (g/cm^3)	Max. Load (kN)	Compressive Strength (Mpa)	Average Density (g/cm^3)	Average Compressive Strength (Mpa)
				1st	2nd	3rd								
UF35-1	06/06/2023	A	L	160.19	160.47	160.44	160.37	253.83	542.30	2.14	68.15	43.06	2.115	41.73
			B	39.55	39.60	39.27	39.47				67.11	42.40		
			H	40.22	40.03	40.06	40.10							
		B	L	161.17	160.76	159.90	160.61	253.17	535.38	2.11	65.10	41.30		
			B	40.09	40.13	40.27	40.16				63.33	40.18		
			H	39.39	39.26	39.10	39.25							

Compressive Strength at 7 days

Mix Code	Date of Test	Sample	Dimensions Readings (mm)				Average (mm)	Volume (cm^3)	Mass (g)	Density (g/cm^3)	Max. Load (kN)	Compressive Strength (Mpa)	Average Density (g/cm^3)	Average Compressive Strength (Mpa)
				1st	2nd	3rd								
HPF15-0.5	09/06/2023	A	L	160.03	159.59	158.94	159.52	250.19	509.5	2.04	52.27	33.33	2.03	34.24
			B	39.88	40.24	39.81	39.98				53.20	33.92		
			H	39.19	39.15	39.36	39.23							
		B	L	160.32	159.86	159.06	159.75	251.52	508	2.02	55.07	34.98		
			B	40.06	39.75	39.93	39.91				54.71	34.75		
			H	39.33	39.37	39.64	39.45							

Compressive Strength at 7 days

Mix Code	Date of Test	Sample	Dimensions Readings (mm)				Average (mm)	Volume (cm^3)	Mass (g)	Density (g/cm^3)	Max. Load (kN)	Compressive Strength (Mpa)	Average Density (g/cm^3)	Average Compressive Strength (Mpa)
				1st	2nd	3rd								
HPF25-0.5	16/06/2023	A	L	161.60	160.86	160.27	160.91	253.00	570.50	2.25	57.32	36.46	2.29	38.41
			B	39.93	40.11	40.22	40.09				58.20	37.02		
			H	39.07	39.44	39.14	39.22							
		B	L	160.29	160.37	160.18	160.28	248.09	576.50	2.32	60.15	38.86		
			B	39.92	39.69	39.67	39.76				63.93	41.30		
			H	38.68	39.48	38.62	38.93							

Compressive Strength at 7 days

Mix Code	Date of Test	Sample	Dimensions Readings (mm)				Average (mm)	Volume (cm^3)	Mass (g)	Density (g/cm^3)	Max. Load (kN)	Compressive Strength (Mpa)	Average Density (g/cm^3)	Average Compressive Strength (Mpa)
				1st	2nd	3rd								
HPF35-0.5	16/06/2023	A	L	160.80	160.62	160.49	160.64	253.18	528.50	2.09	65.21	41.37	2.08	40.69
			B	39.88	39.75	39.68	39.77				64.85	41.15		
			H	39.42	39.30	40.17	39.63							
		B	L	160.91	160.67	160.52	160.70	247.95	529.00	2.13	64.92	41.02		
			B	40.01	39.83	39.84	39.89				62.09	39.23		
			H	39.26	39.69	40.08	38.68							

Compressive Strength at 7 days

Mix Code	Date of Test	Sample	Dimensions Readings (mm)				Average (mm)	Volume (cm^3)	Mass (g)	Density (g/cm^3)	Max. Load (kN)	Compressive Strength (Mpa)	Average Density (g/cm^3)	Average Compressive Strength (Mpa)
				1st	2nd	3rd								
HPF15-1	09/06/2023	A	L	159.70	159.59	158.81	159.37	251.74	548	2.18	62.62	30.64	2.16	38.69
			B	39.91	40.22	39.80	39.98				60.14	38.07		
			H	40.16	39.12	39.24	39.51							
		B	L	160.65	160.26	160.03	160.31	253.11	542.5	2.14	62.11	39.34		
			B	39.95	39.71	39.95	39.87				59.54	37.71		
			H	39.58	39.62	39.59	39.60							

Compressive Strength at 7 days

Mix Code	Date of Test	Sample	Dimensions Readings (mm)				Average (mm)	Volume (cm^3)	Mass (g)	Density (g/cm^3)	Max. Load (kN)	Compressive Strength (Mpa)	Average Density (g/cm^3)	Average Compressive Strength (Mpa)
				1st	2nd	3rd								
HPF25-1	16/06/2023	A	L	160.68	160.80	160.11	160.53	253.58	575	2.27	64.45	40.80	2.27	40.82
			B	39.94	40.19	39.67	39.93				65.82	41.67		
			H	39.25	39.41	40.01	39.56							
		B	L	160.01	160.47	160.04	160.17	254.54	577.5	2.27	63.57	40.00		
			B	39.79	39.48	39.81	39.69				64.85	40.81		
			H	40.35	39.50	40.28	40.04							

Compressive Strength at 7 days

Mix Code	Date of Test	Sample	Dimensions Readings (mm)				Average (mm)	Volume (cm^3)	Mass (g)	Density (g/cm^3)	Max. Load (kN)	Compressive Strength (Mpa)	Average Density (g/cm^3)	Average Compressive Strength (Mpa)
				1st	2nd	3rd								
HPF35-1	16/06/2023	A	L	160.54	160.10	159.87	160.17	258.90	588.5	2.27	64.87	41.13	2.26	41.42
			B	40.14	39.92	39.97	40.01				65.19	40.33		
			H	40.49	40.62	40.08	40.40							
		B	L	160.49	160.32	159.59	160.13	255.70	574.5	2.25	66.72	41.78		
			B	39.88	39.96	40.10	39.98				69.34	43.42		
			H	39.66	39.84	40.33	39.94							

Compressive Strength at 7 days

Mix Code	Date of Test	Sample	Dimensions Readings (mm)				Average (mm)	Volume (cm^3)	Mass (g)	Density (g/cm^3)	Max. Load (kN)	Compressive Strength (Mpa)	Average Density (g/cm^3)	Average Compressive Strength (Mpa)
				1st	2nd	3rd								
SHF15-0.5	23/06/2023	A	L	160.14	161.68	160.95	160.99	265.82	566	2.13	48.66	29.47	2.135	31.47
			B	40.20	40.04	41.05	40.43				53.05	32.12		
			H	40.95	40.82	40.75	40.84							
		B	L	160.95	159.23	159.89	160.02	259.18	553.5	2.14	55.21	34.09		
			B	40.32	39.71	40.93	40.32				48.92	30.20		
			H	40.37	39.46	40.69	40.17							

Compressive Strength at 7 days

Mix Code	Date of Test	Sample	Dimensions Readings (mm)				Average (mm)	Volume (cm^3)	Mass (g)	Density (g/cm^3)	Max. Load (kN)	Compressive Strength (Mpa)	Average Density (g/cm^3)	Average Compressive Strength (Mpa)
				1st	2nd	3rd								
SHF25-0.5	23/06/2023	A	L	159.86	160.80	160.20	160.29	244.76	509.5	2.08	56.71	36.46	2.06	37.02
			B	39.69	39.57	39.61	39.62				55.93	37.02		
			H	39.10	38.45	38.06	38.54							
		B	L	160.49	159.89	159.90	160.09	250.16	511	2.04	59.22	38.86		
			B	40.10	40.77	39.61	40.16				56.89	41.30		
			H	39.66	39.84	40.33	39.94							

Compressive Strength at 7 days

Mix Code	Date of Test	Sample	Dimensions Readings (mm)				Average (mm)	Volume (cm^3)	Mass (g)	Density (g/cm^3)	Max. Load (kN)	Compressive Strength (Mpa)	Average Density (g/cm^3)	Average Compressive Strength (Mpa)
				1st	2nd	3rd								
SHF35-0.5	23/06/2023	A	L	160.01	160.54	159.39	159.98	262.58	587.5	2.24	65.96	41.37	2.215	41.02
			B	40.01	39.91	40.56	40.16				68.28	41.15		
			H	41.33	40.51	40.77	40.87							
		B	L	160.35	160.43	159.56	160.11	257.39	562.5	2.19	64.48	41.02		
			B	40.54	39.95	39.83	40.11				62.25	39.23		
			H	40.10	39.79	40.34	40.08							

Compressive Strength at 7 days

Mix Code	Date of Test	Sample	Dimensions Readings (mm)				Average (mm)	Volume (cm^3)	Mass (g)	Density (g/cm^3)	Max. Load (kN)	Compressive Strength (Mpa)	Average Density (g/cm^3)	Average Compressive Strength (Mpa)
				1st	2nd	3rd								
SHF15-1	23/06/2023	A	L	160.80	161.49	160.40	160.90	256.03	555	2.17	59.09	37.14	2.23	36.81
			B	39.99	39.90	39.79	39.89				53.66	33.72		
			H	39.70	40.90	39.08	39.89							
		B	L	161.22	161.75	160.85	161.27	257.00	588.5	2.29	61.62	38.75		
			B	39.78	39.80	40.35	39.98				59.81	37.62		
			H	39.71	39.45	40.32	39.86							

Compressive Strength at 7 days

Mix Code	Date of Test	Sample	Dimensions Readings (mm)				Average (mm)	Volume (cm^3)	Mass (g)	Density (g/cm^3)	Max. Load (kN)	Compressive Strength (Mpa)	Average Density (g/cm^3)	Average Compressive Strength (Mpa)
				1st	2nd	3rd								
SHF25-1	23/06/2023	A	L	160.13	160.39	160.19	160.24	257.92	586.5	2.28	59.25	36.81	2.16	39.03
			B	40.47	40.30	40.27	40.35				64.75	40.23		
			H	39.93	39.98	39.75	39.89							
		B	L	160.32	160.50	160.07	160.30	256.80	526.5	2.04	60.82	37.97		
			B	39.97	40.02	40.37	40.12				65.84	41.10		
			H	40.72	39.73	39.33	39.93							

Compressive Strength at 7 days

Mix Code	Date of Test	Sample	Dimensions Readings (mm)				Average (mm)	Volume (cm^3)	Mass (g)	Density (g/cm^3)	Max. Load (kN)	Compressive Strength (Mpa)	Average Density (g/cm^3)	Average Compressive Strength (Mpa)
				1st	2nd	3rd								
SHF35-1	23/06/2023	A	L	160.06	159.92	159.54	159.84	259.14	523.5	2.02	71.25	43.95	2.14	43.32
			B	40.23	40.45	39.96	40.21				65.43	40.36		
			H	40.50	40.57	39.90	40.32							
		B	L	160.22	160.40	159.52	160.05	256.08	578	2.26	68.40	42.75		
			B	40.03	39.79	39.74	39.85				73.99	46.24		
			H	39.71	39.45	40.32	39.86							

APPENDIX G

Information on Chicken Feather Fibres (CFF)

A site visit was conducted to Smina, which is a poultry processing plant, to obtain further information regarding chicken waste. From information gathered, it was found that around 4000 chickens a day are slaughtered daily for meat production. Every chicken approximately yields 90g of feathers, resulting in a daily accumulation of 360kg of chicken feather waste.

Apart from feathers, chicken waste consists also includes intestines and bones. About 3 tonnes of chicken waste are transported to the WasteServ plant for disposal on a daily basis. Waster is another important component used in the processing plant for cleaning procedures. It is estimated that half a gallon of water is used for every chicken during the processing which takes about 1.5 hours to complete. The slaughtering process begins with the off-loading of chickens from the farms. The following steps involved in the process are:

***Slaughtering and Killing**:* The chickens are hung upside down by their legs on a moving slaughter line. They are usually stunned with an electric current and their throats are cut as the line moves mechanically, resulting in their death due to blood loss.

Scalding: Once the chickens have bled, they pass through a hot tank of around 57^{o}C for the removal of feathers. The hot water helps soften the skin, making it easier to remove the feathers from their bodies. The collected feathers are then stored in a crate.

Removal of heads and legs: The slaughter line continues to move, and their heads and legs are pulled off mechanically.

Cleaning: The chickens are thoroughly washed to remove any remaining blood. The internal organs and intestines are also removed, and the chickens undergo another round of washing.

Cooling: The chickens are then stored in a refrigerator at a temperature of 5^{o}C for approximately 1 hour to reduce the risk of bacterial growth.

Processing: The chickens are weighed and further processed into different products such as chicken wings, drumsticks, or chicken breasts. They are packed and then distributed to several shops.

The investigation on Agave fibres was carried instead of CFF, as the primary focus was to explore the properties and potential applications of Agave fibres. CFF were also excluded from this study due to time constraints.